Julius–Maximilians–Universität
Würzburg

Institut für Physik und Astronomie
Theoretische Physik II
Prof.Dr.Rückl

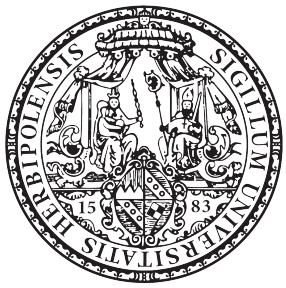

Diplomarbeit zur Erlangung des akademischen Grads eines Diplom-Physikers (Dipl.Phys)

Flavor violating squark and gluino decays

Christian Oppenländer

31.09.08

Betreut von Prof. Werner Porod

Gewidmet meiner Lebensgefährtin Stefania und meiner Mutter Helga

Abstract

In this work we will discuss flavor violating squark and gluino decays. At three of the most typical data points, we will add flavor violating, soft-SUSY breaking offdiagonal elements to the squark masses and trilinear couplings. At first, only one of the parameters is varied - we then use low energy observables originating in the B physics sector to constrain this parameter and illustrate its effects on the branching ratios of flavor violating squark and gluino decays in the allowed region of parameter space. Exemplary for these decays are $\tilde{u}_1 \to \tilde{\chi}_1^0 c$ with 30%, $\tilde{u}_2 \to \tilde{\chi}_1^0 c$ and $\tilde{d}_1 \to \tilde{\chi}_1^0 s$ with 10%, all at the γ data point, and $\tilde{d}_2 \to \tilde{\chi}_1^0 s$ with 30% at the SPS1a' data point. Considering gluino decays, we have $\tilde{g} \to \tilde{u}_1 c$ with 10%, to give an example.

Furthermore, the flavor violating parameters will be combined in pairs to probe their interference effects and to further constrain the parameter space of the nMFV MSSM. In these parameter planes, we look for significant increases in the branching ratios of flavor violating decays. Especially the decays $\tilde{d}_2 \to \tilde{\chi}_1^- c$ and $\tilde{d}_2 \to \tilde{\chi}_2^0 s$ in the MQ23/TD23 and MQ23/TU23 parameter planes, in which the trilinear couplings affect the allowed region of MQ23, show large branching ratio increases.

The results could be interesting to identify SUSY signals in future experiments at the LHC.

Kurzfassung

In der vorliegenden Arbeit werden flavorverletzende Squark- und Gluinozerfälle untersucht. Dazu werden zu drei der typischsten Datenpunkten flavorverletzende, soft-SUSY brechende offdiagonale Elemente der Squarkmassen und trilinearen Kopplungen addiert. Zunächst wird jeweils ein Parameter variiert und Niederenergieobservablen aus der B-Physik verwendet, um den erlaubten Bereich des Parameterraumes einzuschränken. Im Anschluß werden die Auswirkungen der Parameter auf flavorverletzende Squark- und Gluinozerfälle untersucht, um die Größenordnung der Verzweigungsverhältnisse jener Zerfälle im erlaubten Bereich bestimmen zu können. Beispiele hierfür sind $\tilde{u}_1 \to \tilde{\chi}_1^0 c$ mit 30%, $\tilde{u}_2 \to \tilde{\chi}_1^0 c$ und $\tilde{d}_1 \to \tilde{\chi}_1^0 s$ mit je 10% ,alle am γ Datenpunkt, sowie $\tilde{d}_2 \to \tilde{\chi}_1^0 s$ mit 30% am SPS1a' Datenpunkt, an Gluinozerfällen z.B. $\tilde{g} \to \tilde{u}_1 c$ mit 10%.

Darüber hinaus werden die flavorverletzenden Parameter auch in Paaren kombiniert, um die gegenseitige Wechselwirkung zur weiteren Einschränkung des nMFV MSSM Parameterraumes zu verwenden. In diesen Parameterebenen wird nun nach

starken Erhöhungen der Verzweigungsverhältnisse jener flavorverletzenden Zerfälle gesucht. Gefunden wurden diese insbesondere bei den Zerfällen $\tilde{d}_2 \to \tilde{\chi}_1^- c$ und $\tilde{d}_2 \to \tilde{\chi}_2^0 s$ in den Ebenen MQ23/TD23 und MQ23/TU23, in welchen die trilinearen Kopplungen den erlaubten Bereich von MQ23 verschieben.

Die Ergebnisse könnten in zukünftigen Experimenten am LHC von Bedeutung sein, um SUSY-Signale zu identifizieren.

Contents

1 Introduction **1**
1.1 SUSY and B-physics motivation 1

2 SUSY basics **3**
2.1 Weyl and Dirac Spinors 3
2.2 Supersymmetry operators 4
2.3 Supermultiplets 5
2.3.1 Higgs multiplets 6
2.3.2 Auxiliary fields 6
2.4 The SUSY group 6
2.4.1 Supersymmetric translations 6
2.4.2 Superfields 7
2.4.3 SUSY transformations and algebra 8
2.5 Supersymmetric Lagrangian 8
2.5.1 Superpotential and the MSSM 9
2.5.2 Complete unbroken lagrangian 10
2.5.3 The scalar potential 11
2.5.4 Soft SUSY breaking 11
2.6 Higgs sector 13
2.6.1 Higgs potential 13
2.6.2 Physical Higgs particles 13
2.7 Mass eigenstates of SUSY particles 14
2.7.1 Sfermion mixing 14
2.7.2 Neutralino mixing 16
2.7.3 Chargino mixing 17
2.7.4 Gluinos 18

3 B-Physics **21**
3.1 Penguin diagrams 21
3.1.1 SM penguins 22
3.2 Theoretical Considerations 24
3.2.1 Effective penguin theory 24
3.2.2 Penguin-Box Expansion 25
3.2.3 Universal functions 26

3.3 Rare decays and meson mixing . . . 27
3.3.1 B $\to X_s\gamma$ . . . 27
3.3.2 $\bar{B} \to X_s l^+ l^-$ . . . 28
3.3.3 $B_s \to \mu^+\mu^-$ . . . 29
3.3.4 $\bar{B_s} - B_s$ mixing . . . 30
3.4 SUSY penguins/boxes . . . 30

4 Lagrangian for squark decays **33**
4.1 $\mathcal{L}_I$ in gauge eigenstates . . . 33
4.1.1 Interactions with gauginos/gauge bosons . . . 34
4.2 Rotation into physical fields . . . 37
4.2.1 $\mathcal{L}_I$ in mass eigenstates . . . 37

5 Decay rates Γ **39**
5.1 Transition amplitudes . . . 39
5.1.1 Higgs boson radiation . . . 39
5.1.2 Decay into two fermions . . . 39
5.1.3 Gauge boson radiation . . . 40
5.2 Two-body decays in general . . . 41
5.3 Squark decay rates . . . 43

6 Evaluation and Results **45**
6.1 SPheno . . . 45
6.2 Parameters and conventions . . . 45
6.3 Parameter interplay . . . 46
6.3.1 MQ23 / MD23 . . . 46
6.3.2 MQ23 / TD23 . . . 47
6.3.3 MQ23 / TD32 . . . 48
6.3.4 MD23 / TD23 . . . 49
6.3.5 MD23 / TD32 . . . 50
6.3.6 TD23 / TD32 . . . 52
6.3.7 Up-Sector . . . 52
6.4 Squark and gluino decays . . . 54
6.4.1 $\tilde{u}_1$ decays . . . 56
6.4.2 $\tilde{u}_2$ decays . . . 58
6.4.3 $\tilde{d}_1$ decays . . . 60
6.4.4 $\tilde{d}_2$ decays . . . 61
6.4.5 Gluino decays . . . 62
6.5 Squark and gluino decay maxima . . . 64

7 Summary and Outlook **67**

8 Appendix **69**
8.1 Rotation into physical fields - calculations 69
8.1.1 $\mathcal{L}_I$ in mass eigenstates 69
8.1.2 Dirac notation 75

Bibliography **79**

1 Introduction

1.1 SUSY and B-physics motivation

Supersymmetric extensions of the standard model became very popular in the last decades, especially due to their ability to directly or indirectly solve some of the most critical issues with the SM. The core concept of SUSY is a space-time symmetry between bosonic and fermionic states. For such a symmetry, we need half-integer spin operators which obey a lorentz-invariant anticommutation relation:

$$\{Q_\alpha, Q^\dagger_\beta\} = 2\sigma^\mu_{\alpha\beta} P^\mu \tag{1.1}$$

As an anticommutator matrix with positive diagonal elements, it cannot vanish and P^μ is a positive, conserved vector quantity. Extensions oft the Coleman-Mandula-Theorem tell us that in more than two dimensions, the only conserved vector quantity is the energy-momentum 4-vector, and the operators Q_i cannot have higher spin than 1/2, or else any scattering is ruled out. Since the symmetry involves P^μ, every field in the theory is affected and gets a new supersymmetric partner assigned to it, i.e. the particle content is (at least) doubled with respect to the SM.

Since we do not observe any mass-degenerate SUSY partners of known particles, the symmetry has to be broken. If one assumes an energy difference of a few hundred GeV to the SM particles, he would also find a Higgs particle of the correct mass size.

The most striking effects appear in renormalizations of the theories: the scalar self-energy is cancelled by the fermion loop contribution to this energy; a symmetry between bosons and fermions protects the scalar masses from divergent loop corrections, thus giving a solution to the famous *hierarchy problem*. Furthermore, the new particles would affect the running coupling constants, which - as a not suspected side-effect - leads to a better unification of the couplings at very high energy scale. It is even possible to include gravity in this kind of theory, partnering

the force-mediating graviton with a fermionic gravitino and generalizing Einstein's theories to this new field.

Given all these exciting prospects and the ability to verify supersymmetric theories in experiment by the next few years, it is worth exploring the details of SUSY.

Some of the main questions in our search after SUSY particles includes the ability to constrain the parameter space by the phenomenology of the theory, thus being able to tell if a signal can be a SUSY particle at all - and if yes, having options on the details. Rare decays of K and B mesons already are an important tool in checking the standard model, and can also be used to constrain the parameter space of SUSY.

This work will apply known experimental bounds from (very) rare $b \to s$ decays and B meson mixing to the next-to-minimal flavor violating minimal supersymmetric standard model (nMFV MSSM) and constrain the parameter space in respect to off-diagonal squark mass matrix entries. It will check how large branching ratios of flavor violating squark and gluino decays in allowed regions of the parameter space can become, and investigate dependencies on and interferences of the flavor violating parameters. There are three common data points used - SPS1a' , γ, and I" [1, 2] - which main difference is a dissimilar value of $tan\beta$, the ratio of the Higgs VEVs in SUSY.

2 SUSY basics

This introduction will mainly follow [3] and give a short insight into the underlying theory, as well as the theoretical basics for the vertex calculations.

2.1 Weyl and Dirac Spinors

In SUSY, fermionic particle states are represented by (usually) left-handed Weyl spinors rather than Dirac spinors, which then partner a bosonic state and build up a so-called *supermultiplet*. A Dirac spinor is written as

$$\Psi^{(e^-)} = \begin{pmatrix} \chi_{L\alpha}^{(e^-)} \\ \psi_{R\alpha}^{(e^-)} \end{pmatrix} = \begin{pmatrix} \chi_{L\alpha}^{(e^-)} \\ i\sigma_2 \psi_{L\alpha}^{(e^+)*} \end{pmatrix} \equiv \begin{pmatrix} \chi_\alpha \\ \overline{\psi}^{\dot{\alpha}} \end{pmatrix} \tag{2.1}$$

and thus as a combination of the left handed particle Weyl spinor and the charge conjugate of the left-handed antiparticle field. $i\sigma_2 = \epsilon^{\alpha\beta}$ is a factor ensuring Lorentz invariance of spinor products and can be used to raise the spinor index α. The last step in the above equation is a plausible *definition* due to the same transformation behavior of ψ_α^* and $\psi_{\dot{\alpha}}$. In summary, spinors transforming according to $SU(2)_L$ have a lower, undotted spinor index and spinors transforming according to $SU(2)_R$ a high, dotted index. For notation issues, one should consult [3]. In a similar way, one could also use right-handed Weyl spinors to represent the whole particle content; in literature, usually left handed spinors are used due to their unique relationship to $SU(2)$. There are various different notations in literature, and can sometimes be confusing. For better comparison with similar results, we will largely adapt the notations and conventions of [3] and [4].

Some useful relations between Weyl and Dirac spinors are presented for later use:

$$\Psi_D = \begin{pmatrix} \chi_\alpha \\ \overline{\psi}^{\dot{\beta}} \end{pmatrix} \qquad \overline{\Psi}_D = \begin{pmatrix} (\psi^\alpha)^T & (\overline{\chi}_{\dot{\beta}})^T \end{pmatrix}$$

$$\overline{\Psi}_D \Psi_D = (\psi^\alpha)^T \chi_\alpha + h.c. = \psi\chi + h.c.$$

$$\begin{aligned}
&\overline{\Psi}_1 \Psi_2 = \psi_1^\alpha \chi_{2\alpha} + \overline{\chi}_{1\dot{\beta}} \overline{\psi}_2^{\dot{\beta}} = \psi_1\chi_2 + \overline{\chi}_1\overline{\psi}_2 \\
&\overline{\Psi}_1 \gamma_5 \Psi_2 = -\psi_1\chi_2 + \overline{\chi}_1\overline{\psi}_2 \\
&\overline{\Psi}_1 \gamma^\mu \Psi_2 = \overline{\chi}_1\overline{\sigma}^\mu\chi_2 - \overline{\psi}_2\overline{\sigma}^\mu\psi_1 \\
&\overline{\Psi}_1 \gamma^\mu \gamma_5 \Psi_2 = -\overline{\chi}_1\overline{\sigma}^\mu\chi_2 - \overline{\psi}_2\overline{\sigma}^\mu\psi_1 \\
&\overline{\Psi}_1 \gamma^\mu \partial_\mu \Psi_2 = \overline{\chi}_1\overline{\sigma}^\mu\partial_\mu\chi_2 - \overline{\psi}_2\overline{\sigma}^\mu\partial_\mu\psi_1
\end{aligned} \tag{2.2}$$

Defining the usual left- and righthanded projection operators, we can also write Weyl spinor expressions as Dirac spinors.

$$\begin{aligned}
&P_L = \frac{1}{2}(1-\gamma_5) \qquad P_R = \frac{1}{2}(1+\gamma_5) \\
&\psi_1\chi_2 = \overline{\Psi}_1 P_L \Psi_2 \qquad \overline{\chi}_1\overline{\psi}_2 = \overline{\Psi}_1 P_R \Psi_2 \\
&\overline{\chi}_1\overline{\sigma}^\mu\chi_2 = \overline{\Psi}_1\gamma^\mu P_L\Psi_2 \qquad \overline{\psi}_2\overline{\sigma}^\mu\psi_1 = -\overline{\Psi}_1\gamma^\mu P_R\Psi_2 \\
&\overline{\chi}_1\overline{\sigma}^\mu\partial_\mu\chi_2 = \overline{\Psi}_1\gamma^\mu P_L\partial_\mu\Psi_2 \qquad \overline{\psi}_2\overline{\sigma}^\mu\partial_\mu\psi_1 = \overline{\Psi}_1\gamma^\mu P_R\partial_\mu\Psi_2
\end{aligned} \tag{2.3}$$

2.2 Supersymmetry operators

The operator Q transforming bosons into fermions and vice versa has to be an anticommutating spinor object, together with its hermitian conjugate. One can construct supersymmetric theories with more than one unconjugated operator, but without compactified dimensions, these theories are ruled out by not allowing right- and lefthanded particles to be treated in a different way. So, when speaking of SUSY, one usually means "$N = 1$" supersymmetry, meaning the number of unconjugated operators.

Spacetime symmetries using spin-$\frac{1}{2}$ operators in more than two dimensions are heavily restricted by extensions of the "Coleman-Mandula-Theorem" [5], the so-called "Haag-Sohnius-Lopuszanski-Theorem" [6] for the S-Matrix, ruling out any scattering if the operators don't obey the schematic commutation relations

$$\begin{aligned} \{Q, Q^\dagger\} &= 2\sigma^\mu_{\alpha\dot{\alpha}} P_\mu \\ \{Q, Q\} &= \{Q^\dagger, Q^\dagger\} = 0 \\ [P^\mu, Q] &= [P^\mu, Q^\dagger] \end{aligned} \tag{2.4}$$

Thus supersymmetry is the largest allowed symmetry leading to a nontrivial S-matrix. Supersymmetry operators do not only commute with the squared mass operator $(P^\mu)^2$, leading to degenerate masses (at least in an unbroken symmetry), but also with all standard model gauge operators, leading to the exact same quantum numbers of SM particle and its supersymmetric partner.

2.3 Supermultiplets

Irreducible representations of the Susy algebra are called **supermultiplets** and contain - in N=1 SUSY - two particles of same quantum numbers, same amount of *degrees of freedom* [3], but spin differing by $\frac{1}{2}$. The easiest way to construct a multiplet with these properties is with complex spin-0 bosons and spin-$\frac{1}{2}$ fermions, called **chiral**, **matter** or **scalar** multiplet. The next possibility of constructing a multiplet is of spin-$\frac{1}{2}$ fermions and massless spin-1 vector bosons, called **vector** or **gauge** supermultiplet. Excluding gravity, every possible higher supermultiplet can be written as a combination of these two kinds of multiplets, at least if the theory is renormalizeable.

Since gauge bosons transform in the adjoint representation of the gauge group, their partnering fermions must also. But the adjoint representation does not make any difference between left- and right chiral states, and thus the fermions partnering standard model gauge bosons, the so-called **gauginos** (wino, bino...), can not be identified as SM fermions. The latter have to be in chiral multiplets, accompanied by a new boson each, denoted by a praefix "s" (selectrons, squarks, sneutrinos...).

2.3.1 Higgs multiplets

The Higgs sector in supersymmetry needs to be extended in respect to the SM. Since the SM Higgs boson is a spin-0-particle, it should be part of a chiral supermultiplet, accompanied by a spin-$\frac{1}{2}$ fermion, a higgsino. But several issues arise here: one single higgsino spoils the anomaly cancellation of the SM, and in supersymmetric theories, there are two Higgs multiplets with $Y = \pm\frac{1}{2}$ needed to give mass to all the quarks and leptons. Therefore, we have to introduce a second chiral supermultiplet containing a Higgs and a higgsino. The weak isospin states of these particles contain a neutral and charged particle each, so 8 in total (see table "particle content" at the end of the chapter [Fig.2.1.]).

2.3.2 Auxiliary fields

When trying to create supersymmetric lagrangians out of the components of chiral supermultiplets, one encounters a problem: for lagrangians containing chiral supermultiplets, supersymmetry seems only to be valid on-shell, because off-shell, Weyl fermions recieve two more degrees of freedom, spoiling the equivalence to the complex bosons - in SUSY, bosons and fermions are required to have the same number of degrees of freedom. The solution is to add a non-propagating, complex auxiliary field F of mass dimension 2, which affects supersymmetric transformations, but vanishes when going on-shell.

Something similar has to be done for gauge/vector supermultiplets. The degrees of freedom off-shell differ by 1 ins respect to on-shell, thus a real bosonic auxiliary field D has to be added. Auxiliary fields do not have a kinetic term and therefore no propagator.

The components of a chiral or vector supermultiplet together with their auxiliary field are called **component fields**.

2.4 The SUSY group

2.4.1 Supersymmetric translations

Since supersymmetry is a space-time symmetry, it enlarges space-time to *superspace*. It is mathematically convenient to introduce new fermionic spinor "degrees of freedom", θ_α and $\overline{\theta}_{\dot{\alpha}}$, which components are Grassmann numbers with $\theta_i^2 = 0$. The effect of a general SUSY transformation on the new space-time coordinates can

be seen by multipling two general elements $U(x,\theta,\overline{\theta})$ and $U(x,\xi,\overline{\xi})$ of the SUSY group:

$$U(x,\xi,\overline{\xi})U(x,\theta,\overline{\theta}) = e^{ix\cdot P}e^{i\xi\cdot Q}e^{i\overline{\xi}\cdot\overline{Q}}e^{ix\cdot P}e^{i\theta\cdot Q}e^{i\overline{\theta}\cdot\overline{Q}} \tag{2.5}$$

After some simplifications, one then sees that the above product induces the following transformations:

$$\begin{aligned} 0 &\Rightarrow \theta \Rightarrow \theta + \xi \\ 0 &\Rightarrow \overline{\theta} \Rightarrow \overline{\theta} + \overline{\xi} \\ 0 &\Rightarrow x^\mu \Rightarrow x^\mu + a^\mu - i\theta^\alpha(\sigma^\mu)_{\alpha\beta}\xi^{\beta *} \end{aligned} \tag{2.6}$$

2.4.2 Superfields

We will briefly explain the **superfield** formalism, which is a more sophisticated way to calculate supersymmetric vertices [4]. A superfield is a linear representation of the SUSY algebra and an object containing the same information as a set of *component fields* describing either a gauge or chiral multiplet, and called *chiral superfield* or *gauge/vector superfield*. A superfield explicitly depends on location x and at least one of the fermionic parameters - there are two irreducible representations of this algebra, in the sense that a set of components only transform among themselves: they are called right- and lefthanded representations. One can also find an enlarged superfield explicitly depending on both fermionic parameters, but this turns out to be a reducible representation of the algebra. Therefore, it is sufficient to take fields only depending on θ, which are *left* chiral superfields.

If a chiral superfield Φ is expanded in powers of θ, the expansion has to end after second order, since $\theta_1^2 = \theta_2^2$. The expansion coefficients of this left chiral superfield can be interpreted as the component fields ψ, a left chiral field, its partner-boson ϕ, and the auxiliary field F.

$$\begin{aligned} \Phi(y,\theta) &= \phi(y) + \theta\cdot\chi(y) + \frac{1}{2}\theta\cdot\theta F(y) \\ y^\mu &= x^\mu + i\theta\sigma^\mu\theta \end{aligned} \tag{2.7}$$

A chiral superfield always has the mass dimension of its lower spin component field, and superfields in general offer a compact formulation of interaction terms, so-called superpotentials and more.

2.4.3 SUSY transformations and algebra

The group algebra is defined by a series of (anti)commutation relations of the supersymmetric operators Q and differential operators D inducing the same transformations and obeying the same relations. Barred operators represent, as in [4], hermitian conjugates of the operators and fields.

$$\begin{aligned} &\{Q_\alpha, \bar{Q}_{\dot{\alpha}}\} = 2\sigma^\mu_{\alpha\dot{\alpha}} P_\mu \\ &\{Q_\alpha, Q_\beta\} = \{\bar{Q}_{\dot{\alpha}}, \bar{Q}_{\dot{\beta}}\} = [P_\mu, Q_\alpha] = [P_\mu, \bar{Q}_{\bar{\alpha}}] = [P_\mu, P_\nu] = 0 \\ &D_\alpha = \frac{\partial}{\partial\theta^\alpha} - i\sigma^\mu_{\alpha\dot{\alpha}}\overline{\theta}^{\dot{\alpha}}\partial_\mu \qquad \overline{D}_{\dot{\alpha}} = -\frac{\partial}{\partial\theta^{\dot{\alpha}}} + i\theta^\alpha\sigma^\mu_{\alpha\dot{\alpha}}\partial_\mu \end{aligned} \tag{2.8}$$

Futhermore, any supersymmetric langrangian needs to be invariant under the following supersymmetry transformations of the fields. In this nomenclature, A^a_μ are SM vector bosons, λ^a_α denote gaugino fields, D^a the auxiliary field of vector supermultiplets, and $F^{\mu\nu}$ is the field tensor of the corresponding gauge group.

$$\begin{aligned} \delta_\theta\phi &= \sqrt{2}\theta\psi \\ \delta_\theta\psi &= i\sqrt{2}\sigma^\mu\overline{\theta}\partial_\mu\phi + \sqrt{2}\theta F \\ \delta_\theta F &= i\sqrt{2}\overline{\theta}\overline{\sigma}^\mu\partial_\mu\psi \\ \delta_\theta A^a_\mu &= \overline{\theta}\overline{\sigma}_\mu\lambda^a + \lambda^{\dagger a}\overline{\sigma}_\mu\theta \\ \delta_\theta\lambda^a_\alpha &= \frac{i}{2}(\sigma^\mu\overline{\sigma}^\nu\theta)_\alpha F^a_{\mu\nu} + \theta_\alpha D^a \\ \delta_\theta D^a &= i(\overline{\theta}\overline{\sigma}^\mu D_\mu\lambda^a - D_\mu\lambda^{\dagger a}\overline{\sigma}^\mu\theta) \end{aligned} \tag{2.9}$$

2.5 Supersymmetric Lagrangian

Before we start, there is one serious notational issue here when looking at interaction terms regarding gauginos. Neutral gauginos mix, together with neutral higgsinos, to physical particles called **neutralinos** $\tilde{\chi}^0_i$, charged gauginos and higgsinos to

charginos $\tilde{\chi}_i^{\pm}$. The definition of gaugino/higgsino gauge eigenstates is often taken to be

$$\psi_C = \begin{pmatrix} -i\tilde{\omega}^+ \\ \tilde{h}_2^+ \\ -i\tilde{\omega}^- \\ \tilde{h}_1^- \end{pmatrix} \qquad \psi_N = \begin{pmatrix} -i\tilde{b} \\ -i\tilde{\omega} \\ \tilde{h}_1^0 \\ \tilde{h}_2^0 \end{pmatrix} \tag{2.10}$$

with an additional complex factor ***-i*** for electroweak gauginos. Some SUSY introduction scripts like [4] do this without telling the reader and introduce gauginos which are already multiplied by this complex factor. Thus, there is a danger that unaware readers might do this definition a second time when trying to compare results with another script, spoiling the results. To avoid confusion when comparing to [3] and [4],we write redefined gauginos using capital letters:

$$\psi_C = \begin{pmatrix} \tilde{W}^+ \\ \tilde{H}_2^+ \\ \tilde{W}^- \\ \tilde{H}_1^- \end{pmatrix} = \begin{pmatrix} -i\tilde{\omega}^+ \\ \tilde{h}_2^+ \\ -i\tilde{\omega}^- \\ \tilde{h}_1^- \end{pmatrix} \qquad \psi_N = \begin{pmatrix} \tilde{B} \\ \tilde{W} \\ \tilde{H}_1^0 \\ \tilde{H}_2^0 \end{pmatrix} = \begin{pmatrix} -i\tilde{b} \\ -i\tilde{\omega} \\ \tilde{h}_1^0 \\ \tilde{h}_2^0 \end{pmatrix} \tag{2.11}$$

these fields have to be rotated into mass eigenstates to describe physical particles.

2.5.1 Superpotential and the MSSM

The main input defining the exact SUSY model we are working with is the mentioned "superpotential". We are working within the "**MSSM**", the "minimal supersymmetric standard model", using the following superpotential. It is **very** important to check the conventions of this potential, since it is defined slightly different in the various scripts and papers. We adopt the convention of "SUSY Les Houches accord" [7, 8], a paper trying to set a standard and common interface for programs/tools calculating MSSM spectra. The program used lateron, "SPheno" [9], also uses these conventions.

$$\mathcal{W}_{MSSM} = \epsilon_{ab}[(Y_E)_{ij} H_i^a \cdot L_i^b \overline{E}_j + (Y_D)_{ij} H_1^a \cdot Q_i^b \overline{D}_j + (Y_u)_{ij} H_2^b \cdot Q_i^a \overline{U}_j - \mu H_1^a \cdot H_2^b] \tag{2.12}$$

Here, unbarred superfields transform left-handed, barred superfields right-handed [10]. Left-handed superfields also include right-handed antiparticle fields. It is

important to see that bars over superfields are part of their name and tell something about their transformation behaviour, while bars and conjugations over particle fields denote *antiparticles*.

ϵ_{ab} is the antisymmetric symbol used to create SU(2) invariant products, with $\epsilon_{12} = \epsilon^{12} = 1$ in our convention. Y_I are the Yukawa matrices, sometimes transposed in other definitions. Furthermore, $H_1 = H_d$ and $H_2 = H_u$, here expressed in numbers to write the Higgs superfields with ij-indices. μ is the only "new" parameter in *unbroken* SUSY (although it appears in the SM in another context) and describes the inter-Higgs coupling.

In the table at the end of this chapter [Fig.2.1], you can look up the particle content of the MSSM written in superfields. The table was taken out of ref. [10], whose conventions on superfields are used in this work.

2.5.2 Complete unbroken lagrangian

The complete $\mathcal{L}$ of SUSY is very complicated (especially in the broken symmetry) and can be looked up in [10], for example. The author used the superfield formalism to calculate all terms, while we will try the task of calculating the relevant vertices without it. We will split $\mathcal{L}$ in parts, according to the type of multiplets interacting.

$$\begin{aligned}\mathcal{L}_{chiral} = &(D_\mu\phi_i)^\dagger D^\mu\phi_i + \psi_i^\dagger i\overline{\sigma}^\mu D_\mu\psi_i + F_i^\dagger F_i + [\frac{\partial\mathcal{W}}{\partial\phi_i}F_i - \frac{1}{2}\frac{\partial^2\mathcal{W}}{\partial\phi_i\phi_j}\psi_i\cdot\psi_j + h.c.] \\ &- \frac{1}{4}F^\alpha_{\mu\nu}F^{\mu\nu\alpha} + i\lambda^{\alpha\dagger}\overline{\sigma}^\mu(D_\mu\lambda)^\alpha + \frac{1}{2}D^\alpha D^\alpha \\ &- \sqrt{2}g[(\phi_i^\dagger T^\alpha\psi_i)\cdot\lambda^\alpha + \lambda^{\alpha\dagger}\cdot(\psi_i^\dagger T^\alpha\phi_i)] - g(\phi_i^\dagger T^\alpha\phi_i)D^\alpha\end{aligned} \tag{2.13}$$

This first part mainly includes the interaction of squarks with gauge bosons and Higgs particles, and involves the important quantity $\mathcal{W}$, the **superpotential**, which ultimatively defines the supersymmetric model used (see section "superpotential"), and is used here in a form where all fermionic parts are equal to zero. D^μ is a covariant derivative with $D^\mu X_j = \partial^\mu X_j + igA^\alpha_\mu(T^\alpha X)_j$.

λ in the second line is representing a gaugino **already redefined** (see above),
$F^{\mu\nu}$ the field tensor of the corresponding gauge group, and
$D_\mu\lambda^\alpha = \partial_\mu\lambda^\alpha - gf^{\alpha\beta\gamma}W^\beta_\mu\lambda^\gamma$ a covariant derivative, where $f^{\alpha\beta\gamma}$ are the structure constants of the gauge group.

The third line governs the decays of squarks into quarks and gauginos. T^α are the corresponding group generators. If the supermultiplets in the first interaction are the two Higgs multiplets, higgsino-gaugino mixing will occur as a consequence of EWSB (mentioned above, "neutralinos/charginos").

2.5.3 The scalar potential

In the above, the auxiliary fields can be eliminated. From the Euler-Lagrange equations for F [4] we get $F_i^\dagger = -\frac{\partial \mathcal{W}}{\partial \phi_i}$, for D we get $D^\alpha = g\sum_i(\phi_i^\dagger T^\alpha \phi_i)$. Inserting these identities in the lagrangian, we can extract the scalar potential $\mathcal{V}$ in $\mathcal{L} = \mathcal{T} - \mathcal{V}$ as

$$\mathcal{V}(\phi_i, \phi_i^\dagger) = \sum_i \|\frac{\partial \mathcal{W}}{\partial \phi_i}\|^2 + \frac{1}{2}\sum_G \sum_\alpha \sum_{i,j} g_G^2(\phi_i^\dagger T_G^\alpha \phi_i)(\phi_j^\dagger T_G^\alpha \phi_j) \tag{2.14}$$

The first term is called "F-Term", the second "D-Term".

2.5.4 Soft SUSY breaking

Since particles and their SUSY partners are degenerate in mass, it is obvious SUSY has to be broken. There are numerous, more or less convincing approaches to the exact mechanism, but as we simply don't know what causes the breaking, it is the most useful way to parameterize it by adding explicit SUSY-breaking terms to the lagrangian. For the MSSM, the common terms used are

$$\mathcal{L}_{soft} = -\frac{1}{2}M_a\lambda^a\lambda^a + m_i\phi_i\phi_i^\dagger + \frac{1}{6}a^{ijk}\phi_i\phi_j\phi_k + \frac{1}{2}b^{ij}\phi_i\phi_j + c.c. \tag{2.15}$$

i.e. gaugino and squared scalar mass terms as well as three-scalar-couplings. There are other terms/couplings, like so-called "tadpole"-couplings, but for the specific case of the MSSM, they aren't allowed due to the lack of a gauge singlet. It is easy to see that $\mathcal{L}_{soft}$ is breaking SUSY, since it involves terms with only one part of each supermultiplet. Gaugino and scalar masses are always allowed when this $\mathcal{L}_{soft}$ is used, no matter if their superpartners are masseless. Applying the above to the MSSM, we explicitly get

$$\begin{aligned}\mathcal{L}_{softMSSM} = &-\frac{1}{2}(M_1\tilde{B}\tilde{B} + M_2\tilde{W}\tilde{W} + M_3\tilde{g}\tilde{g} + h.c) \\ &- \epsilon_{ab}\sum_{ij}[(T_e)_{ij}H_1^a\overline{L}_{iL}^b\tilde{e}_{jR}^* + (T_D)_{ij}H_1^a\overline{Q}_{iL}^b\tilde{d}_{jR}^* \\ &\qquad +(T_U)_{ij}H_2^b\overline{Q}_{iL}^a\tilde{u}_{jR}^*] + h.c. \\ &- \overline{Q}_{iLa}^*(m_{\overline{Q}}^2)_{ij}\overline{Q}_{jL}^a - \overline{L}_{iLa}^*(m_{\overline{L}}^2)_{ij}\overline{L}_{jL}^a \\ &- \overline{u}_{iR}(m_{\overline{u}}^2)_{ij}\overline{u}_{jR}^* - \overline{d}_{iR}(m_{\overline{d}}^2)_{ij}\overline{d}_{jR}^* - \overline{e}_{iR}(m_{\overline{e}}^2)_{ij}\overline{e}_{jR}^* \\ &- m_{H1}^2H_{1a}^*H_1^a - m_{H2}^2H_{2a}^*H_2^a + (m_3^2\epsilon_{ab}H_1^aH_2^b + h.c.)\end{aligned} \tag{2.16}$$

This notation is according to "SUSY Les Houches Accord" SLHA [7,8]. The gaugino masses M_1 to M_3, the explicit Higgs masses m_{H1}^2 and m_{H2}^2, as well as the Higgs mixing mass parameter m_3^2 are scalars (in this notation, be careful about confusing m_3 and M_3), but the mass terms for sleptons and squarks are symmetric matrices with theoretically unconstrained elements. Unbroken SUSY only provides a new context for the standard model μ-parameter, but the soft breaking and Higgs sectors consist of over 100 of new parameters, and constraining them is a real challenge. This work will try to constrain the off-diagonal elements of the breaking matrices in the squark mass matrices by looking at rare $b \to s$ decays, since they can be responsible for much too large CP-violating and flavor violation effects and huge regions of parameter space are excluded by phenomenology. The scenario in which flavor violation not only resides in the entries of the Yukawa matrices (minimal flavor violation), but also in arbitary off-diagonal entries of the squark mass matrices, is called next-to-minimal flavor violation (nMFV)

Instead of m_3^2, usually the pseudoscalar Higgs parameter $m_A^2 = \frac{m_3^2}{\sin\beta\cos\beta}$ is used (see below). Here, β is a higgs mixing angle, and $tan\beta$ describes the ratio of the Higgs VEVs). If you ever see matrices A_{ij}, they are usually used for a decomposition of the trilinear coupling matrices T_{ij}, together with the corresponding Yukawa matrices. In order to construct the A_{ij}-matrices, one has to assume that the trilinear couplings are proportinal to the Yukawa couplings - a simplification we won't work with here.

$$A_{ij} = \frac{T_{ij}}{Y_{ij}} \tag{2.17}$$

2.6 Higgs sector

2.6.1 Higgs potential

Due to having two Higgs multiplets, this sector is much more complicated than in the SM. We will restrict ourselves mainly to the results of the discussions in [3], [4] etc. - first of all, EWSB can't take place in an unbroken MSSM. The complete Higgs potential, consisting of F-, D-, and SUSY-breaking terms looks like

$$\begin{aligned}\mathcal{V}_{Higgs} &= (|\mu|^2 + m_{H2}^2)(\left|H_2^+\right|^2 + \left|H_2^0\right|^2) + (|\mu|^2 + m_{H1}^2)(\left|H_1^0\right|^2 + \left|H_1^-\right|^2) \\ &+ [\frac{\sin 2\beta m_3^2}{\sin\beta\cos\beta}(H_2^+ H_1^- - H_2^0 H_1^0) + h.c.] \\ &+ \frac{g^2 + g'^2}{8}(\left|H_2^+\right|^2 + \left|H_2^0\right|^2 - \left|H_1^0\right|^2 - \left|H_1^-\right|^2)^2 \\ &+ \frac{g^2}{2}\left|H_2^+ H_1^{0\dagger} + H_2^0 H_1^{-\dagger}\right|^2\end{aligned} \tag{2.18}$$

A minimum for this potential can be found [3], although only for a restricted region of parameter space: a small $m_{A^0}^2$, a small $|\mu|$ and a large negative $m_{H_2}^2$ help to archieve the condition for a minimum in the potential. If EWSB takes place, both neutral Higgs aquire a VEV:

$$\nu^2 = \nu_1^2 + \nu_2^2 = \frac{4M_W^2}{g^2} \approx 250GeV \qquad \tan(\beta) = \frac{\nu_2}{\nu_1} \tag{2.19}$$

ν being the SM Higgs VEV and $\tan(\beta)$ a new parameter needed for the description of the Higgs sector, which is theoretically unbounded for $\beta \in [0, \frac{\pi}{2}]$.

2.6.2 Physical Higgs particles

The Higgs multiplets can be split into parts by

$$\begin{aligned}\begin{pmatrix} H_1^0 \\ H_1^- \end{pmatrix} &= \begin{pmatrix} \frac{1}{\sqrt{2}}(\nu_1 + i\chi_1 + \phi_1) \\ \phi_1^- \end{pmatrix} \\ \begin{pmatrix} H_2^+ \\ H_2^0 \end{pmatrix} &= \begin{pmatrix} \phi_2^+ \\ \frac{1}{\sqrt{2}}(\nu_2 + i\chi_2 + \phi_2) \end{pmatrix}\end{aligned} \tag{2.20}$$

After EWSB, the imaginary, neutral parts create the longitudinal mode for the Z-boson and a new particle, the pseudoscalar (CP-odd) neutral Higgs field A^0, with mixing angle β.

$$\begin{pmatrix} G^0 \\ A^0 \end{pmatrix} = \begin{pmatrix} \cos\beta & \sin\beta \\ -\sin\beta & \cos\beta \end{pmatrix} \begin{pmatrix} \chi_1 \\ \chi_2 \end{pmatrix} \tag{2.21}$$

The charged parts of the multiplets mix to physical charged Higgs bosons with equal mass and longitudinal modes for the $W^{\pm}$-bosons, again with mixing angle β and a mass $m_{H^{\pm}} = \sqrt{m_W^2 + m_{A^0}^2}$.

$$\begin{pmatrix} G^{\pm} \\ H^{\pm} \end{pmatrix} = \begin{pmatrix} \cos\beta & \sin\beta \\ -\sin\beta & \cos\beta \end{pmatrix} \begin{pmatrix} \phi_1^{\pm} \\ \phi_2^{\pm} \end{pmatrix} \tag{2.22}$$

Last but not least, the neutral scalar parts ϕ_i mix to two physical particles with different mass, the lighter one usually referred to as "little Higgs" h^0.

$$\begin{pmatrix} H^0 \\ h^0 \end{pmatrix} = \begin{pmatrix} \cos\alpha & \sin\alpha \\ -\sin\alpha & \cos\alpha \end{pmatrix} \begin{pmatrix} \phi_1 \\ \phi_2 \end{pmatrix} \tag{2.23}$$

$$\begin{aligned} m_{h^0}^2 &= \frac{1}{2}\sqrt{m_{A^0}^2 + m_Z^2 - [(m_{A^0}^2 + m_Z^2)^2 - 4m_{A^0}^2 m_Z^2 \cos^2 2\beta]} \\ m_{H^0}^2 &= \frac{1}{2}\sqrt{m_{A^0}^2 + m_Z^2 + [(m_{A^0}^2 + m_Z^2)^2 - 4m_{A^0}^2 m_Z^2 \cos^2 2\beta]} \end{aligned} \tag{2.24}$$

It is worth mentioning that according to [11], the little Higgs mass has to be smaller than 140GeV and thus is an important test for the validity of the MSSM. This concludes our review of the Higgs sector, for details check [3, 4, 10].

2.7 Mass eigenstates of SUSY particles

2.7.1 Sfermion mixing

For this work, the physical squark eigenstates are obviously of great importance. Sfermions form the largest collection of new particles in the MSSM, and it is crucial

to realize that we need a new boson for *each* chirality of the corresponding SM fermions, for example $\tilde{e}_L$ and $\tilde{e}_R$. These are different particles without chirality, which carry "L" and "R" only in their names. The SUSY breaking terms allow interfamily mixing of particles with same color and charge [4], so we get (6x6) mixing matrices for u-squarks, d-squarks and sleptons, as well as a (3x3) mass matrix for sneutrinos. We will only discuss the squark mixing sector here. It can be seen that this sector allows new sources of flavor violation and even FCNCs at tree-level, in contrast to the SM.

We use the so-called super-CKM basis, in which all fields have been rotated in a way the Yukawa matrices are diagonal. The rotation matrices are, as in the SM, defined

$$\begin{aligned} q^0_{L_j} &= (U_{q_L})_{jk} q_{L_k} & \overline{q}^0_{L_j} &= \overline{q}_{L_k} (U^\dagger_{q_L})_{kj} \\ q^0_{R_j} &= (U_{q_R})_{jk} q_{R_k} & \overline{q}^0_{R_j} &= \overline{q}_{R_k} (U^\dagger_{q_R})_{kj} \\ U^\dagger_{uL} U_{dL} &= V_{CKM} \end{aligned} \tag{2.25}$$

The mass matrices are then defined as

$$\mathcal{L}_{\tilde{q}M} = -\Phi^\dagger_u \mathcal{M}^2_{\tilde{u}} \Phi_u - \Phi^\dagger_d \mathcal{M}^2_{\tilde{d}} \Phi_d \tag{2.26}$$

with $\Phi_u = (\tilde{u}_L, \tilde{c}_L, \tilde{t}_L, \tilde{u}_R, \tilde{c}_R, \tilde{t}_R)$ and $\Phi_d = (\tilde{d}_L, \tilde{s}_L, \tilde{b}_L, \tilde{d}_R, \tilde{s}_R, \tilde{b}_R)$.

Collecting all these terms (see [10] for example), we obtain mass matrices of the form

$$\mathcal{M}^2_{\tilde{u}} = \begin{pmatrix} V^\dagger_{CKM} \hat{m}^2_{\tilde{Q}} V_{CKM} + m^2_u + D_{uLL} & \frac{\nu_2}{\sqrt{2}} \hat{T}^\dagger_U - \mu m_u \cot\beta \\ \frac{\nu_2}{\sqrt{2}} T_U - \mu^* m_u \cot\beta & \hat{m}^2_u + m_u + D_{uRR} \end{pmatrix} \tag{2.27}$$

$$\mathcal{M}^2_{\tilde{d}} = \begin{pmatrix} \hat{m}^2_{\tilde{Q}} + m^2_d + D_{dLL} & \frac{\nu_1}{\sqrt{2}} \hat{T}^\dagger_D - \mu m_d \tan\beta \\ \frac{\nu_1}{\sqrt{2}} T_D - \mu^* m_d \tan\beta & \hat{m}^2_d + m_d + D_{dRR} \end{pmatrix} \tag{2.28}$$

$$
\begin{aligned}
D_{uLL} &= \cos(2\beta)m_Z^2[\frac{1}{2} - \frac{2}{3}\sin^2(\theta_W)]\mathbf{1} \\
D_{uRR} &= -\frac{2}{3}\sin^2(\theta_W)\cos(2\beta)m_Z^2\mathbf{1} \\
D_{dLL} &= \cos(2\beta)m_Z^2[-\frac{1}{2} + \frac{1}{3}\sin^2(\theta_W)]\mathbf{1} \\
D_{dRR} &= +\frac{1}{3}\sin^2(\theta_W)\cos(2\beta)m_Z^2\mathbf{1}
\end{aligned}
\tag{2.29}
$$

$$
\begin{gathered}
\hat{m}_{\tilde{Q}}^2 \equiv U_{d_L}^\dagger m_{\tilde{Q}}^2 U_{d_L} \quad \hat{m}_{\tilde{u}}^2 \equiv U_{u_R}^\dagger m_{\tilde{u}}^{2^T} U_{u_R} \quad \hat{m}_{\tilde{d}}^2 \equiv U_{d_R}^\dagger m_{\tilde{d}}^{2^T} U_{d_R} \\
\hat{T}_U = U_{u_R}^\dagger T_U^T U_{u_L} \quad \hat{T}_D = U_{d_R}^\dagger T_D^T U_{d_L}
\end{gathered}
\tag{2.30}
$$

The 6x6 mass matrices are now diagonalised using Mathematica, the four resulting 6x3 mixing matrices $R_{qL,qR}$ are defined by

$$
\begin{aligned}
\tilde{q}_{Lg} &= (U_{qL})_{gf}(R_{qL})_{fi}\tilde{q}_i \qquad & \tilde{q}_{Lg}^* &= \tilde{q}_i^*(R_{qL}^\dagger)_{if}(U_{uL}^\dagger)_{fg} \\
\tilde{q}_{Rg} &= (U_{qR})_{gf}(R_{qR})_{fi}\tilde{q}_i \qquad & \tilde{q}_{Rg}^* &= \tilde{q}_i^*(R_{qR}^\dagger)_{if}(U_{uR}^\dagger)_{fg}
\end{aligned}
\tag{2.31}
$$

The mass eigenstates $\tilde{q}_i$ are ordered by mass with $m_{q_i} \leq m_{q_j}, i \leq j$.

2.7.2 Neutralino mixing

As mentioned above, interactions between chiral supermultiplets and gauginos of the form

$$
\mathcal{L}_{\phi\psi\lambda} = -\sqrt{2}g[(\phi_i^\dagger T^\alpha \psi_i)\cdot\lambda^\alpha] \tag{2.32}
$$

lead to a mixing between higgsinos and gauginos, if the chiral supermultiplet consists of Higgs particles and its boson can acquire a VEV in consequence of EWSB. The resulting eigenstates of the neutral higgsinos and the neutral gauginos, namely wino $\tilde{W}^0$ and bino $\tilde{B}$, are four physical particles called "neutralinos" $\tilde{\chi}_i$, again ordered in mass from i=1 to i=4. The lightest one of these is a candidate for

non-baryonic dark matter. In the following neutralino mass matrix, there are contributions from the breaking masses of $\tilde{W}$ and $\tilde{B}$ and the Higgs mixing term in the superpotential:

$$M_N = \begin{pmatrix} M_1 & 0 & -c_\beta s_W m_Z & s_\beta s_W m_Z \\ 0 & M_2 & c_\beta c_W m_Z & -s_\beta c_W m_Z \\ -c_\beta s_W m_Z & c_\beta c_W m_Z & 0 & -\mu \\ s_\beta s_W m_Z & -s_\beta c_W m_Z & -\mu & 0 \end{pmatrix} \tag{2.33}$$

This mass matrix is diagonalized and the mixing matrix N_{ij} is defined as follows:

$$\begin{aligned} \tilde{B} &= N_{1j}\tilde{C}^0_j & \overline{\tilde{B}} &= N^*_{1j}\overline{\tilde{C}}^0_j \\ \tilde{W}_3 &= N_{2j}\tilde{C}^0_j & \overline{\tilde{W}}_3 &= N^*_{2j}\overline{\tilde{C}}^0_j \\ \tilde{H}^0_1 &= N_{3j}\tilde{C}^0_j & \overline{\tilde{H}}^0_1 &= N^*_{3j}\overline{\tilde{C}}^0_j \\ \tilde{H}^0_2 &= N_{4j}\tilde{C}^0_j & \overline{\tilde{H}}^0_2 &= N^*_{4j}\overline{\tilde{C}}^0_j \end{aligned} \tag{2.34}$$

Please note that the neutralino Weyl spinors are denoted $\tilde{C}^0_i$ here, as we use $\tilde{\chi}^0_i$ for Majorana spinors only.

2.7.3 Chargino mixing

In a similar way, the charged higgsinos and gauginos mix to **charginos**. Of course, only particles of same charge quantum numbers can mix, so we get two different kinds of charginos $\tilde{\chi}^\pm$, one for each pair of gaugino/higgsino sharing the same charge. The diagonalisation is slightly more complicated - we can write the mass terms for the charged particles in this way:

$$-\frac{1}{2}[(\ \tilde{W}^+,\ \ \tilde{H}^+_2\ )\,\mathbf{X}^T \cdot \begin{pmatrix} \tilde{W}^- \\ \tilde{H}^-_1 \end{pmatrix} + (\ \tilde{W}^-,\ \ \tilde{H}^-_1\ )\,\mathbf{X} \cdot \begin{pmatrix} \tilde{W}^+ \\ \tilde{H}^+_2 \end{pmatrix}] \tag{2.35}$$

Collecting terms (same as in the neutralino case),
we obtain

$$\mathbf{X} = \begin{pmatrix} M_2 & \sqrt{2}s_\beta m_W \\ \sqrt{2}c_\beta m_W & \mu \end{pmatrix} \tag{2.36}$$

As we can see, $\mathbf{X}$ is not necessarily symmetric, which implies the need of *two* mixing matrices, V and U. We used matrices called U_{index} for the quark rotations as well, but as they cancel out in the lagrangian or are compactified to V_{CKM}, this shouldn't be too confusing. The replacements

$$\begin{aligned} \tilde{W}^+ &= V_{1j}^\dagger \tilde{C}_j^+ & \overline{\tilde{W}^+} &= \overline{\tilde{C}^+}_j V_{j1} \\ \tilde{W}^- &= U_{1j}^\dagger \tilde{C}_j^- & \overline{\tilde{W}^-} &= \overline{\tilde{C}^-}_j U_{j1} \\ \tilde{H}_2^+ &= V_{2j}^\dagger \tilde{C}_j^+ & \overline{\tilde{H}_2^+} &= \overline{\tilde{C}^+}_j V_{j2} \\ \tilde{H}_1^- &= U_{2j}^\dagger \tilde{C}_j^- & \overline{\tilde{H}_1^-} &= \overline{\tilde{C}^-}_j U_{j2} \end{aligned} \tag{2.37}$$

reveal the chargino Weyl spinors in mass eigenstates, $\tilde{C}_j^\pm$. V und U diagonalise the mass matrices:

$$U^* X V^{-1} = \begin{pmatrix} m_{\tilde{\chi}_1^\pm} & 0 \\ 0 & m_{\tilde{\chi}_2^\pm} \end{pmatrix} \tag{2.38}$$

$$V X^\dagger U^T = \begin{pmatrix} m_{\tilde{\chi}_1^\pm} & 0 \\ 0 & m_{\tilde{\chi}_2^\pm} \end{pmatrix} \tag{2.39}$$

2.7.4 Gluinos

Gluinos can't mix, since they are octet fermions. They are massive, and decays of squarks into gluinos are, if kinematically allowed, dominating because the relevant interaction vertices have QCD strength.

Φ	φ	ψ	F	Y	T_3	Q	R
L^j	$\begin{pmatrix}\tilde{\nu}\\ \tilde{e}_L\end{pmatrix}$	$\begin{pmatrix}\nu\\ e_L\end{pmatrix}$	$\begin{pmatrix}F_\nu\\ F_{eL}\end{pmatrix}$	$-\frac{1}{2}$	$\begin{pmatrix}\frac{1}{2}\\ -\frac{1}{2}\end{pmatrix}$	$\begin{pmatrix}0\\ -1\end{pmatrix}$	-1
$\bar{L}^j$	$(\tilde{\nu}^*, \tilde{e}_L^*)$	$(\nu, \bar{e}_L)$	(F_ν^*, F_{eL}^*)	$\frac{1}{2}$	$(-\frac{1}{2}, \frac{1}{2})$	$(0, 1)$	-1
E_R	$\tilde{e}_R^*$	$\bar{e}_R$	F_{eR}^*	1	0	1	-1
$\bar{E}_R$	$\tilde{e}_R$	e_R	F_{eR}	-1	0	-1	-1
Q^j	$\begin{pmatrix}\tilde{u}_L\\ \tilde{d}_L\end{pmatrix}$	$\begin{pmatrix}u_L\\ d_L\end{pmatrix}$	$\begin{pmatrix}F_{uL}\\ F_{dL}\end{pmatrix}$	$\frac{1}{6}$	$\begin{pmatrix}\frac{1}{2}\\ -\frac{1}{2}\end{pmatrix}$	$\begin{pmatrix}\frac{2}{3}\\ -\frac{1}{3}\end{pmatrix}$	-1
$\bar{Q}^j$	$(\tilde{u}_L^*, \tilde{d}_L^*)$	$(\bar{u}_L, \bar{d}_L)$	(F_{uL}^*, F_{dL}^*)	$-\frac{1}{6}$	$(-\frac{1}{2}, \frac{1}{2})$	$(-\frac{2}{3}, \frac{1}{3})$	-1
U	$\tilde{u}_R^*$	$\bar{u}_R$	F_{uR}^*	$-\frac{2}{3}$	0	$-\frac{2}{3}$	-1
$\bar{U}$	$\tilde{u}_R$	u_R	F_{uR}	$\frac{2}{3}$	0	$\frac{2}{3}$	-1
D	$\tilde{d}_R^*$	$\bar{d}_R$	F_{dR}^*	$\frac{1}{3}$	0	$\frac{1}{3}$	-1
$\bar{D}$	$\tilde{d}_R$	d_R	F_{dR}	$-\frac{1}{3}$	0	$-\frac{1}{3}$	-1
H_1^j	${h_1}^j$	$\tilde{h}_1{}^j$	F_1^j	$-\frac{1}{2}$	$\begin{pmatrix}\frac{1}{2}\\ -\frac{1}{2}\end{pmatrix}$	$\begin{pmatrix}0\\ -1\end{pmatrix}$	1
$\bar{H}_1{}^j$	h_1^{*j}	$\tilde{\bar{h}}_1{}^j$	F_1^{*j}	$\frac{1}{2}$	$(-\frac{1}{2}, \frac{1}{2})$	$(0, 1)$	1
H_2^j	${h_2}^j$	$\tilde{h}_2{}^j$	F_2^j	$\frac{1}{2}$	$\begin{pmatrix}\frac{1}{2}\\ -\frac{1}{2}\end{pmatrix}$	$\begin{pmatrix}1\\ 0\end{pmatrix}$	1
$\bar{H}_2{}^j$	h_2^{*j}	$\tilde{\bar{h}}_2{}^j$	F_2^{*j}	$-\frac{1}{2}$	$(-\frac{1}{2}, \frac{1}{2})$	$(-1, 0)$	1

V	v_μ	λ	$\bar{\lambda}$	D	**Generator**	**Gauge group**
B	B_μ	$\tilde{b}$	$\tilde{\bar{b}}$	D_B	$\mathbf{Y} = \frac{1}{2}y$	$U(1)_Y$
W^a	W_μ^a	$\tilde{w}^a$	$\tilde{\bar{w}}^a$	D_W^a	$\mathbf{T}^a = \frac{1}{2}\tau^a$	$SU(2)_I$
G^b	G_μ^b	$\tilde{g}^b$	$\tilde{\bar{g}}^b$	D_G^b	$\mathbf{F}^b = \frac{1}{2}\lambda^b$	$SU(3)_{color}$

Figure 2.1: MSSM particle content and auxiliary fields, taken from [10]

3 B-Physics

The sector of B meson and Kaon physics has been very successful in testing the SM and its possible extensions. Since the b quark was revealed in 1977, B physics is a relatively new discipline. Interesting aspects are low energy observables, meaning branching ratios of rare to very rare decays, and meson mixing. Most extensions of the SM would affect these observables as well as their flavor and CP violating consequences. We can learn alot about what is possible in new theories by looking at experimental data constraining these effects. In this work, we use rare b $\rightarrow$ s transitions and B meson mixing to learn about the parameter space of SUSY and to examine squark/gluino decays in the allowed region.

This section will give a very brief introduction into the observables needed and an idea of the underlying theory. But since we are not interested in very precise experimental and theoretical bounds, but try to get a general overview about the impact of rare decay constraints in the nMFV MSSM, the reader will have to look in other excellent reports (like [12]) for details.

3.1 Penguin diagrams

The rare flavor violating decays in the B and K sector have contributions from so-called "penguin" diagrams: as we know, FCNC processes in the SM are forbidden at tree level, and the simplest loop inducing flavor violation looks like [Fig.3.1.] [13]:

Figure 3.1: self-energy graph, the simplest off-shell flavor violating transition

In this self-energy graph, the V_{CKM} is involved into the b → s transition via the interaction with the top quarks and leads to flavor violation. Of course, on-shell it isn't complete, because an additional particle has to be emitted to get 4-momentum-conservation straight. Diagrams of this kind were named "penguins" when the loop emits a particle (see below), for reasons which will become apparent lateron. For FCNC b decays, penguins are of critical importance, since there are large contributions from new physics, and penguins are theoretically easy to calculate. The penguin loops involve heavy particles and and are therefore sensitive to new, very heavy particles predicted by NP theories.

3.1.1 SM penguins

Electromagnetic penguins

For b→ $s\gamma$, the penguin loop emits a real, hard photon, which provides an excellent experimental signal. The decay can be used to probe the CKM ($|\frac{V_{td}}{V_{ts}}|$) and is one of the most important and researched transitions [Fig.3.2].

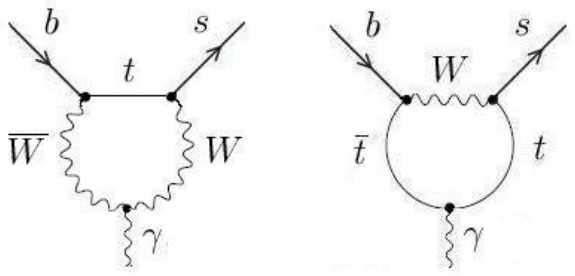

Figure 3.2: electromagnetic penguins (radiating a real photon) [14]

Electroweak penguins

Instead of a real photon, the penguin loop can also produce virtual photons and Z bosons which decay into pairs of leptons, thus governing the process $b \to sl^+l^-$, together with electroweak box diagrams [Fig.3.3]. These diagrams are important for the $b \to s\overline{\nu}\nu$ transition as well - excluding the virtual photon diagram, since neutrinos don't couple to photons.

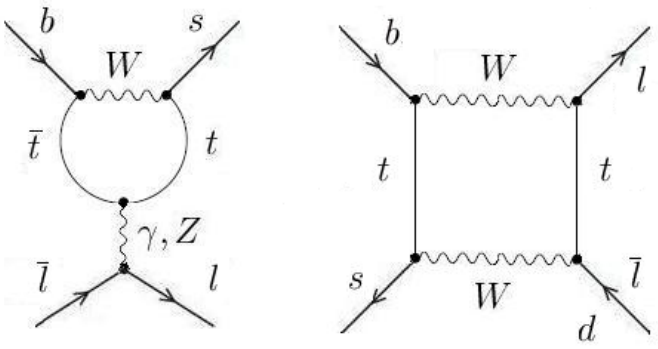

Figure 3.3: Examples for electroweak penguins and box diagrams [14]

Annihilation penguins

For $B_q \rightarrow l^+l^-$ decays, like $B_s \rightarrow \mu^+\mu^-$ used in this work, there is a similar set of penguins annihilating both particles of the meson to either photons or a pair of leptons [Fig.3.4]. Penguins with internal photons do not contribute to the lepton pair generation, because a lepton-antilepton pair with zero angular momentum has C = 1, while a photon has C = -1.

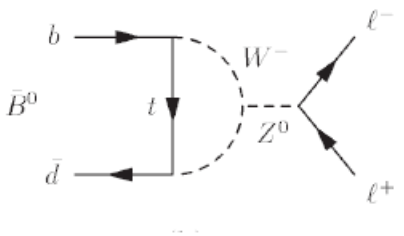

Figure 3.4: Examples for annihilation penguins [13]

There is also a box diagram with two W bosons contributing to this decay, yet it is supressed in respect to the penguins.

Hadronic final states

For interactions involving mesons, there are contributions from penguin diagrams which create a pair of quarks out of the internally emitted photon, Z, or gluon (gluonic or QCD penguins). The latter are not easily accessible, because they have only hadronic final states, but these final states aren't excusively created by gluonic penguins.

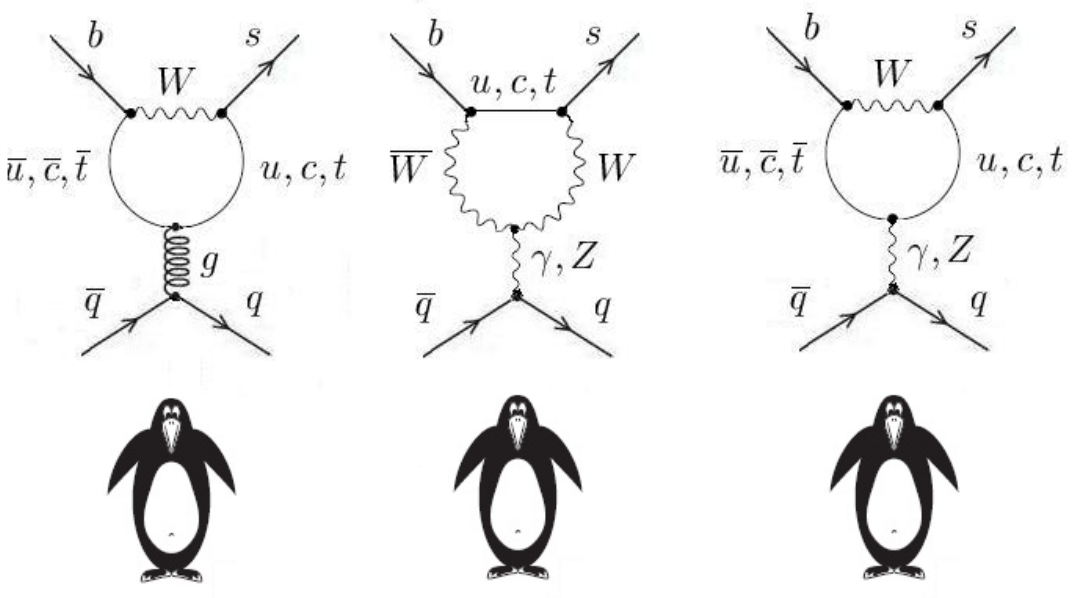

Figure 3.5: Typical penguins with hadronic final states (For these diagrams, you have to imagine a happy penguin in order to understand the outgoing lines.)

3.2 Theoretical Considerations

3.2.1 Effective penguin theory

The above diagrams govern the quark decays at a low energy scale. In theory, you calculate the diagrams at 80 GeV and scale down to 5 GeV to obtain information about low energy observables. An effective theory with point-like interactions can be expressed as an expansion in local, scale(μ)-dependant operators $Q_i(\mu)$ weightened by so-called Wilson coefficients $C_i(\mu)$ and multiplied by the relevant CKM matrix elements - here an example for exclusive b $\rightarrow$ s penguin decays:

$$\mathcal{H}_{eff} = -\frac{4G_F}{\sqrt{2}} V_{tb} V_{ts}^* \sum_{i=1}^{10} C_i(\mu) Q_i(\mu) \tag{3.1}$$

The Q_i are current-current operators, EW penguins and QCD penguins: [14]

$$
\begin{aligned}
Q_{CC1} &= (\overline{s}_\alpha u_\beta)_{V-A}(\overline{u}_\beta d_\alpha)_{V-A} \quad Q_{CC2} = (\overline{s}u)_{V-A}(\overline{u}d)_{V-A} \\
Q_{QCD3} &= (\overline{s}d)_{V-A}\sum_{q=u,d,s}(\overline{q}q)_{V-A} \quad Q_{QCD4} = (\overline{s}_\alpha d_\beta)_{V-A}\sum_{q=u,d,s}(\overline{q}_\beta q_\alpha)_{V-A} \\
Q_{QCD5} &= (\overline{s}d)_{V-A}\sum_{q=u,d,s}(\overline{q}q)_{V+A} \quad Q_{QCD6} = (\overline{s}_\alpha d_\beta)_{V-A}\sum_{q=u,d,s}(\overline{q}_\beta q_\alpha)_{V+A} \\
Q_{EW7} &= \frac{3}{2}(\overline{s}d)_{V-A}\sum_{q=u,d,s}e_q(\overline{q}q)_{V+A} \quad Q_{EW8} = \frac{3}{2}(\overline{s}_\alpha d_\beta)_{V-A}\sum_{q=u,d,s}e_q(\overline{q}_\beta q_\alpha)_{V+A} \\
Q_{EW9} &= \frac{3}{2}(\overline{s}d)_{V-A}\sum_{q=u,d,s}e_q(\overline{q}q)_{V-A} \quad Q_{EW10} = \frac{3}{2}(\overline{s}_\alpha d_\beta)_{V-A}\sum_{q=u,d,s}e_q(\overline{q}_\beta q_\alpha)_{V-A}
\end{aligned}
\tag{3.2}
$$

The Wilson coefficients of the above operators represent the influence of heavy degrees of freedom (t, Z, W), which are integrated out in the rescaling process. In practice, the calculation takes place at 80 GeV and is run down by RGEs, which effective couplings and running masses are also affected by the heavy particles. The RGEs mix the Wilson coefficients, but there is usually still a typical set of relevant coefficients for each decay, like C_7 for $b \to$ s γ or C_7, C_9, C_{10} for $b \to sl^+l^-$. Theoretically, the scale-dependence of the operators and their coefficients should cancel out exactly, but due to the pertubative nature of the calculations, there is always a small leftover and thus, a theoretical error. The observables also depend on the renormalization scheme used, so it is important to have access to higher order (NNLO) calculations.

Unlike the Wilson coefficients, the matrix elements of the operators can't be calculated pertubatively due to confinement - one has to use lattice calculations or other non-pertubative approaches to calculate decay rates of mesons, and this results in the dominant uncertanties for the amplitudes of exclusive decays.

3.2.2 Penguin-Box Expansion

The SM meson decays can also be expressed by a similar expansion of the amplitude, using a set of process-independent universal functions $F_r(\frac{m_t^2}{m_W^2})$ [14] :

$$
A(M \to F) = P_0(M \to F) + \sum_r P_r(M \to F)F_r(\frac{m_t^2}{m_W^2}) \tag{3.3}
$$

The coefficients P_0 and P_r depend on the process, on hadronic matrix elements of local operators and CKM factors. If any new particles exchange in the penguin and box loops, these coefficients would only change considerably if new local operators contribute. Otherwise, the only change happens in the universal functions, which now depend on the masses of new particles - therefore, we could see new physics as a change in $F_r(\frac{m_t^2}{m_W^2})$. P_0 describes mainly the contributions from internal charm quark loops and is often negligible.

3.2.3 Universal functions

The universal functions governing our rare decays are listened below, whereas the subscript 0 indicates that QCD corrections are not (yet) included. [14]

$$
\begin{array}{ll}
B_0(m_t) & \Delta F = 1 \quad \text{box diagram} \\
C_0(m_t) & \Delta F = 1 \quad Z^0\text{-penguin} \\
D_0(m_t) & \Delta F = 1 \quad \gamma\text{-penguin} \\
X_0(m_t) & C_0 - 4B_0 \quad \text{gauge invariant combination} \\
Y_0(m_t) & C_0 - B_0 \quad \text{gauge invariant combination} \\
Z_0(m_t) & C_0 + \frac{1}{4}D_0 \quad \text{gauge invariant combination} \\
S_0(m_t) & \Delta F = 2 \quad \text{box diagram with tt-exchange} \\
E_0(m_t) & \text{QCD penguin with off-shell gluon} \\
E_0'(m_t) & \text{QCD penguin with on-shell gluon} \\
D_0'(m_t) & \gamma\text{-penguin with on-shell photon}
\end{array}
\tag{3.4}
$$

Rare decays used in this work depend on the following functions:

$$
\begin{array}{ll}
B \to X_s\gamma & D_0'(m_t), E_0'(m_t) \\
B \to X_s\mu^+\mu^- & Y_0(m_t), Z_0(m_t), E_0(m_t), D_0'(m_t), E_0'(m_t) \\
B \to X_{d,s}\nu\overline{\nu} & X_0(m_t)
\end{array}
\tag{3.5}
$$

3.3 Rare decays and meson mixing

3.3.1 B $\rightarrow X_s\gamma$

Theory

For the inclusive decay rate, meaning a summation over all final states,

$$A(B \rightarrow X)_{incl} = \frac{G_F}{\sqrt{2}} \sum_{f \in X} V^i_{CKM} C_i(\mu) < f|Q_i(\mu)|B > \tag{3.6}$$

the amplitude can be approximated by a spectator model of a pertubative b quark decay plus nonperturbative corrections [15–21]. Radiative B decays in general are heavily affected by pertubative QCD corrections, where we now have access to NNLO calculations [22–34]:

$$\Gamma(\bar{B} \rightarrow X_s\gamma)_{E_\gamma > E_0} = \Gamma(b \rightarrow X_s^{partons}\gamma)_{E_\gamma > E_0} + O(\frac{\Lambda^2}{m_b^2}, \frac{\Lambda^2}{m_c^2}, \frac{\Lambda\alpha_s}{m_b}) \tag{3.7}$$

Λ is of the order of Λ_{QCD}. There may be additional non-pertubative corrections to this decay rate when the photon energy cut is chosen too large or too small [35–39]. The leading order for the pertubative part is represented by one-loop diagrams with, for example, internal top-quark exchanges, then followed by NLO and NNLO contributions and QCD corrections. Expanding the pertubative part in α_s, one has to resum over large logarithms $ln(\frac{m_W^2}{m_b^2})$ - in order to do that, one uses the effective low-scale ($\approx m_b$) theory in which the top-quarks and the electroweak bosons are decoupled. The Wilson coefficients for the local operators are evaluated at a scale of the order m_t and then scaled down to the effective theory, finally the matrix elements of the local operators are computed. This has been done up to next-to-next-to-leading-log [22], with the following result for a photon energy cut of $E_\gamma > 1.6GeV$:

$$\mathcal{B}(\bar{B} \rightarrow X_s\gamma)_{theo} = (3.15 \pm 0.23) \cdot 10^{-4} \tag{3.8}$$

The error consists of the non-pertubative effects (5%), errors from input parameters (3%), higher-order effects (3%) and m_c-interpolation (3%). The biggest error emerges from the non-pertubative $\frac{\Lambda\alpha_s}{m_b}$ -part on four-quark-operators [16].

Experiment

This mode has been measured by pseudoinclusive and fully inclusive methods (BaBar, BELLE, Cleo) [40–43]. Altough each experiment has its own methods, restrictions and errors, the results agree quite well and are summarized by the world average,

$$\mathcal{B}(\bar{B} \to X_s\gamma)_{exp} = (3.55 \pm 0.30) \cdot 10^{-4} \tag{3.9}$$

yet one always has to ask how well theoretical errors can be compared to experimental errors, and thus we will work with much broader error bars of (3.5 ± 0.8) in this work, assuming SUSY effects of roughly the same order as the SM errors, which will already constrain the flavor parameter space well enough, while being relatively sure that no information is lost.

The current world average is limited by mainly systematic errors, the loss of X_s fractions for pseudoinclusive methods as well as background effects for fully inclusive methods.

3.3.2 $\bar{B} \to X_s l^+ l^-$

This electroweak penguin decay consists only of one-loop contributions and is therefore very useful to probe NP effects. As stated earlier, it is sensitive to Q_7, Q_9 and Q_{10}, but radiative corrections add partly process-independent dependencies to the remaining seven operators, which can also be expressed by the penguin-box expansion.

The experimental probing of these decays is difficult due to their small branching ratios, and only few exclusive decays are accessible, like $b \to s\mu^+\mu^-$, (which we will use) $b \to se^+e^-$ and the simplest hadronic final states. However, future B factories are capable of significantly improving the experimental data. With the newest NNLO corrections, the decay is theoretically clean - however,we won't look into the details, because we aren't interested in precise theoretical errors. We will just cite [12] and choose much larger error bars:

$$\begin{aligned} \mathcal{B}(\bar{B} \to X_s\mu^+\mu^-)_{theo} &= (1.59 \pm 0.11) \cdot 10^{-6} \\ \mathcal{B}(\bar{B} \to X_s\mu^+\mu^-)_{here} &= (1.59 \pm 0.55) \cdot 10^{-6} \end{aligned} \tag{3.10}$$

3.3.3 $B_s \rightarrow \mu^+\mu^-$

This very rare leptonic decay is a smoking gun for neutral Higgs effects in SUSY with large $tan\beta$ and is useful for constraining parameters in many models, and testing the SM. On the loop level, both SUSY Higgs doublets can couple to any fermion, with couplings proportional to a breaking term and μ. The loop contribution suppression factors are compensated by a factor of $tan\beta$, thus, in models with large $tan\beta$, the branching ratio can exceed SM expectations by 10^3 [12], scaling like:

$$\mathcal{B}(B_s \rightarrow \mu^+\mu^-)_{SUSY} \propto \frac{m_b^2 m_l^2 (\tan\beta)^6}{M_{A^0}^4} \tag{3.11}$$

In the SM, the theoretical predicitions suffer from uncertancies, roughly in the order of 20% (see below). Here, f_{B_s} and τ_{B_s} are decay constant and lifetime of the B_s-meson.

$$\mathcal{B}(B_s \rightarrow \mu^+\mu^-)_{SM} = (3.86 \pm 0.15) \cdot 10^{-9} \times \frac{\tau_{B_s}}{1.527ps}[\frac{|V_{ts}|}{0.0408}][\frac{f_{B_s}}{240MeV}] \tag{3.12}$$

From the experimental side, we only have upper bounds on this class of very rare decays. Regarding $B_s \rightarrow \mu^+\mu^-$, the strongest bound is from the D0-experiment using 2 fb^{-2} of $p\bar{p}$ data [44]:

$$(B_s \rightarrow \mu^+\mu^-)_{exp} \leq 93 \cdot 10^{-9} \ \ @95\%CL \tag{3.13}$$

The bound can vary depending on the amount of data used, luminosity etc., and we will assume a more generous bound of $(2 \cdot 10^{-8})$ including SUSY effects. In near future, the LHC experiments will improve this bound with several different approaches - the main problem hereby is having to deal with a massive background.

3.3.4 $\bar{B}_s - B_s$ mixing

Out of the many possible observables in this sector, we will only look at the mass difference Δm_{B_s} of the two B_s meson mass eigenstates (particle/antiparticle) oscillating into each other. The mass difference depends on the 12-entry of the mass matrix between $\bar{B}_s$ and B_s:

$$\Delta m_s = 2|M_{12}^s| \tag{3.14}$$

Pertubative NLO corrections to these matrix elements have been computed in [45], the resulting SM prediction is obtained from the CKMfitter collaboration [46]. Experimental data comes from the CDF collaboration [47], which used semileptonic and hadronic decay modes with improved particle identification and a neural network for the event selection. The results are consistent with the SM prediction.

$$\begin{aligned} \Delta m_{s_{SM}} &= (18.9^{+5.7}_{-2.8}) ps^{-1} \\ \Delta m_{s_{exp}} &= (17.77 \pm 0.010 \pm 0.07) ps^{-1} \end{aligned} \tag{3.15}$$

The possible effects of new physics are parametrized in respect to the SM value by C_{B_s} below, citing ref. [48], while some regions seem to be excluded if the underlying error analysis is correct. To get a general idea about the constraints by B_s mixing, we use a looser bound:

$$\begin{aligned} C_{B_s} &= \frac{|M_{12}^s|^{SM+NP}}{|M_{12}^s|^{SM}} = 1.03 \pm 0.29 \\ \Delta m_{s_{here}} &= (17.3 \pm 3.8) ps^{-1} \end{aligned} \tag{3.16}$$

3.4 SUSY penguins/boxes

As stated earlier, SUSY changes the Wilson coefficients by adding diagrams with heavy particles in the loops. There are numerous possibilities with squarks, gluinos, higgsinos and gauginos - the resulting diagrams are called "super-penguins" [Fig.3.6]:

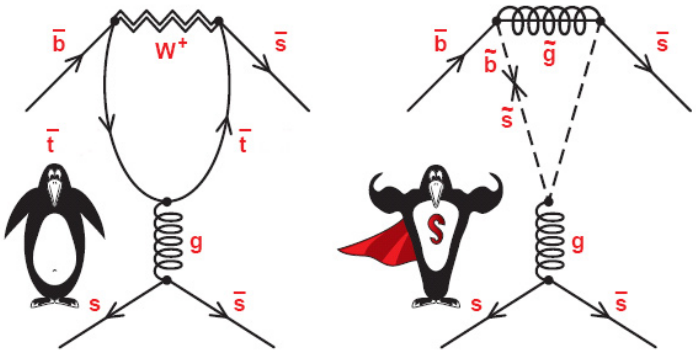

Figure 3.6: Standard model penguins and penguins involving SUSY particles [49]

In order to find all contributions, one has to look through all possible interactions between quarks, since every class of SUSY particle is heavy enough to appear in such a loop. The new penguin graphs look like [Fig.3.7], while the number represents the "penguin legs"[Fig.3.8] below that fit the graph.

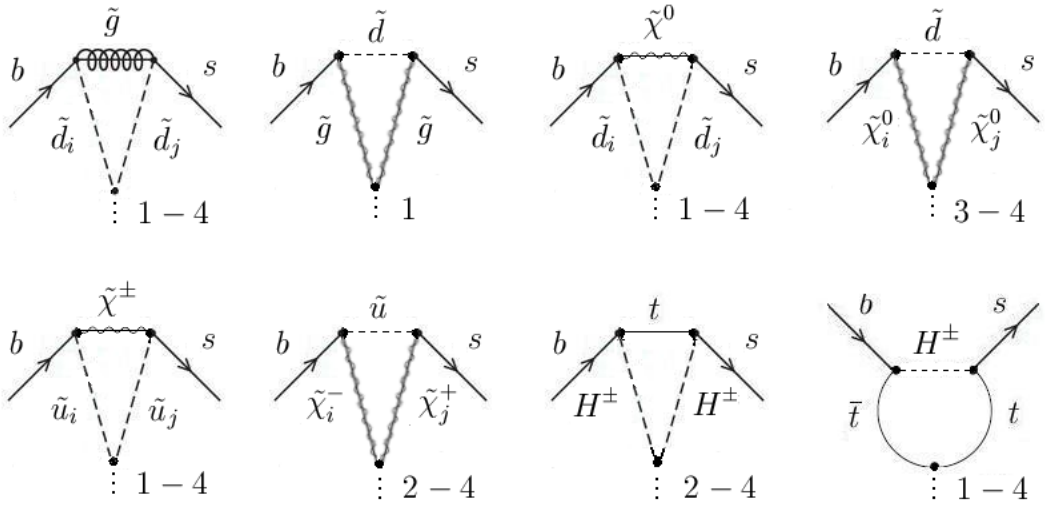

Figure 3.7: new SUSY contributions to the $b \to s$ transistions

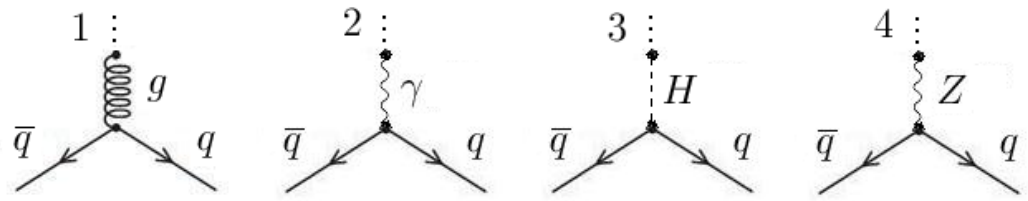

Figure 3.8: The above diagrams can be combined with these penguin legs

There are similar box diagrams exchanging the same particles, here are some examples [Fig.3.9]:

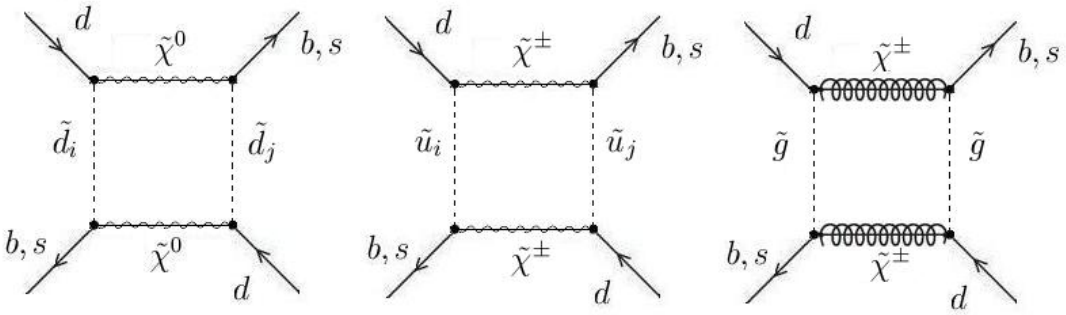

Figure 3.9: Examples for box diagrams involving supersymmetric particles

The effects of these diagrams were not explicitly calculated in this work, we use results from other publications [50–52] integrated in SPheno [9] to obtain theoretical values for the decays and compare them to experimental results.

4 Lagrangian for squark decays

Starting in gauge eigenstates and rotating to mass eigenstates, all vertices governing two-body decays of squarks will be calculated in the following sections. Using these results, we can then evaluate squark decay rates. We will later probe the behaviour of u_1,u_2, d_1 and d_2 decay rates when sweeping off-diagonal mass matrix elements.

4.1 $\mathcal{L}_I$ in gauge eigenstates

As stated above, the interaction term between chiral and gauge supermultiplets reads (in the given gaugino definition!):

$$\begin{aligned}
\mathcal{L}_I|_{\Phi_i\lambda} &= -\sum_i \sqrt{2}g[(\phi_i^\dagger T^\alpha \psi_i)\cdot\lambda^\alpha + \lambda^{\alpha\dagger}\cdot(\psi_i^\dagger T^\alpha \phi_i)] \\
&= \sum_f -\frac{\sqrt{2}}{2}g[(\tilde{u}^*_{fL}\tau^a d^0_{fL})\tilde{W}^a + \overline{\tilde{W}^a}(\overline{u^0}_{fL}\tau^a \tilde{d}_{fL}) + (\tilde{d}^*_{fL}\tau^a u^0_{fL})\tilde{W}^a + \overline{\tilde{W}^a}(\overline{d^0}_{fL}\tau^a \tilde{u}_{fL})] \\
&\quad -\sqrt{2}g'[\frac{1}{6}\tilde{u}^*_{fL}\tilde{B}u^0_{fL} + \frac{1}{6}\overline{u^0}_{fL}\overline{\tilde{B}}\tilde{u}_{fL} - \frac{2}{3}\tilde{u}^*_{fR}\overline{\tilde{B}}u^0_{fR} - \frac{2}{3}\overline{u^0}_{fR}\tilde{B}\tilde{u}_{fR} \\
&\qquad \frac{1}{6}\tilde{d}^*_{fL}\tilde{B}d^0_{fL} + \frac{1}{6}\overline{d^0}_{fL}\overline{\tilde{B}}\tilde{d}_{fL} + \frac{1}{3}\tilde{d}^*_{fR}\overline{\tilde{B}}d^0_{fR} + \frac{1}{3}\overline{d^0}_{fR}\tilde{B}\tilde{d}_{fR}] \\
&\quad -\frac{g_3}{\sqrt{2}}[\tilde{u}^*_{fL}\lambda^a_{GM}u^0_{fL}\tilde{G}^a + \overline{u^0}_{fL}\lambda^a_{GM}\tilde{u}_{fL}\overline{\tilde{G}^a} - \tilde{u}^*_{fR}\lambda^a_{GM}u^0_{fR}\overline{\tilde{G}^a} - \overline{u^0}_{fR}\lambda^a_{GM}\tilde{u}_{fR}\tilde{G}^a \\
&\qquad +\tilde{d}^*_{fL}\lambda^a_{GM}d^0_{fL}\tilde{G}^a + \overline{d^0}_{fL}\lambda^a_{GM}\tilde{d}_{fL}\overline{\tilde{G}^a} - \tilde{d}^*_{fR}\lambda^a_{GM}d^0_{fR}\overline{\tilde{G}^a} - \overline{d^0}_{fR}\lambda^a_{GM}\tilde{d}_{fR}\tilde{G}^a]
\end{aligned} \tag{4.1}$$

When writing down the interaction lagrangian, we have to take into account that right handed particles like $\tilde{q}_R$ transform as an antitriplet under $SU(3)$, which leads to an additional minus sign in the corresponding group generator.

Together with the corresponding terms in the MSSM superpotential,

$$\mathcal{W}_{MSSM_{Squarks}} = \epsilon_{ab}[(Y_D)_{ij} H_1^a \cdot Q_i^b \overline{D}_j + (Y_u)_{ij} H_2^b \cdot Q_i^a \overline{U}_j] \tag{4.2}$$

$$\begin{aligned}
\mathcal{L}_{Superpot} =& -\epsilon_{ab}[(Y_D)_{ij} H_1^a \cdot Q_i^b \overline{D}_j + (Y_u)_{ij} H_2^b \cdot Q_i^a \overline{U}_j] + h.c. \\
=& -(Y_D)_{ij}(\tilde{H}_1^0 \tilde{d}_{L_i} \overline{d^0}_{R_j} - \tilde{H}_1^- \tilde{u}_{L_i} \overline{d^0}_{R_j}) + (Y_U)_{ij}(\tilde{H}_2^+ \tilde{d}_{L_i} \overline{u^0}_{R_j} - \tilde{H}_2^0 \tilde{u}_{L_i} \overline{u^0}_{R_j}) \\
& -(Y_D)_{ij}(\tilde{H}_1^0 d_{L_i}^0 \tilde{d}_{R_j}^* - \tilde{H}_1^- u_{L_i}^0 \tilde{d}_{R_j}^*) + (Y_U)_{ij}(\tilde{H}_2^+ d_{L_i}^0 \tilde{u}_{R_j}^* - \tilde{H}_2^0 u_{L_i}^0 \tilde{u}_{R_j}^*) \\
& -(Y_D)_{ji}^*(\overline{\tilde{H}_1^0} \tilde{d}_{L_j}^* d_{R_i}^0 - \tilde{H}_1^+ \tilde{u}_{L_j}^* d_{R_i}^0) + (Y_U)_{ji}^*(\tilde{H}_2^- \tilde{d}_{L_j}^* u_{R_i}^0 - \overline{\tilde{H}_2^0} \tilde{u}_{L_j}^* u_{R_i}^0) \\
& -(Y_D)_{ji}^*(\overline{\tilde{H}_1^0} \overline{d^0}_{L_j} \tilde{d}_{R_i} - \tilde{H}_1^+ \overline{u^0}_{L_j} \tilde{d}_{R_i}) + (Y_U)_{ji}^*(\tilde{H}_2^- \overline{d^0}_{L_j} u_{R_i} - \overline{\tilde{H}_2^0} \overline{u^0}_{L_j} \tilde{u}_{R_i})
\end{aligned} \tag{4.3}$$

we get the interaction in gauge eigenstates responsible for the decay of a squark into one quark and higgsinos. Interactions of squarks with gauge bosons are governed by the same covariant derivative as in the standard model (please note that we will not discuss decays into photons and gluons, because these decays can never be flavor violating):

$$\begin{aligned}
\mathcal{L}_{\Phi V} &= \sum_i (D^\mu \phi_i)^\dagger D_\mu \phi_i \\
&= (\partial^\mu + ig\frac{\tau^a}{2} W^{\mu a} + ig'\frac{Y}{2} B^\mu)\phi^\dagger (\partial_\mu - ig\frac{\tau^a}{2} W_\mu^a - ig'\frac{Y}{2} B_\mu)\phi
\end{aligned} \tag{4.4}$$

4.1.1 Interactions with gauginos/gauge bosons

Now we can start collecting terms for charginos, neutralinos and gluinos. Regarding EWSB, the winos behave like the W-bosons:

$$\tilde{W}^\pm = \frac{1}{\sqrt{2}}(\tilde{W}^1 \mp i\tilde{W}^2) \tag{4.5}$$

Charginos $\tilde{q} \to \tilde{\chi}^{\pm} + q$

Terms including charged winos and higgsinos:

$$\begin{aligned}\mathcal{L}_I|_{\tilde{q}q\tilde{\chi}^{\pm}} = &-\sum_{f=1}^{3} g[\tilde{u}^*_{fL} d^0_{fL} \tilde{W}^+ + \tilde{d}^*_{fL} u^0_{fL} \tilde{W}^- + \overline{\tilde{W}^-}\,\overline{u^0}_{fL} \tilde{d}_{fL} + \overline{\tilde{W}^+}\,\overline{d^0}_{fL} \tilde{u}_{fL}] \\ &+ (Y_D)_{ij}[\tilde{H}_1^- \tilde{u}_{L_i} \overline{d^0}_{R_j} + \tilde{H}_1^- u^0_{L_i} \tilde{d}^*_{R_j}] + (Y_U)_{ij}[\tilde{H}_2^+ \tilde{d}_{L_i} \overline{u^0}_{R_j} + \tilde{H}_2^+ d^0_{L_i} \tilde{u}^*_{R_j}] \\ &+ (Y_D)^*_{ji}[\tilde{H}_1^+ \tilde{u}^*_{L_j} d^0_{R_i} + \tilde{H}_1^+ \overline{u^0}_{L_j} \tilde{d}_{R_i}] + (Y_U)^*_{ji}[\tilde{H}_2^- \tilde{d}^*_{L_j} u^0_{R_i} + \tilde{H}_2^- \overline{d^0}_{L_j} \tilde{u}_{R_i}]\end{aligned} \tag{4.6}$$

Neutralinos $\tilde{q} \to \tilde{\chi}^0 + q$

Terms including the neutral wino, the bino and neutral higgsinos:

$$\begin{aligned}\mathcal{L}_I|_{\tilde{q}q\tilde{\chi}^0} = \sum_{f=1}^{3} &-\sqrt{2} g'[\frac{1}{6}\tilde{u}^*_{fL} \tilde{B} u^0_{fL} + \frac{1}{6}\overline{u^0}_{fL} \overline{\tilde{B}} \tilde{u}_{fL} - \frac{2}{3}\tilde{u}^*_{fR} \overline{\tilde{B}} u^0_{fR} - \frac{2}{3}\overline{u^0}_{fR} \tilde{B} \tilde{u}_{fR} \\ &+\frac{1}{6}\tilde{d}^*_{fL} \tilde{B} d^0_{fL} + \frac{1}{6}\overline{d^0}_{fL} \overline{\tilde{B}} \tilde{d}_{fL} + \frac{1}{3}\tilde{d}^*_{fR} \overline{\tilde{B}} d^0_{fR} + \frac{1}{3}\overline{d^0}_{fR} \tilde{B} \tilde{d}_{fR}] \\ &-\frac{1}{\sqrt{2}} g[\tilde{u}^*_{fL} \tilde{W}^3 u^0_{fL} + \tilde{d}^*_{fL} \tilde{W}^3 d^0_{fL} + \overline{u^0}_{fL} \overline{\tilde{W}^3} \tilde{u}_{fL} + \overline{d^0}_{fL} \overline{\tilde{W}^3} \tilde{d}_{fL}] \\ &- (Y_D)_{ij}[\tilde{H}_1^0 \tilde{d}_{L_i} \overline{d^0}_{R_j} + \tilde{H}_1^0 d^0_{L_i} \tilde{d}^*_{R_j}] - (Y_U)_{ij}[\tilde{H}_2^0 \tilde{u}_{L_i} \overline{u^0}_{R_j} + \tilde{H}_2^0 u^0_{L_i} \tilde{u}^*_{R_j}] \\ &- (Y_D)^*_{ji}[\overline{\tilde{H}_1^0} \tilde{d}^*_{L_j} d^0_{R_i} + \overline{\tilde{H}_1^0}\,\overline{d^0}_{L_j} \tilde{d}_{R_i}] - (Y_U)^*_{ji}[\overline{\tilde{H}_2^0} \tilde{u}^*_{L_j} u^0_{R_i} + \overline{\tilde{H}_2^0}\,\overline{u^0}_{L_j} \tilde{u}_{R_i}]\end{aligned} \tag{4.7}$$

Gluinos $\tilde{q} \to \tilde{g} + q$

Terms including gluinos:

$$\begin{aligned}\mathcal{L}_I|_{\tilde{q}q\tilde{G}} = \sum_{f=1}^{3} -\frac{g_3}{\sqrt{2}}[&\tilde{u}^*_{fL}\lambda^a_{GM}u^0_{fL}\tilde{G}^a + \overline{u^0}_{fL}\lambda^a_{GM}\tilde{u}_{fL}\overline{\tilde{G}^a} \\ &-\tilde{u}^*_{fR}\lambda^a_{GM}u^0_{fR}\overline{\tilde{G}^a} - \overline{u^0}_{fR}\lambda^a_{GM}\tilde{u}_{fR}\tilde{G}^a \\ &+\tilde{d}^*_{fL}\lambda^a_{GM}d^0_{fL}\tilde{G}^a + \overline{d^0}_{fL}\lambda^a_{GM}\tilde{d}_{fL}\overline{\tilde{G}^a} \\ &-\tilde{d}^*_{fR}\lambda^a_{GM}d^0_{fR}\overline{\tilde{G}^a} - \overline{d^0}_{fR}\lambda^a_{GM}\tilde{d}_{fR}\tilde{G}^a]\end{aligned} \tag{4.8}$$

Gauge Bosons $\tilde{q} \to \tilde{q} + V$

We need the terms of $(D^\mu\phi)^\dagger D_\mu\phi$ which contribute to $(\tilde{q}\tilde{q}V)$ vertices, and apply EWSB.

$$\begin{aligned}\mathcal{L}|_{\phi\phi V} &= -\partial^\mu\phi^\dagger ig\frac{\tau^a}{2}W^a_\mu\phi + ig\frac{\tau^a}{2}W^a_\mu\phi^\dagger\partial^\mu\phi - \partial^\mu\phi^\dagger ig'\frac{Y}{2}B_\mu\phi + ig'\frac{Y}{2}B_\mu\phi^\dagger\partial^\mu\phi \\ &= (-ig\frac{\tau^a}{2}W^a_\mu - ig'\frac{Y}{2}B_\mu)[(\partial^\mu\phi^\dagger)\phi - \phi^\dagger(\partial^\mu\phi)] \\ &= (-ig\frac{\tau^a}{2}W^a_\mu - ig'\frac{Y}{2}B_\mu)[\phi^\dagger\partial^\mu_{\leftrightarrow}\phi]\end{aligned}$$

$$\begin{aligned}\mathcal{L}|_{\tilde{q}\tilde{q}V} = \sum_{f=1}^{3} &-i\frac{g}{\sqrt{2}}\tilde{u}^*_{fL}\partial^\mu_{\leftrightarrow}\tilde{d}_{fL}W^+_\mu - i\frac{g}{\sqrt{2}}\tilde{d}^*_{fL}\partial^\mu_{\leftrightarrow}\tilde{u}_{fL}W^-_\mu \\ &-i\frac{g}{c_W}(\frac{1}{2} - \frac{2}{3}s^2_W)\tilde{u}^*_{fL}\partial^\mu_{\leftrightarrow}\tilde{u}_{fL}Z_\mu - i\frac{g}{c_W}(-\frac{1}{2} + \frac{1}{3}s^2_W)\tilde{d}^*_{fL}\partial^\mu_{\leftrightarrow}\tilde{d}_{fL}Z_\mu \\ &-i\frac{g}{c_W}(\frac{1}{3}s^2_W)\tilde{d}^*_{fR}\partial^\mu_{\leftrightarrow}\tilde{d}_{fR}Z_\mu + i\frac{g}{c_W}(\frac{2}{3}s^2_W)\tilde{u}^*_{fR}\partial^\mu_{\leftrightarrow}\tilde{u}_{fR}Z_\mu\end{aligned} \tag{4.9}$$

4.2 Rotation into physical fields

4.2.1 $\mathcal{L}_I$ in mass eigenstates

We use the transformations from section [2.7] to rotate the fields into mass eigenstates. Only the results are given here, you can find the complete calculation in the appendix.

We introduce the Dirac spinors of the Charginos and Quarks, as well as the Majorana spinors for Gluons and Neutralinos

$$
\begin{aligned}
\tilde{\chi}_j^+ &= \begin{pmatrix} \tilde{C}_j^+ \\ \overline{\tilde{C}_j^-} \end{pmatrix} & \tilde{\chi}_j^- &= \begin{pmatrix} \tilde{C}_j^- \\ \overline{\tilde{C}_j^+} \end{pmatrix} \\
\overline{\tilde{\chi}_j^+} &= \begin{pmatrix} \tilde{C}_j^- & \overline{\tilde{C}_j^+} \end{pmatrix} & \overline{\tilde{\chi}_j^-} &= \begin{pmatrix} \tilde{C}_j^+ & \overline{\tilde{C}_j^-} \end{pmatrix} \\
\tilde{\chi}_j^0 &= \begin{pmatrix} \tilde{C}_j^0 \\ \overline{\tilde{C}_j^0} \end{pmatrix} & \overline{\tilde{\chi}_j^0} &= \begin{pmatrix} \tilde{C}_j^0 & \overline{\tilde{C}_j^0} \end{pmatrix} \\
\tilde{g} &= \begin{pmatrix} \tilde{G} \\ \overline{\tilde{G}} \end{pmatrix} & \overline{\tilde{g}} &= \begin{pmatrix} \tilde{G} & \overline{\tilde{G}} \end{pmatrix} \\
\mathbf{\Psi}_u &= \begin{pmatrix} u_L \\ u_R \end{pmatrix} & \mathbf{\Psi}_d &= \begin{pmatrix} d_L \\ d_R \end{pmatrix} \\
\overline{\mathbf{\Psi}}_u &= \begin{pmatrix} \overline{u}_R & \overline{u}_L \end{pmatrix} & \overline{\mathbf{\Psi}}_d &= \begin{pmatrix} \overline{d}_R & \overline{d}_L \end{pmatrix}
\end{aligned}
\tag{4.10}
$$

and use them to write down the Lagrangians in dirac notation. We also replace $\frac{1}{\nu_1} = \frac{g}{2m_W c_\beta}$ and $\frac{1}{\nu_2} = \frac{g}{2m_W s_\beta}$.

Charginos

$$\begin{aligned}\mathcal{L}_I = \overline{\mathbf{\Psi}}_u[\hat{P}_L(&\frac{g}{\sqrt{2}m_W s_\beta}V_{2j}^*\hat{m}_u V_{CKM}R_{dL}) \\ &+\hat{P}_R(\frac{g}{\sqrt{2}m_W c_\beta}U_{2j}V_{CKM}\hat{m}_d R_{dR} - gU_{1j}V_{CKM}R_{dL})]\tilde{\chi}_j^+\vec{\tilde{\mathbf{d}}} \\ + \overline{\mathbf{\Psi}}_d[\hat{P}_L(&\frac{g}{\sqrt{2}m_W c_\beta}U_{2j}^*\hat{m}_d V_{CKM}^\dagger R_{uL}) \\ &+\hat{P}_R(\frac{g}{\sqrt{2}m_W s_\beta}V_{2j}V_{CKM}^\dagger\hat{m}_u R_{uR} - gV_{1j}V_{CKM}^\dagger R_{uL})]\tilde{\chi}_j^-\vec{\tilde{\mathbf{u}}} \\ &+\mathbf{h.c.}\end{aligned} \tag{4.11}$$

Neutralinos

$$\begin{aligned}\mathcal{L}_I = \overline{\mathbf{\Psi}}_u[\hat{P}_L(&\frac{2\sqrt{2}g'}{3}N_{1j}^*R_{uR} - \frac{\hat{m}_u g}{\sqrt{2}m_W s_\beta}N_{4j}^*R_{uL}) \\ &+\hat{P}_R(-\frac{\sqrt{2}g'}{6}N_{1j}R_{uL} - \frac{\sqrt{2}g}{2}N_{2j}R_{uL} - \frac{\hat{m}_u g}{\sqrt{2}m_W s_\beta}N_{4j}R_{uR})]\tilde{\chi}_j^0\vec{\tilde{\mathbf{u}}} \\ + \overline{\mathbf{\Psi}}_d[\hat{P}_L(&\frac{-\sqrt{2}g'}{3}N_{1j}^*R_{dR} - \frac{\hat{m}_d g}{\sqrt{2}m_W c_\beta}N_{3j}^*R_{dL}) \\ &+\hat{P}_R(\frac{-\sqrt{2}g'}{6}N_{1j}R_{dL} + \frac{\sqrt{2}g}{2}N_{2j}R_{dL} - \frac{\hat{m}_d g}{\sqrt{2}m_W c_\beta}N_{3j}R_{dR})]\tilde{\chi}_j^0\vec{\tilde{\mathbf{d}}} \\ &+\mathbf{h.c.}\end{aligned} \tag{4.12}$$

Gluinos

$$\begin{aligned}\mathcal{L}_I = \overline{\mathbf{\Psi}}_u[\hat{P}_L(&\frac{g_3}{\sqrt{2}}\lambda_{GM}R_{uR}) + \hat{P}_R(-\frac{g_3}{\sqrt{2}}\lambda_{GM}R_{uL})]\tilde{g}\vec{\tilde{\mathbf{u}}} \\ + \overline{\mathbf{\Psi}}_d[\hat{P}_L(&\frac{g_3}{\sqrt{2}}\lambda_{GM}R_{dR}) + \hat{P}_R(-\frac{g_3}{\sqrt{2}}\lambda_{GM}R_{dL})]\tilde{g}\vec{\tilde{\mathbf{d}}} \\ &+\mathbf{h.c.}\end{aligned} \tag{4.13}$$

5 Decay rates Γ

5.1 Transition amplitudes

We are interested in the decay rates of squarks governed by the above lagrangian. For these, we need the transition amplitude for each decay. All possible two-body squark decays at tree-level can be arranged into three classes, each of them sharing the same general structure in amplitude, kinematics - and thus, decay rate:

5.1.1 Higgs boson radiation

Being the simplest decay mode (at least in structure), the squared transition amplitude of this all-bosonic coupling only depends on the coefficients in the corresponding interaction Lagrangian, so with $\mathcal{L}_{int} = a_{ijk}\tilde{q}_i^*\tilde{q}_j H_k$ we get

$$|\mathcal{M}_{ijk}|^2 = |a_{ijk}|^2 \tag{5.1}$$

5.1.2 Decay into two fermions

The amplitude of this general coupling will be explicitly calculated via elementary dirac algebra, listed in the appendix. Given the structure of the interaction, with $\hat{P}_L = \frac{1-\gamma_5}{2}$ and $\hat{P}_R = \frac{1+\gamma_5}{2}$ being the projection operators on the left- and righthanded helicity states, respectively,

$$\mathcal{L}_{int} = \sum_k -\overline{f}_k(a_{ijk}\hat{P}_L + b_{ijk}\hat{P}_R)f_i\tilde{q}_j^* + h.c. \tag{5.2}$$

suppressing spin indices.The amplitude, still carrying spin information, reads

$$M_{ijk} = \overline{u}_i(p_f)(a_{ijk}\hat{P}_L + b_{ijk}\hat{P}_R)v_k(p_{\overline{f}}) \tag{5.3}$$

Using the spin sum relations $\sum_{spins} \overline{u}u = \not{p} + m_f$ for fermions and $\sum_{spins} \overline{v}v = \not{p} - m_{\overline{f}}$ for antifermions, we elaborate

$$\begin{aligned}
\sum_{spins} |M_{ijk}|^2 &= \frac{1}{4} tr[(\not{p}_f + m_f)(a_{ijk}\hat{P}_L + b_{ijk}\hat{P}_R)(\not{p}_{\overline{f}} - m_{\overline{f}})(a^*_{ijk}\hat{P}_R + b^*_{ijk}\hat{P}_L)] \\
&= \frac{1}{4} tr[((p_f)_\mu \gamma^\mu a_{ijk}(\frac{1-\gamma_5}{2}) + (p_f)_\mu \gamma^\mu b_{ijk}(\frac{1+\gamma_5}{2}) \\
&\quad + \mathbf{1} m_f a_{ijk}(\frac{1-\gamma_5}{2}) + \mathbf{1} m_f b_{ijk}(\frac{1+\gamma_5}{2})) \\
&\quad (p_{\overline{f}})_\nu \gamma^\nu a^*_{ijk}(\frac{1+\gamma_5}{2}) + (p_{\overline{f}})_\nu \gamma^\nu b^*_{ijk}(\frac{1-\gamma_5}{2}) \\
&\quad - \mathbf{1} m_{\overline{f}} a^*_{ijk}(\frac{1+\gamma_5}{2}) - \mathbf{1} m_{\overline{f}} b^*_{ijk}(\frac{1-\gamma_5}{2}))] \\
&= \frac{1}{4} tr[(p_f)_\mu \gamma^\mu (p_{\overline{f}})_\mu \gamma^\mu |a_{ijk}|^2 (\frac{1-\gamma_5}{2}) \\
&+ \frac{1}{4} tr[(p_f)_\mu \gamma^\mu (p_{\overline{f}})_\mu \gamma^\mu |b_{ijk}|^2 (\frac{1+\gamma_5}{2}) \\
&- \mathbf{1} m_f a_{ijk}(\frac{1-\gamma_5}{2}) \mathbf{1} m_{\overline{f}} b^*_{ijk} - \mathbf{1} m_f a^*_{ijk}(\frac{1+\gamma_5}{2}) \mathbf{1} m_{\overline{f}} b_{ijk} \\
&= \frac{1}{2}(p_f \cdot p_{\overline{f}})(|a_{ijk}|^2 + |b_{ijk}|^2) - \frac{1}{2} m_f m_{\overline{f}}(a_{ijk} b^*_{ijk} + a^*_{ijk} b_{ijk})
\end{aligned} \tag{5.4}$$

Thus, the final squared transition amplitude reads

$$|\mathcal{M}_{ijk}|^2 = 2(p_f \cdot p_{\overline{f}})(|a_{ijk}|^2 + |b_{ijk}|^2) - 2 m_f m_{\overline{f}}(a_{ijk} b^*_{ijk} + a^*_{ijk} b_{ijk}) \tag{5.5}$$

5.1.3 Gauge boson radiation

The interaction with gauge bosons leads to numerous possible decay channels, governed by Lagrangians of the form

$$\mathcal{L}_{int} = \sum a_{ijk}(\tilde{q}^*_i \partial^\mu \tilde{q}_j - \partial^\mu \tilde{q}^*_i \tilde{q}_j) V_{k\mu} \tag{5.6}$$

in mass eigenstates. Using gauge eigenstates, one has to add another squark index representing the position in the corresponding fermion doublet. Now, taking advantage of the gauge boson spin sum relation $\sum_{spins} \epsilon^*_\mu \epsilon_\nu = (-g_{\mu\nu} + \frac{p_{V\mu} p_{V\nu}}{m^2_V})$ and $P^\mu = i\partial^\mu$, we evaluate

$$\mathcal{L}_{int} = \sum i(p_{in} + p_{out})^{\mu} a_{ijk} \tilde{q}_i^* \tilde{q}_j V_{k\mu} \tag{5.7}$$

which leads to

$$M_{ijk} = -i a_{ijk} (p_{in} + p_{out})^{\mu} \epsilon_{\mu}^* \tag{5.8}$$

$$\begin{aligned} \frac{1}{2} \sum_{spins} |M_{ijk}|^2 &= |a_{ijk}|^2 (p_{in} + p_{out})^{\mu} (p_{in} + p_{out})^{\nu} (-g_{\mu\nu} + \frac{p_{V\mu} p_{V\nu}}{m_V^2}) \\ &= |a_{ijk}|^2 (-(p_{in} + p_{out}) \cdot (p_{in} + p_{out}) + \frac{1}{m_V^2} ((p_{in} + p_{out}) \cdot p_V)^2) \end{aligned} \tag{5.9}$$

and a final transition amplitude of

$$|\mathcal{M}_{ijk}|^2 = 2|a_{ijk}|^2 [-(p_{in} + p_{out})^2 + \frac{1}{m_V^2} ((p_{in} + p_{out}) \cdot p_V)^2] \tag{5.10}$$

5.2 Two-body decays in general

The differential decay rate is given by

$$d\Gamma = \frac{(2\pi)^4}{2E} |\mathcal{M}|^2 \underbrace{\delta^4(P - p_1 - p_2) \frac{d^3 p_1}{(2\pi)^3 2E_1} \frac{d^3 p_2}{(2\pi)^3 2E_2}}_{\text{differential phase spase factor}} \tag{5.11}$$

while $P = (E, \vec{P})$ is the 4-momentum of the mother particle and $p_i = (E_i, p_i)$ of the daughter particles, respectively. The main task is now to integrate the differential decay rate over all components of p_1 and p_2. In the simplest case of two-body decay, the spin-averaged square of the invariant matrix element $\mathcal{M}$ is a **constant** which simplifies the integration considerably.

If one integrates over one of the 4-momenta, for example p_2, the three-dimensional delta function $\delta(\vec{P} - \vec{p_i})$ vanishes and only energy conservation remains:

$$d\Gamma = \frac{(2\pi)^4}{2E}|\mathcal{M}|^2\delta(E - E_1 - E_2)\frac{d^3p_1}{4(2\pi)^6 E_1 E_2} \tag{5.12}$$

Due to the lorentz invariance of the phase space factor, we can enter the rest frame of the mother particle, which simplifies the energies to $E = M$, $E_1 = \sqrt{p_1^2 + m_1^2}$, $E_2 = \sqrt{(\vec{P} - \vec{p_1})^2 + m_2^2} = \sqrt{p_1^2 + m_2^2}$. Furthermore, the integration over d^3p_1 can be written in polar coordinates as $p^2 dp d\Omega$:

$$\Gamma = \frac{1}{32\pi^2 M}|\mathcal{M}|^2 \int \delta(M - E_1 - E_2)\frac{p_1^2 dp_1 d\Omega}{E_1 E_2} \tag{5.13}$$

We now need to express our results for the invariant matrix elements by particle masses, using 4-momentum-conversation to obtain inner products of particle momenta, for example

$$\begin{aligned} P^2 = M^2 = (p_f + p_{\overline{f}})^2 &= m_f^2 + 2(p_f \cdot p_{\overline{f}}) + m_{\overline{f}}^2 \\ \Rightarrow (p_f \cdot p_{\overline{f}}) &= \frac{1}{2}(M^2 - m_f^2 - m_{\overline{f}}^2) \end{aligned} \tag{5.14}$$

and the corresponding equations for the squared masses of other particles.

Since the above integrand has no angular dependence, integration over $d\Omega$ simply gives a factor of 4π. We can now do a substitution by $E_1 dE_1 = p_1 dp_1$ to only have energies to be integrated:

$$d\Gamma = \frac{1}{8\pi M}|\mathcal{M}|^2 \int \delta(M - E_1 - E_2)\frac{p_1 dE_1}{E_2} \tag{5.15}$$

Due to momentum conservation, $E_2 = p_1 = \sqrt{E_1^2 - M^2}$. If we now denote $f(E_1) = M - E_1 - E_2$ and use the identity $f(E_1) = |f'(E_0)|^{-1}\delta(E_1 - E_0)$, the decay rate becomes

$$\Gamma = \frac{1}{8\pi M^2}|\mathcal{M}|^2|p_1| = \frac{1}{8\pi M^2}|\mathcal{M}|^2\frac{\sqrt{[M^2 - (m_1 - m_2)^2][M^2 - (m_1 + m_2)^2]}}{2M} \tag{5.16}$$

5.3 Squark decay rates

By using four-momentum-conservation, we replace all momenta with particle masses and calculate the total decay rates.

Decay into Neutralinos, Charginos and Gluinos

All the gauginos in mass eigenstates are denoted $\tilde{\chi}$ in the following equation, assuming real vertex coefficients a_{ijk} and b_{ijk}.

$$\begin{aligned}\Gamma_{ijk_{\tilde{\chi}}} = \frac{1}{16\pi M_{\tilde{q}_i}^3}[(M_{\tilde{q}_i}^2 - m_{q_k}^2 - m_{\tilde{\chi}_j}^2)(|a_{ijk}|^2 + |b_{ijk}|^2) - 4m_{q_k}m_{\tilde{\chi}_j}(a_{ijk}b_{ijk})] \\ \cdot \sqrt{[M_{\tilde{q}_i}^2 - (m_{q_k} - m_{\tilde{\chi}_j})^2][M_{\tilde{q}_i}^2 - (m_{q_k} + m_{\tilde{\chi}_j})^2]}\end{aligned} \tag{5.17}$$

Decay into Vector Bosons

$$\begin{aligned}\Gamma_{ijk_V} = \frac{|a_{ijk}|^2}{8\pi M_{\tilde{q}_i}^3}[\frac{(M_{\tilde{q}_i}^2 - m_{\tilde{q}_j}^2)^2}{m_{V_k}^2} - (2M_{\tilde{q}_i}^2 + 2m_{\tilde{q}_j}^2 - m_{V_k}^2)] \\ \cdot \sqrt{[M_{\tilde{q}_i}^2 - (m_{\tilde{q}_j} - m_{V_k})^2][M_{\tilde{q}_i}^2 - (m_{\tilde{q}_j} + m_{V_k})^2]}\end{aligned} \tag{5.18}$$

Decay into Higgs Bosons

$$\Gamma = \frac{1}{16\pi M_{\tilde{q}_i}^3}|a_{ijk}|^2\sqrt{[M_{\tilde{q}_i}^2 - (m_{\tilde{q}_j} - m_{H_k})^2][M_{\tilde{q}_i}^2 - (m_{\tilde{q}_j} + m_{H_k})^2]} \tag{5.19}$$

6 Evaluation and Results

6.1 SPheno

SPheno (SUSY Phenomenology) [9] is a Fortran program written to calculate supersymmetric spectra using high scale input in the SLHA standard [7,8]. It supports nMFV and calculates two- and three-body branching ratios of supersymmetric particles, Higgs bosons, rare decays in the B sector, B meson mixing, other observables like the anomalous magnetic moment of the muon. This work uses SPheno for all spectra calculations and the CAS Mathematica as an interface and visualisation device.

6.2 Parameters and conventions

In detail, only the breaking parameters appearing in offdiagonal-elements of the squark mass matrices are probed, and exclusively for the $2 \to 3$ sector, since it is the least constrained. These parameters include $\hat{m}^2_{Q_{23}}$, $\hat{m}^2_{d_{23}}$, $\hat{m}^2_{u_{23}}$, $\hat{T}_{U_{23}}$, $\hat{T}_{U_{32}}$, $\hat{T}_{D_{23}}$ and $\hat{T}_{D_{32}}$, where you have to take into account that the soft SUSY breaking squared mass matrices are hermitean.

It is convenient to normalize the off-diagonal elements by the diagonal ones. The $\hat{m}^2_{i_{23}}$ are divided by the trace of their matrix, the off-diagonal trilinear couplings are normalized by the trace of $\hat{m}^2_Q$:

$$\begin{aligned} \delta_{MQ_{23}} &= \frac{3\hat{m}^2_{Q_{23}}}{\sum_{i=1}^3 \hat{m}^2_{Q_{ii}}} \qquad \delta_{MD_{23}} = \frac{3\hat{m}^2_{d_{23}}}{\sum_{i=1}^3 \hat{m}^2_{d_{ii}}} \qquad \delta_{MU_{23}} = \frac{3\hat{m}^2_{u_{23}}}{\sum_{i=1}^3 \hat{m}^2_{u_{ii}}} \\ \delta_{TU_{23,32}} &= \frac{3\nu_2 \hat{T}^2_{U_{23,32}}}{\sqrt{2}\sum_{i=1}^3 \hat{m}^2_{Q_{ii}}} \qquad \delta_{TD_{23,32}} = \frac{3\nu_1 \hat{T}^2_{D_{23,32}}}{\sqrt{2}\sum_{i=1}^3 \hat{m}^2_{Q_{ii}}} \end{aligned} \tag{6.1}$$

Using these definitions, we will analyze the interplay between pairs of the above parameters and their impact on the flavor violating branching ratios of the first- and

second-lightest squarks as well as gluinos. We will then check how large flavor violation transistions in the allowed region of parameter space can become.

6.3 Parameter interplay

In the following subsections, we will probe all relevant combinations of two distinct nMFV parameters and probe their interference effects. The parameter planes would be affected if we added a third parameter, resulting in a complex three-dimensional structure. It is next to impossible to get an idea of the complete interplay between all parameters, but for a rough estimate of the constraints, it is suitable to limit the observations to two interacting parameters. The region of parameter space allowed by the low energy observables is shown in red color.

6.3.1 MQ23 / MD23

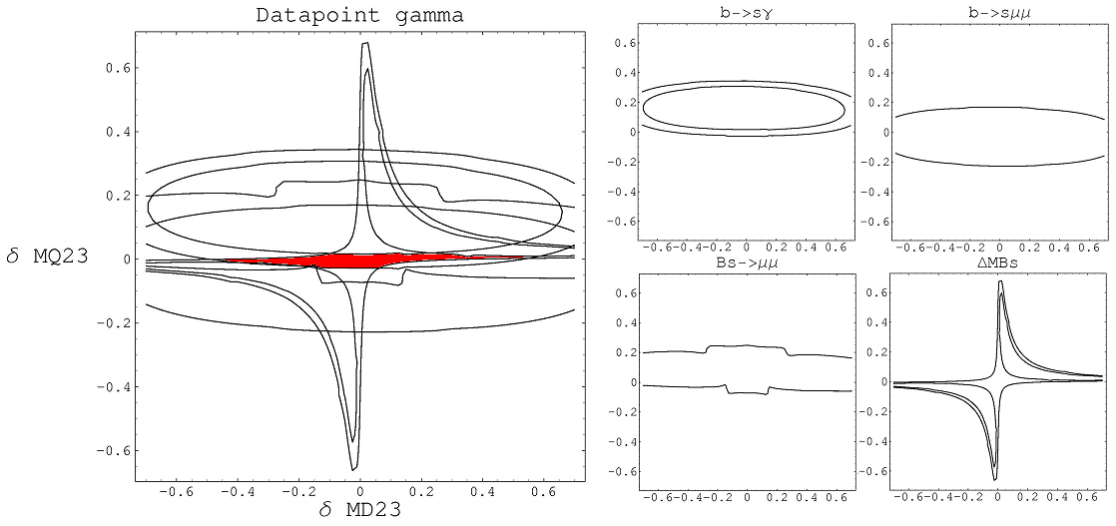

Figure 6.1: MQ23/MD23 parameter plane at γ

We use the γ data point here to illustrate the dependencies [Fig.6.1]. For SPS1a', the picture looks very similar, apart from missing constraints by $B_s \to \mu^+\mu^-$ in the chosen region, and a more bended $b \to s\gamma$ band resulting in a slightly more constrained MD23. You can see that MD23 is in general poorly constrained, which changes a bit when MQ23 varies from zero. MQ23 itself has a strong effect on the calculated low energy observables and the allowed values are therefore confined to

a small region of parameter space. For I", the allowed region is even more narrow, resulting in higher constraints on MQ23.

6.3.2 MQ23 / TD23

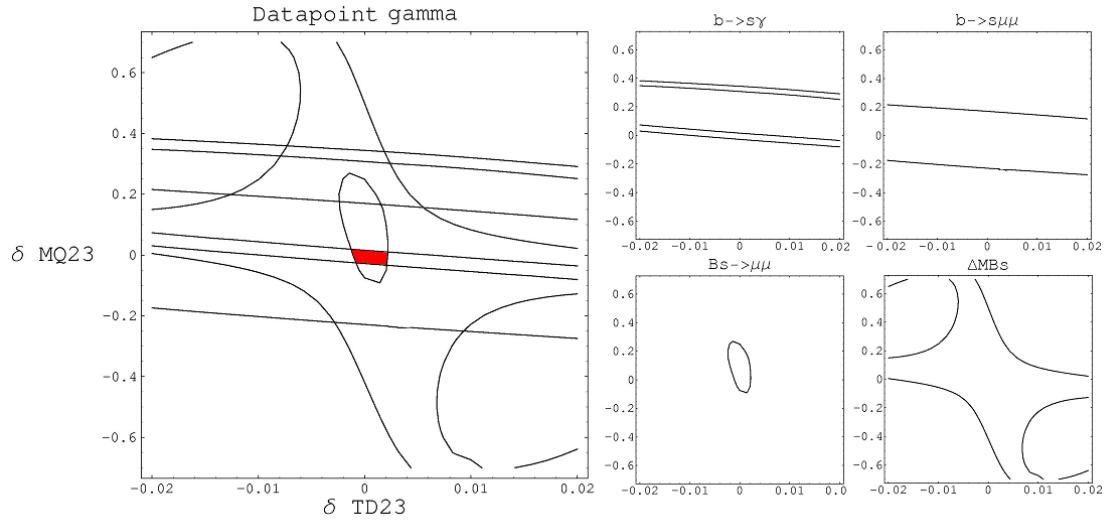

Figure 6.2: MQ23/TD23 parameter plane at γ

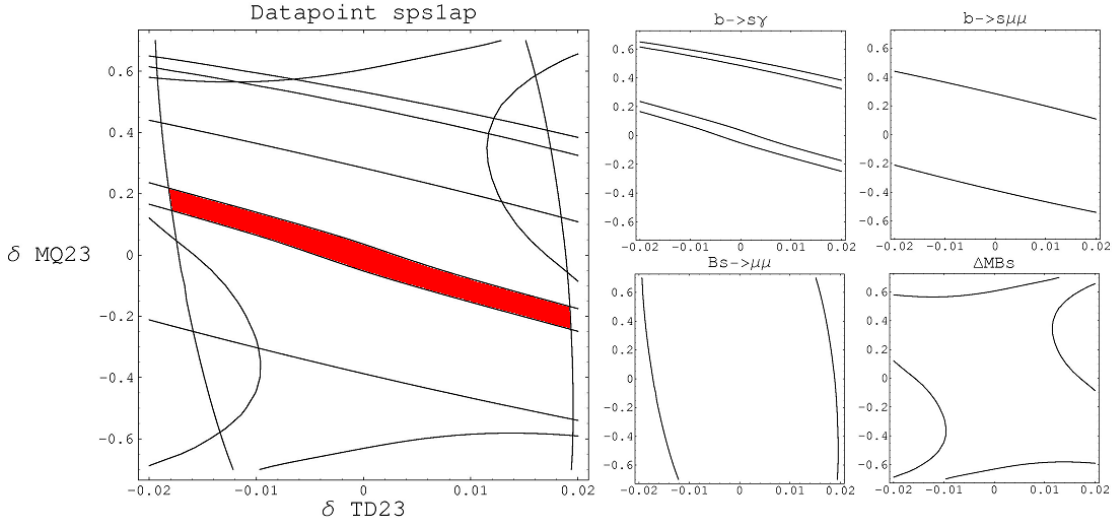

Figure 6.3: MQ23/TD23 parameter plane at SPS1a'

Again, there are strong $B_s \to \mu^+\mu^-$ constraints in γ missing in SPS1a'[Fig.6.3], which now heavily affects the shape of the allowed region. It is interesting to see

that for γ [Fig.6.2], TD23 is fixed to a very limited range, whereas in SPS1a', its allowed range scales with MQ23.

6.3.3 MQ23 / TD32

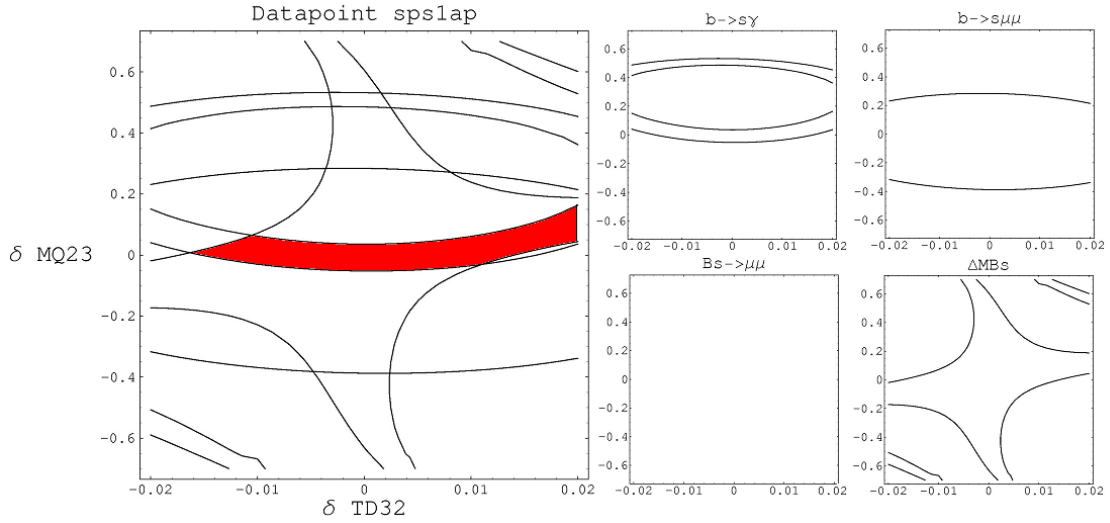

Figure 6.4: MQ23/TD32 parameter plane at SPS1a'

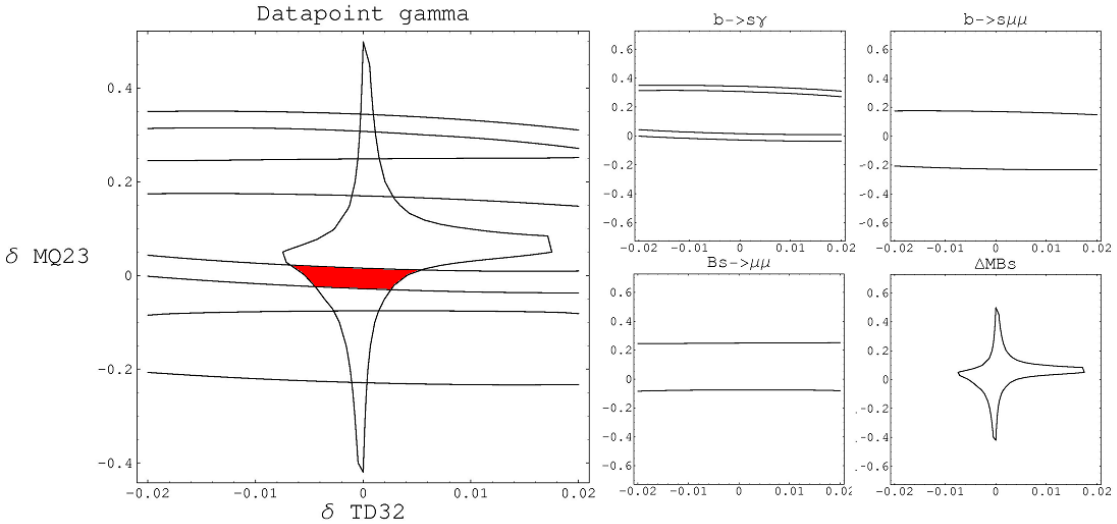

Figure 6.5: MQ23/TD32 parameter plane at SPS1a'

As in almost all pictures, $b \to s\gamma$ is the dominant constraining decay. We have a bended band in SPS1a' [Fig.6.4] fitting well in the ΔM_{B_s} figure and giving TD32 a

lot of freedom. It is striking that for γ [Fig.6.5], the picture is similar, but with more straight lines instead of bended bands and figures. This leads to an allowed region smaller than in SPS1a', but there is still enough room to vary TD32 independent of MQ23.

6.3.4 MD23 / TD23

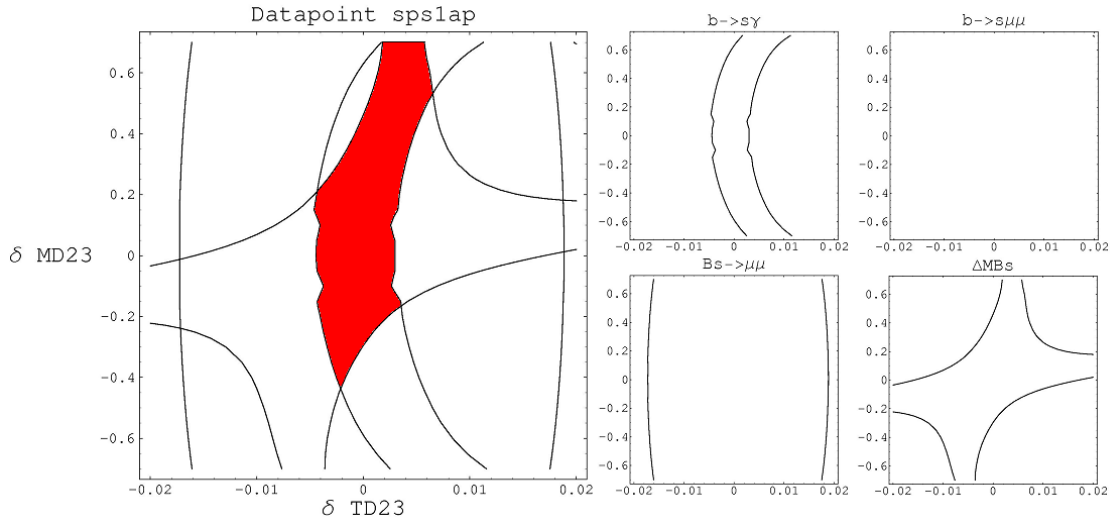

Figure 6.6: MD23/TD23 parameter plane at SPS1a'

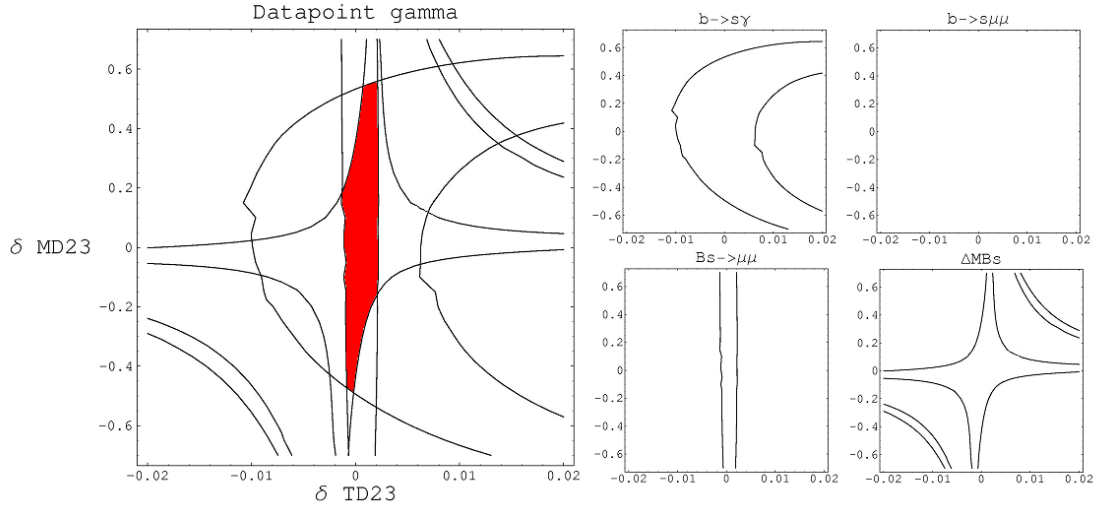

Figure 6.7: MD23/TD23 parameter plane at γ

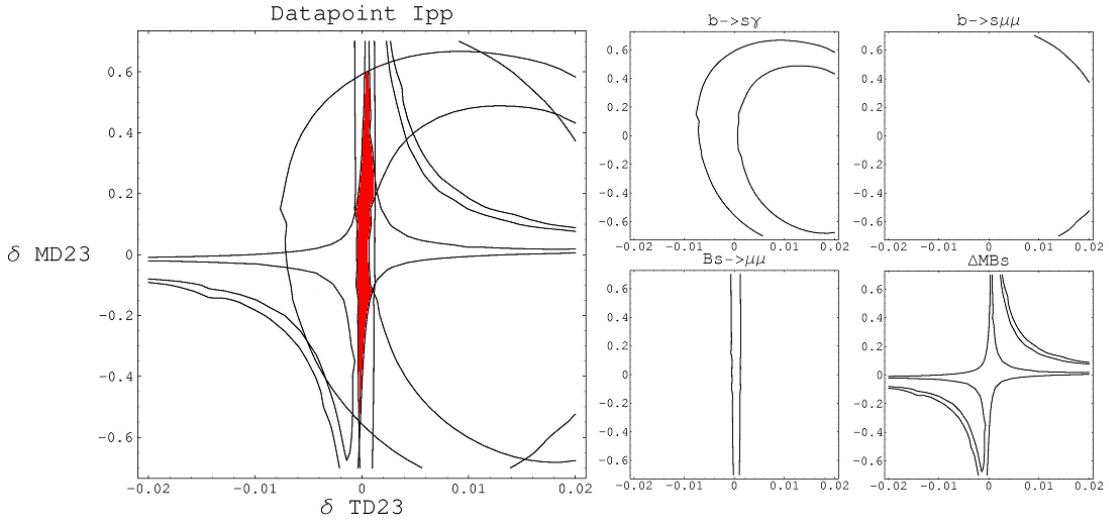

Figure 6.8: MD23/TD23 parameter plane at I"

When looking at graphs like the above [Fig.6.6-6.8], one should remember that the TD23 and TD32 normalizations depend on ν_1, which varies by roughly a factor of two between SPS1a' and γ, and a factor of four between SPS1a' and I". This leads to differently "zoomed in" graphs and allowed regions. We can again see that our bound on $B_s \to \mu^+\mu^-$ does not apply constraints on SPS1a', but is very important for data points with higher $tan\beta$

6.3.5 MD23 / TD32

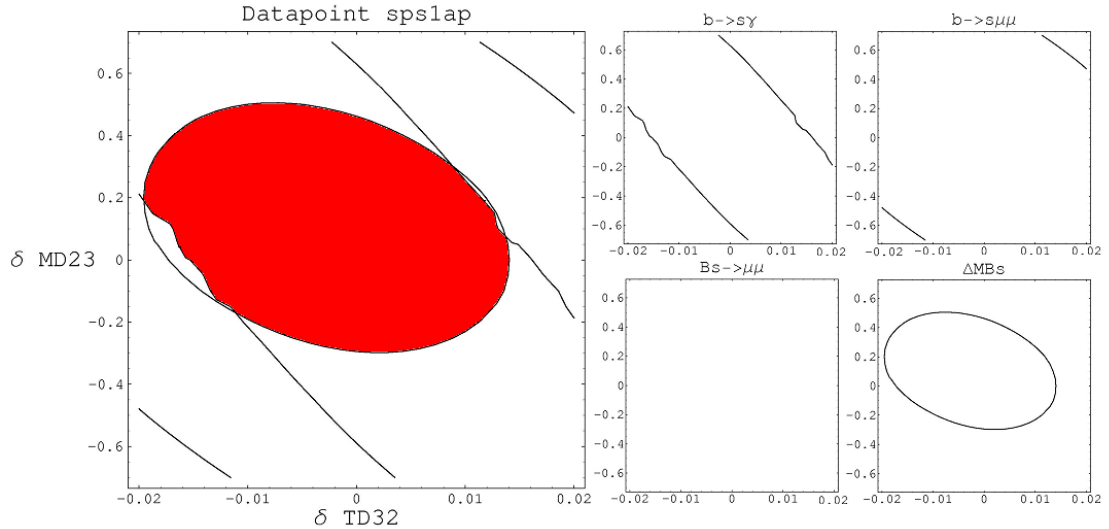

Figure 6.9: MD23/TD32 parameter plane at SPS1a'

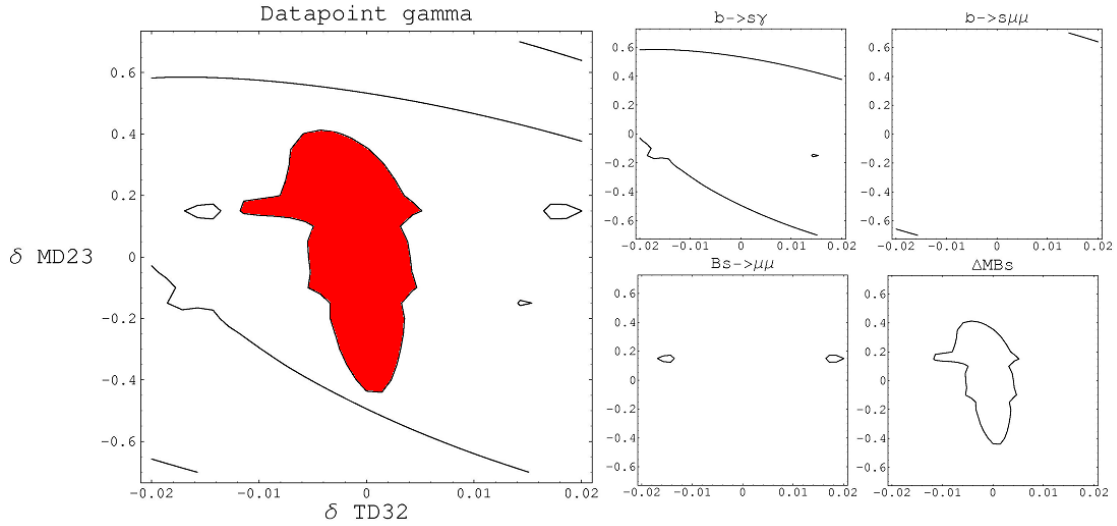

Figure 6.10: MD23/TD32 parameter plane at γ

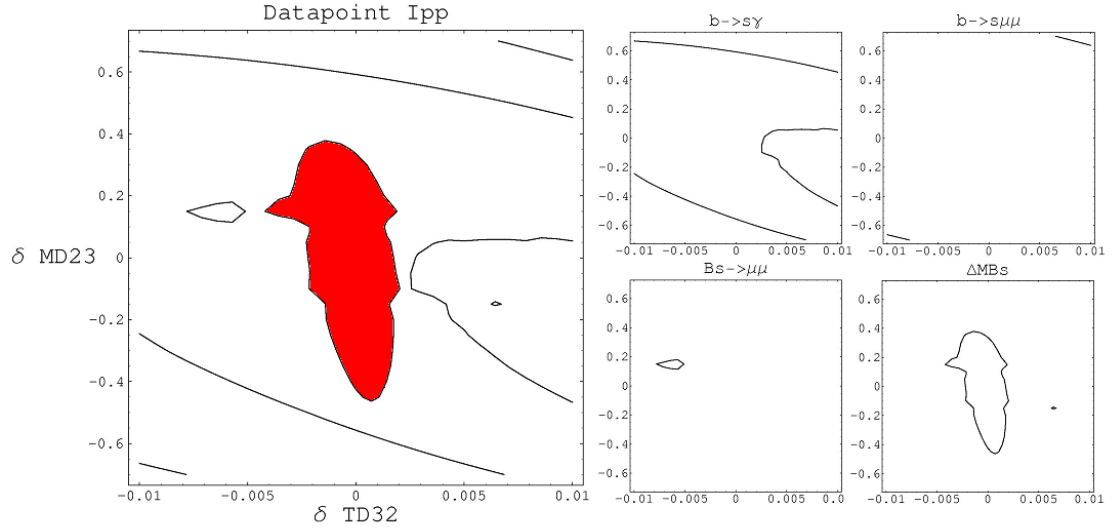

Figure 6.11: MD23/TD32 parameter plane at I"

In all data points [Fig.6.9-6.11], we have an asymmetrical allowed region, preferring negative values of TD32 and positive values of MD23. Each parameter slightly affects the allowed range of the other one shown, given mostly by ΔM_{B_s}, with growing effect in the extreme regions.

6.3.6 TD23 / TD32

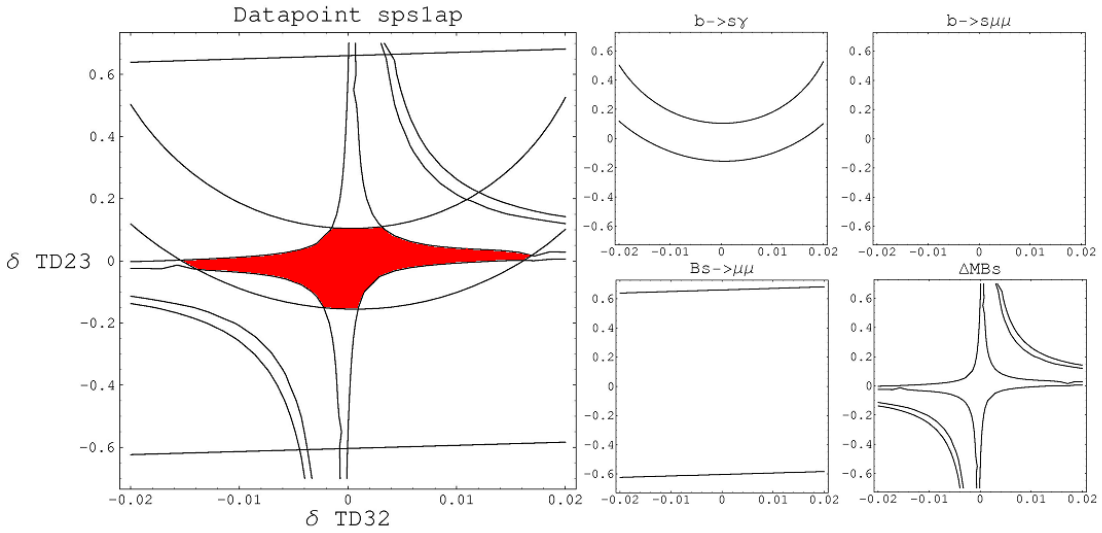

Figure 6.12: TD23/TD32 parameter plane at SPS1a'

The most striking effect of this graph [Fig.6.12] is that higher values of TD23 affect the usually poorly constrained TD32, thus leading to almost unconstrained MD23 in these regions (in the approximation of no 3-parameter-interplay).

6.3.7 Up-Sector

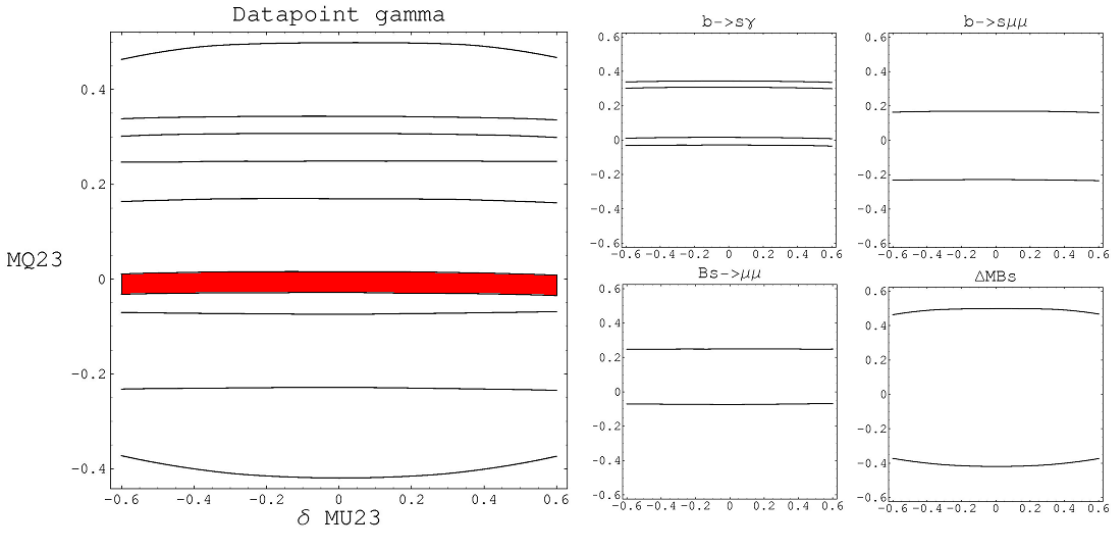

Figure 6.13: Example for MU23 effects on the constraining bands

The bounds from our low energy observables on the U-sector are, except for TU23, very loose. MU23 and TU32 lead to small changes in the bending of the constraining bands [Fig.6.13], but there is no serious information gained looking at them. For the I" data point, the bending of $b \to s\gamma$ is big enough to actually apply constraints on MU23, but they are still very loose ($\delta MU23 = -0.5...0.5$).

At all data points, $b \to s\gamma$ is the observable eventually constraining the TU parameters [Fig.6.14]. Unlike other interplays, decays like $B_s \to \mu^+\mu^-$ do not add any additional constraints at the γ and I" data points, compared to SPS1a'.

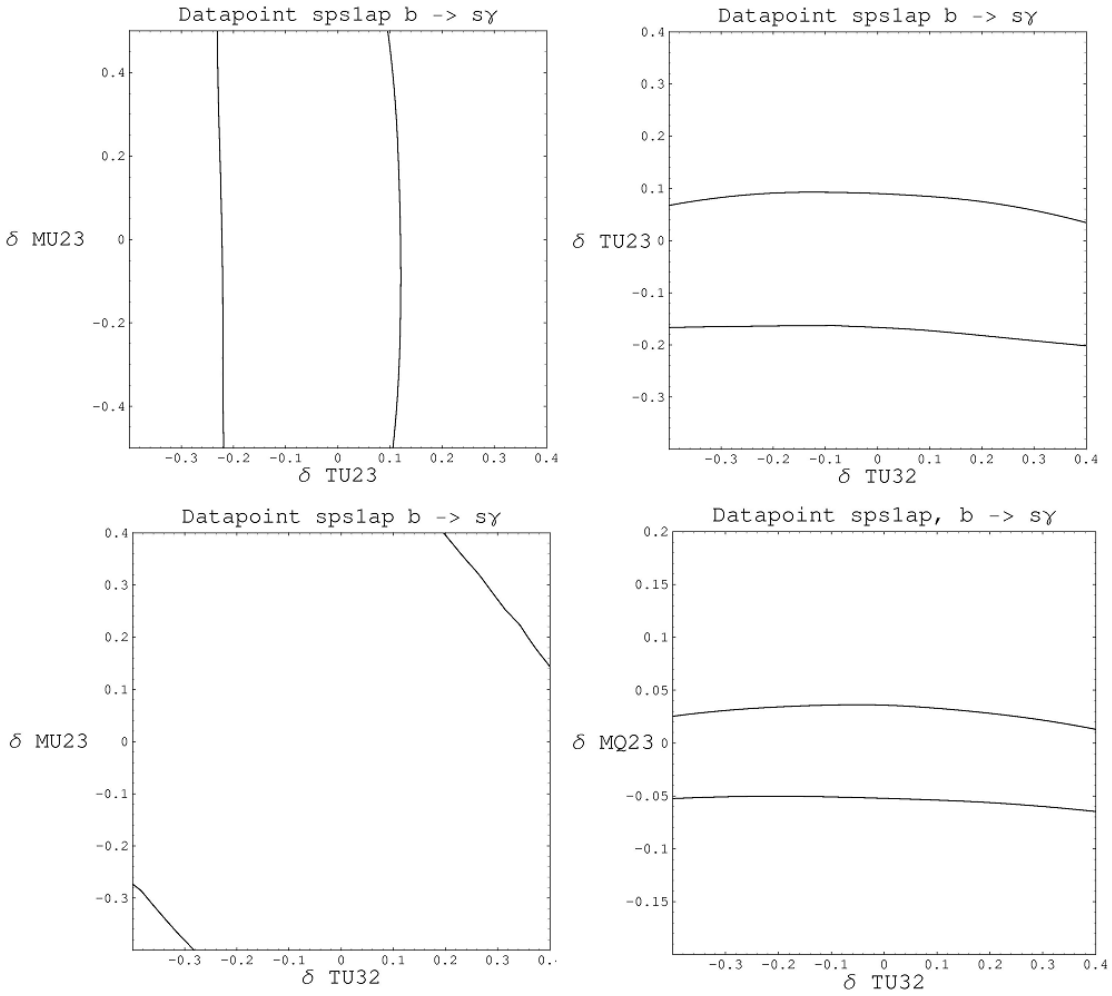

Figure 6.14: $b \to s\gamma$ constraints on TU parameters. They look very similar at all data points and represent the only important constraints

The most interesting interplay happens between MQ23 and TU23 [Fig.6.15]. Due to its small allowed area, the induced band shift by TU23 is of importance for the constraints on MQ23. Because multiple squark and gluino decays are senstitive to the latter, we can expect to find considerable changes in the branching ratios of interesting decays when taking into account the interplay between MQ23 and TU23.

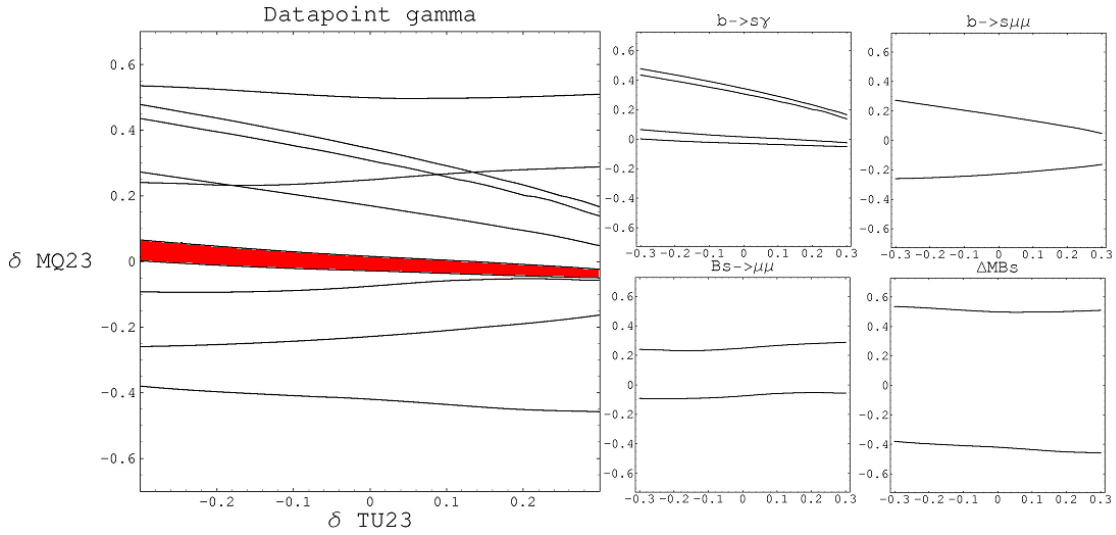

Figure 6.15: MQ23 / TU23 interplay at the γ data point. At SPS1a', the constraints by $B_s \to \mu^+\mu^-$ are missing in this case, but this doesn't alter the allowed region

6.4 Squark and gluino decays

In this section, we will give examples of flavor violating decays of the two lightest up- and down-squarks, as well as light gluinos. We show that the mixing in the allowed regions of parameter space can be significant by switching on flavor violating parameters, and give insight into the underlying mixing matrices. All FV decays are discussed, provided the mixing is large enough to induce branching ratios roughly in the same order of magnitude for the the flavor conserving decay on the one hand, and the flavor violating decay on the other hand. In the following mixing matrix pictures, Ru/Rd means u/d-squark mixing matrix, the first number represents the mass eigenstate, the second number the squark family index (1..3 lefthanded, 4..6 righthanded) and the letters are abbreviations for the shape of the graph (S = solid line, D = dashed, PD = point-dashed, P = points only). If the graphs for the three data points are very similar, one out of them is taken as an example.

For the correct understanding of the following flavor violating decays, it is important to look at the mixing matrix elements which - besides gauge and Yukawa couplings - govern the decays. Since the physical particles are a mixture of left- and right-squarks, they also have mixed decay preferences, depending on which gauge eigenstate they are alike.

Right-squark-like eigenstates almost exclusively decay into a bino and a quark, while left-squark-like eigenstates predominantly decay into charged winos ($\approx 60\%$), neutral winos ($\approx 30\%$) and more rarely a bino ($\approx 10\%$). Usually, one can assume that $\tilde{\chi}_1$ are bino-like particles, and $\tilde{\chi}_2$ wino-like. If either of these two become too higgsino-like, other effects like strong Yukawa couplings need to be taken into account, and the above percentages can change.

6.4.1 $\tilde{u}_1$ decays

decay	data point SPS1a'	data point γ	data point I"
$\tilde{u}_1 \to \tilde{\chi}_1^0 t$	0.224	0.209	0.201
$\tilde{u}_1 \to \tilde{\chi}_2^0 t$	0.0580	0.137	0.147
$\tilde{u}_1 \to \tilde{\chi}_1^+ b$	0.717	0.403	0.457
$\tilde{u}_2 \to \tilde{\chi}_1^0 c$	0.987	$\leq$1%	$\leq$1%
$\tilde{u}_2 \to \tilde{\chi}_1^0 t$	$\leq$1%	0.0238	0.0273
$\tilde{u}_2 \to \tilde{\chi}_2^0 t$	$\leq$1%	0.0979	0.0806
$\tilde{u}_2 \to \tilde{\chi}_3^0 t$	$\leq$1%	0.0913	0.0855
$\tilde{u}_2 \to \tilde{\chi}_4^0 t$	$\leq$1%	0.242	0.237
$\tilde{u}_2 \to \tilde{\chi}_1^+ b$	$\leq$1%	0.261	0.214
$\tilde{u}_2 \to \tilde{\chi}_2^+ b$	$\leq$1%	0.237	0.241
$\tilde{u}_2 \to \tilde{u}_1 Z$	$\leq$1%	0.0325	0.0886
$\tilde{u}_2 \to \tilde{u}_1 h_0$	$\leq$1%	0.0126	0.0218

Figure 6.16: branching ratios (larger than 1%) of the two lightest up-squarks, when all flavor violating parameters are switched off.

The most important parameters for these decays are MU23, TU23 and TU32, while MQ23 has almost no effect, mainly due to its small allowed region confined by the low energy observables. When all FV parameters are switched off, we have roughly 20% of $\tilde{u}_1 \to \tilde{\chi}_1^0 t$ and no decay into charm quarks at all data points. When switching on MU23 [Fig.6.17], mixing occurs and we observe branching ratios for $\tilde{u}_1 \to \tilde{\chi}_1^0 c$ up to 30 % for γ and SPS1a', 15% for I". At MU23 = 0, the $\tilde{u}_1$ is completely stop-like with a small LR-mixing. With growing MU23, RR-mixing induces decays into $\tilde{\chi}_1^0 c$. The sum of the right-like parts becomes larger at the cost of the $\tilde{t}_L$-like part of the $\tilde{u}_1$. leading to increased branching ratios of both $\tilde{u}_1 \to \tilde{\chi}_1^0 c$ and $\tilde{u}_1 \to \tilde{\chi}_1^0 t$.

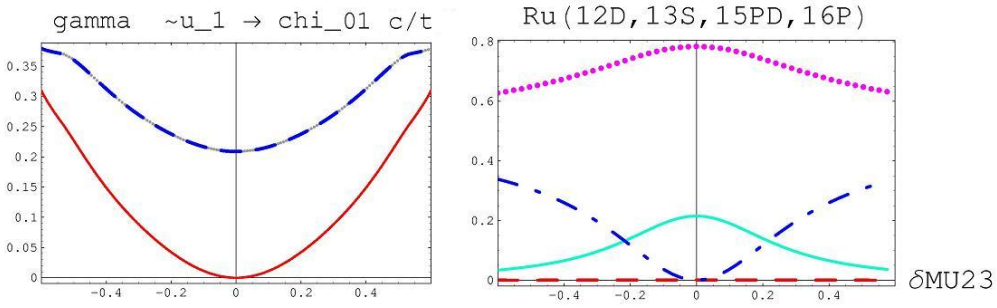

Figure 6.17: $\tilde{u}_1$ decays depending on MU23, γ data point. *left*: solid line: FV decay into charm quarks, dashed line: decay into top quarks. *right*: corresponding mixing matrix entries

TU23 leads to flavor violation via $\tilde{u}_1 \to \tilde{\chi}_2^0 c$ and $\tilde{u}_1 \to \tilde{\chi}_1^+ s$ [Fig.6.18]. At γ and I", these decays look very similar while at SPS1a', the branching ratio for the decay into the second lightest neutralinos is about half as large, and the decay into charginos is almost doubled. We here have an example of additional kinematic and gaugino/higgsino interference effects. The very dominating decay into $\tilde{\chi}_1^+$ at SPS1a' is also a consequence of the strong top-Yukawa-coupling to the higgsino-like parts of the chargino.

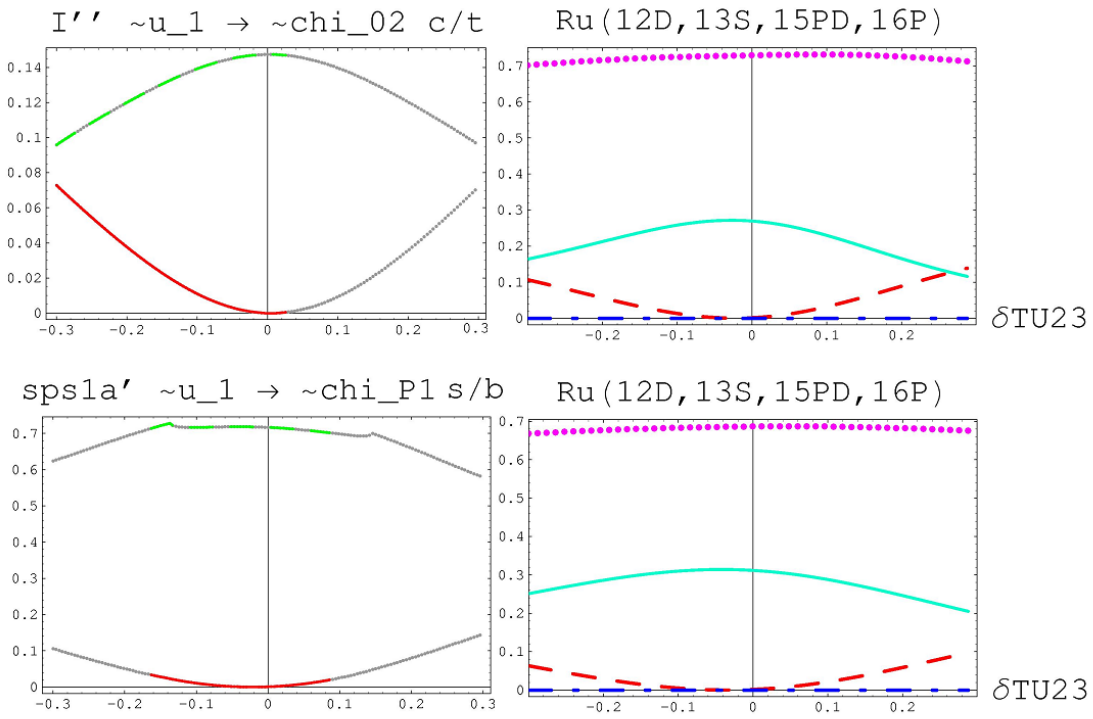

Figure 6.18: effect of TU23 on the $\tilde{u}_1$ sector. *left*: The solid lines are FV decays into second generation squarks, the dashed lines into third generation quarks. *right*: corresponding mixing matrix elements

When switching on TU32, we observe flavor violation via $\tilde{u}_1 \to \tilde{\chi}_1^0 c$ [Fig.6.19]. At first, the $\tilde{u}_1$ is (as expected) completely stop-like with considerable LR-mixing. TU32 induces a change in the hierarchy and the increasing $\tilde{c}_R$-like parts decay almost completely into $\tilde{\chi}_1^0 c$, resulting - together with the decrease of decays into tops - in a large increase of its branching ratio. Again, at γ and I", these decays are almost identical, while at SPS1a', we observe even larger branching ratios for $\tilde{u}_1 \to \tilde{\chi}_1^0 c$.

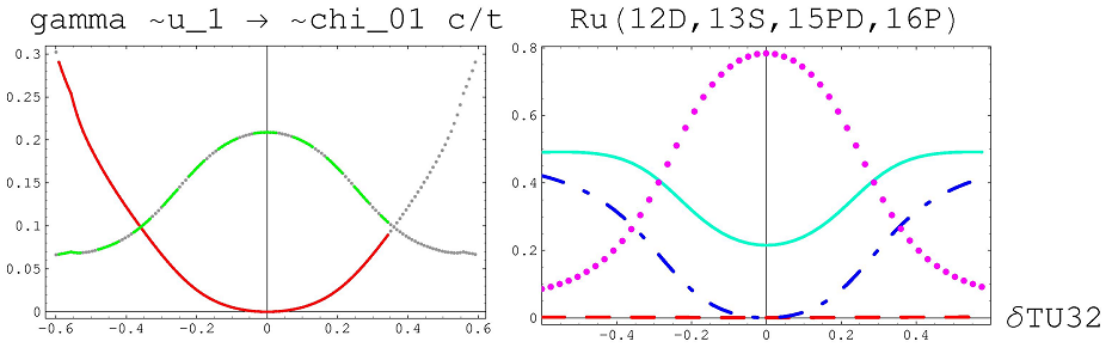

Figure 6.19: $\tilde{u}_1$ flavor violation induced by TU32. *left*: The solid line represents FV decays into charm quarks, the dashed line is the flavor conserving decay.(valid until BR ≈10%, where their roles begin to switch) *right*: corresponding mixing matrix elements

6.4.2 $\tilde{u}_2$ decays

MQ23, TU32 and MU23 do affect this sector slightly. MQ23 doesn't induce large mixings in general, due to its small region allowed by the low energy observables. With FV turned off, we have roughly 3% $\tilde{u}_2 \to \tilde{\chi}_1^0 t$, 10% $\tilde{u}_2 \to \tilde{\chi}_2^0 t$ and 25-30% $\tilde{u}_2 \to \tilde{\chi}_1^+ b$ for I" and γ.

TU32 induces flavor violating decays into charm quarks ($\tilde{u}_2 \to \tilde{\chi}_1^0 c$) at I" and γ [Fig.6.20], and into top quarks ($\tilde{u}_2 \to \tilde{\chi}_1^0 t$) at SPS1a'[Fig.6.21], respectively. Since the $\tilde{u}_2$ is - at γ and I" - predominantly $\tilde{t}_L$-like, these decays are not very important without flavor violating parameters. Now, a change in TU32 results in rapidly growing right-like parts and thus, increasing branching ratios of the mentioned decays. At SPS1a' though, the $\tilde{u}_2$ is nearly 100% $\tilde{c}_R$-like and stop-like parts grow with TU32.

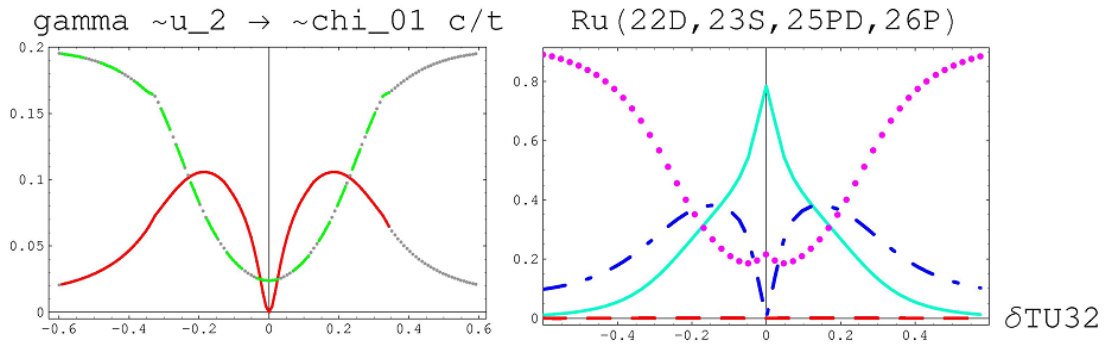

Figure 6.20: Consequences of TU32 on $\tilde{u}_2$ decays. left solid line: decay into charm, left dashed line: decay into top

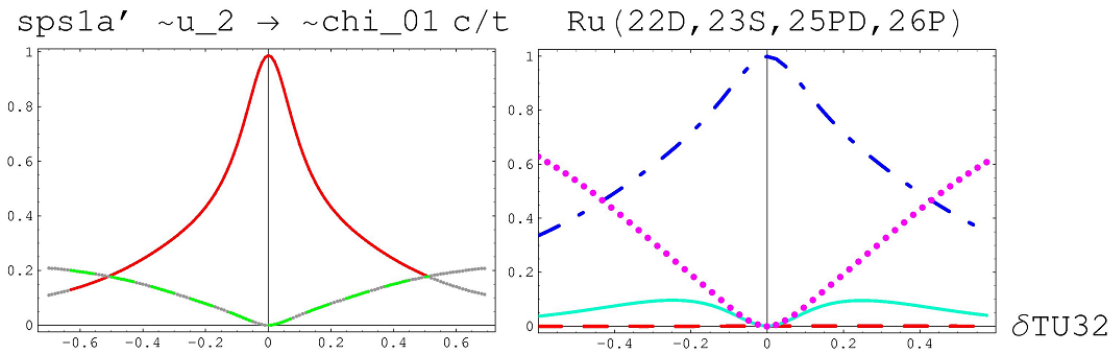

Figure 6.21: Effects of TU32 at SPS1a'. left solid line: decay into charm, left dashed line: decay into top

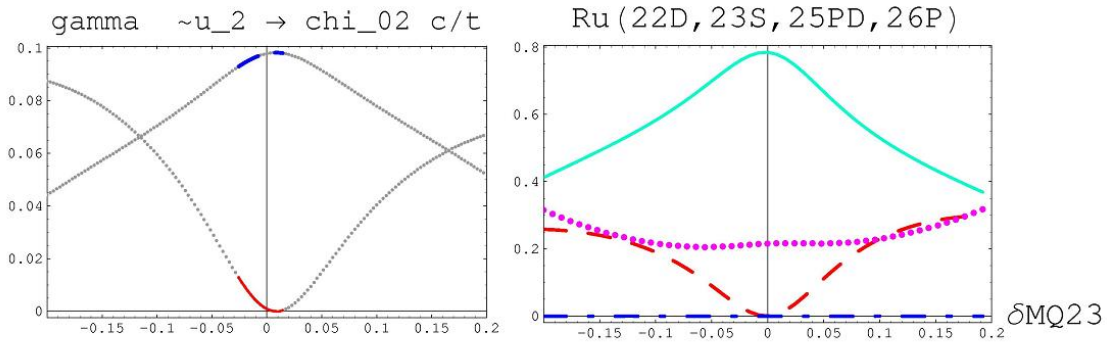

Figure 6.22: $\tilde{u}_2$ decay with MQ23 switched on. left solid line: decay into charm, left dashed line: decay into top

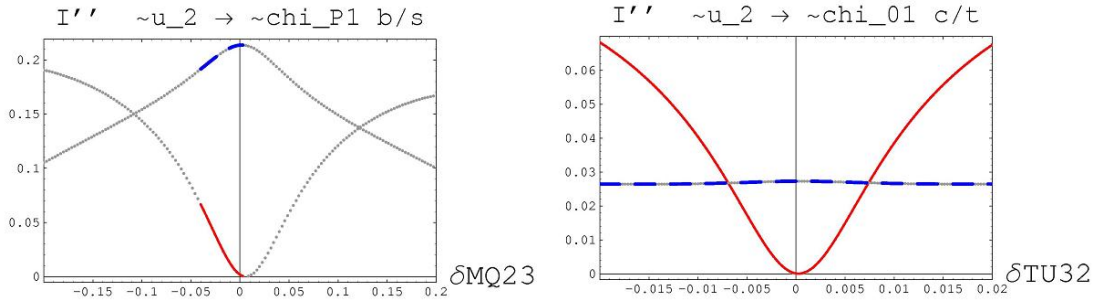

Figure 6.23: Examples of $\tilde{u}_2$ decays at I", solid line: decays into second generation quarks. dashed line: decay into third generation quarks

6.4.3 $\tilde{d}_1$ decays

decay	data point SPS1a'	data point γ	data point I"
$\tilde{d}_1 \to \tilde{\chi}_1^0 b$	0.0346	0.0692	0.06906
$\tilde{d}_1 \to \tilde{\chi}_2^0 b$	0.295	0.281	0.282
$\tilde{d}_1 \to \tilde{\chi}_3^0 b$	$\leq$1%	0.0819	0.0808
$\tilde{d}_1 \to \tilde{\chi}_4^0 b$	$\leq$1%	0.0484	0.0479
$\tilde{d}_1 \to \tilde{\chi}_1^- t$	0.366	0.413	0.412
$\tilde{d}_1 \to \tilde{\chi}_2^- t$	$\leq$1%	0.105	0.101
$\tilde{d}_1 \to \tilde{u}_1 W^-$	0.296	$\leq$1%	$\leq$1%
$\tilde{d}_2 \to \tilde{\chi}_1^0 b$	0.256	0.190	0.0182
$\tilde{d}_2 \to \tilde{\chi}_2^0 b$	0.105	0.0592	0.0547
$\tilde{d}_2 \to \tilde{\chi}_3^0 b$	0.0342	0.137	0.129
$\tilde{d}_2 \to \tilde{\chi}_4^0 b$	0.0438	0.152	0.143
$\tilde{d}_2 \to \tilde{\chi}_1^- t$	0.136	0.0794	0.0730
$\tilde{d}_2 \to \tilde{\chi}_2^- t$	$\leq$1%	0.495	0.462
$\tilde{d}_2 \to \tilde{u}_1 W^-$	0.426	0.0583	0.0120

Figure 6.24: branching ratios (larger than 1%) of the two lightest down-squarks, when all flavor violating parameters are switched off.

Looking into the down sector, we observe that MQ23, TD32 and especially MD23 induce significantly large flavor violating decays, while the largest are found at the SPS1a' data point. Without any perturbation, $\tilde{d}_1 \to \tilde{\chi}_1^0 b$ contributes 5-8 %, $\tilde{d}_1 \to \tilde{\chi}_1^- t$ about 35 %. The flavor violating $\tilde{d}_1 \to \tilde{\chi}_1^- c$ becomes large enough only at SPS1a' by altering MQ23. A considerable change in MD23 leads to very large FV decays for all three data points [Fig.6.25] - the larger $\tan\beta$, the smaller the branching ratio. (up to 12 % at SPS1a')

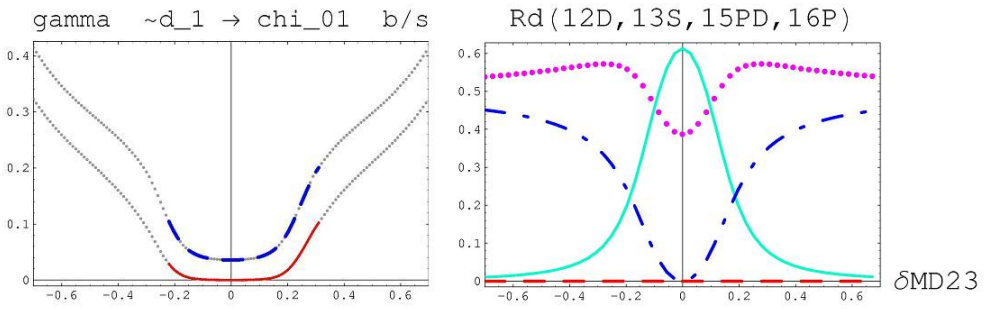

Figure 6.25: $\tilde{d}_1$ decays at γ, with corresponding mixing matrix elements left solid line: decay into strange quarks, left dashed line: decay into bottom quarks

At first, we only have LR-mixing, and with growing MD23, the lighter mixed right-like state becomes comparable in mass with the left-like, and eventually we find near 45 degree mixing in the RR part and vanishing left-like contributions. Since the $\tilde{d}_1$ consists almost 100% of right-like parts at large MD23, decays into $\tilde{\chi}_1^0 s$ and $\tilde{\chi}_1^0 b$ strongly increase.

6.4.4 $\tilde{d}_2$ decays

Without perturbation, we have 2% $\tilde{d}_2 \to \tilde{\chi}_1^0 b$ for I", 12 % for γ and 25 % for SPS1a'. 6 % $\tilde{d}_2 \to \tilde{\chi}_2^0 b$ for I" and γ,10 % for SPS1a', as well as 8-15 % $\tilde{d}_2 \to \tilde{\chi}_1^- t$ for all data points. With turned on FV, we can see a larger effect of MQ23 at SPS1a' for the first time [Fig.6.26]: $\tilde{s}_L$-like parts appear, slowly taking the place of the $\tilde{b}_L$-like parts in decays into charginos. For large TD32, the very $\tilde{b}_R$-like $\tilde{d}_2$ switches into being $\tilde{s}_R$-like [Fig.6.27], massively increasing $\tilde{d}_2 \to \tilde{\chi}_1^0 s$, again at SPS1a'. In the well-defined regions of flavor violation, we observe a branching ratio of $\approx 30\%$. At higher TD32, $\tilde{d}_2 \to \tilde{\chi}_1^0 s$ becomes the flavor conserving decay. The flavor violating effects on the $\tilde{d}_2$ squark decays are much less significant at I".

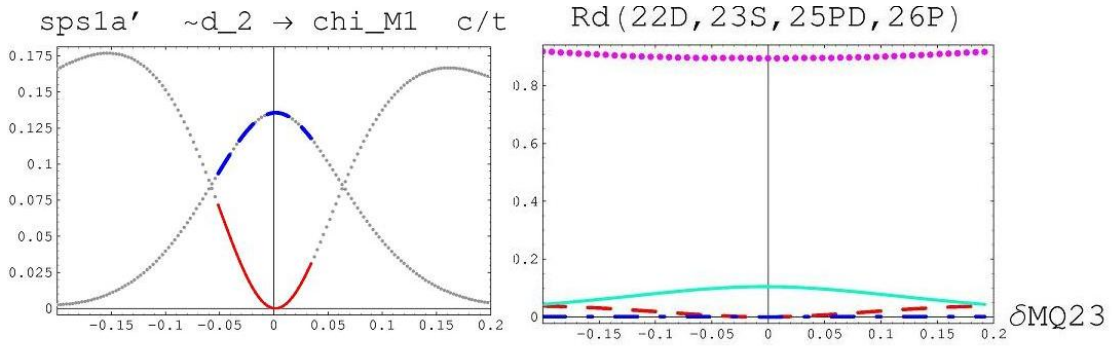

Figure 6.26: $\tilde{d}_2$ MQ23 decays and mixing matrix elements. left solid line: decay into strange quark. left dashed line: decay into bottom quark

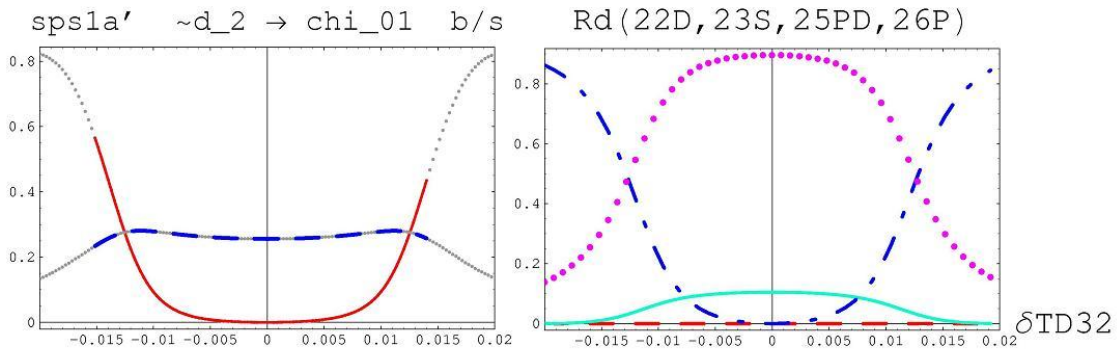

Figure 6.27: $\tilde{d}_2$ TD32 decays and mixing matrix elements. left solid line: decay into strange quark. left dashed line: decay into bottom quark

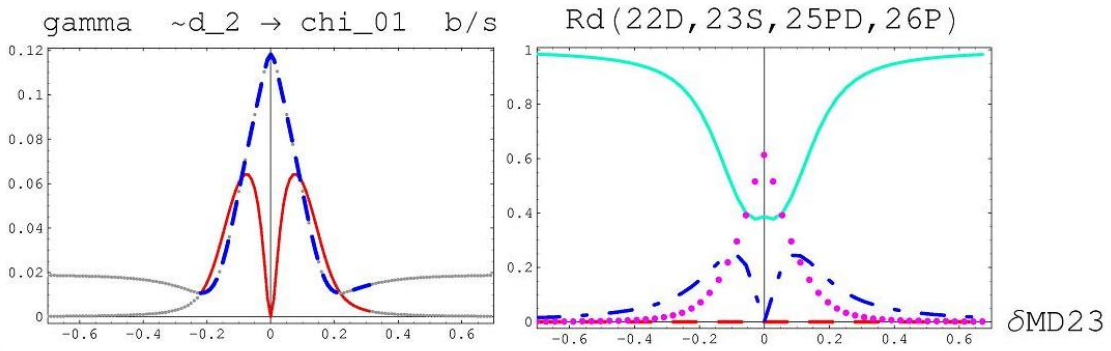

Figure 6.28: $\tilde{d}_2$ MD23 decays and mixing matrix elements. left solid line: decay into strange quark. left dashed line: decay into bottom quark

6.4.5 Gluino decays

decay	data point SPS1a'	data point γ	data point I"
$\tilde{g} \to \tilde{u}_1 t$	0.0983	0.0673	0.0778
$\tilde{g} \to \tilde{u}_2 c$	0.0421	$\leq$1%	$\leq$1%
$\tilde{g} \to \tilde{u}_3 u$	0.0422	$\leq$1%	$\leq$1%
$\tilde{g} \to \tilde{u}_3 c$	$\leq$1%	0.0401	0.0385
$\tilde{g} \to \tilde{u}_4 u$	$\leq$1%	0.0401	0.0385
$\tilde{g} \to \tilde{u}_4 c$	0.0217	$\leq$1%	$\leq$1%
$\tilde{g} \to \tilde{u}_5 u$	0.0216	0.0218	0.0211
$\tilde{g} \to \tilde{u}_6 c$	$\leq$1%	0.0217	0.0208
$\tilde{g} \to \tilde{d}_1 b$	0.110	0.124	0.124
$\tilde{g} \to \tilde{d}_2 b$	0.0453	0.0601	0.0598
$\tilde{g} \to \tilde{d}_3 s$	0.0426	0.0414	0.0398
$\tilde{g} \to \tilde{d}_4 d$	0.0426	0.0414	0.0398
$\tilde{g} \to \tilde{d}_5 s$	0.0150	0.0181	0.0175
$\tilde{g} \to \tilde{d}_6 d$	0.0150	0.0181	0.0175

Figure 6.29: branching ratios (larger than 1%) of gluinos, when all flavor violating parameters are switched off.

For flavor violating gluino decays, MQ23 is of minor importance, and we only present MU23 and MD23 sweeps for the u- and d-sector respectively, as well as TU23 and TU32. You can see the comparison of the FV decay modes into down squarks at γ and I" below [Fig.6.30], as well as a typical FV decay in the u-sector,

$\tilde{g} \to \tilde{u}_1 c$ [Fig.6.31], which looks very similar at all data points. The SPS1a' decays into down squarks are also compareable to I". The TU23/TU32 dependant gluino decays are also very similar at all data points, the only noteable difference is at I", where the allowed parameter region is shifted almost completely towards negative values of the parameter.

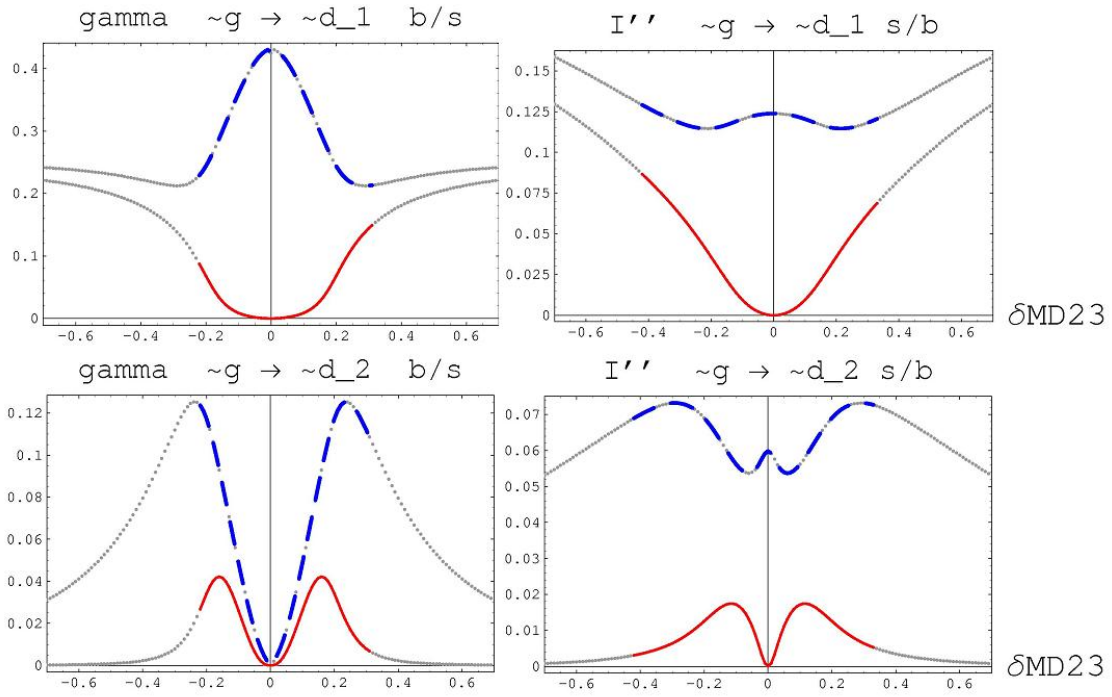

Figure 6.30: comparison between γ and I" gluino decays sensitive to MD23, left solid line: decay into strange quarks, left dashed line: decay into bottom quarks.

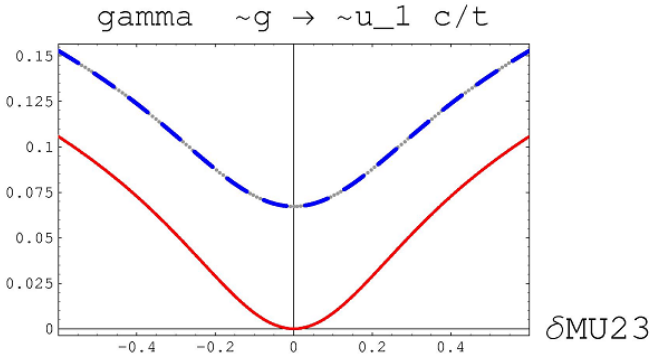

Figure 6.31: typical decay in the u-sector, here shown at γ.left solid line: decay into strange quarks, left dashed line: decay into bottom quarks.

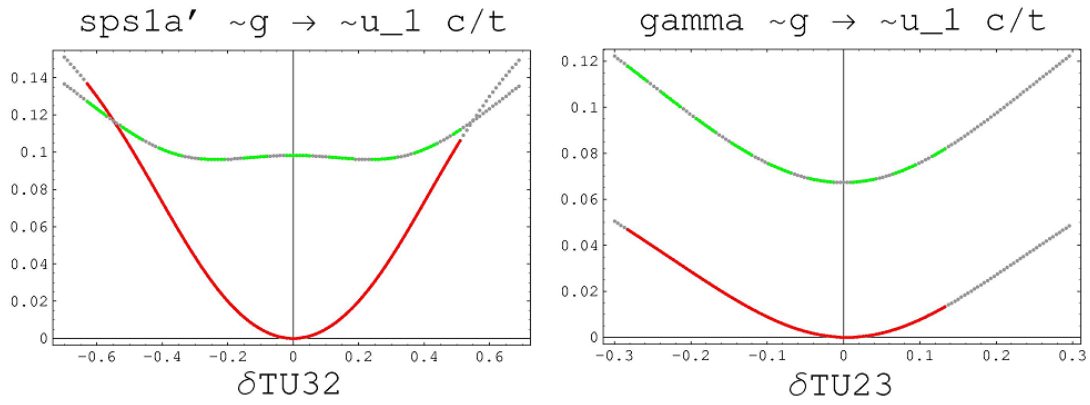

Figure 6.32: Gluino decays depending on TU23/TU32. left solid line: decay into charm quarks. left dashed line: decay into top quarks.

6.5 Squark and gluino decay maxima

In this section, we check if the discussed flavor violating decays can become significantly (factor three or above) larger when adding a second parameter. Each interesting decay was probed in every possible parameter interplay. There were few suprising results, yet we did find a change in the branching ratio of some decays up to the factor of five.

At SPS1a', there was a striking discrepancy between the sweep of MQ23 alone and its parameter interplay with TD23 [Fig.6.33]. The branching ratios of the decays $\tilde{d}_1 \to \tilde{\chi}_1^- c$, $\tilde{d}_2 \to \tilde{\chi}_1^- c$ and $\tilde{d}_2 \to \tilde{\chi}_2^0 s$ vastly increased by a factor 3 up to factor 6. The reason for this becomes clear if we again take a look at the parameter interplay between MQ23 and TD23: MQ23 is confined by $b \to s\gamma$ to a narrow band in the parameter space. Yet, TD23 determines where the allowed region of MQ23 is located, and allows for significantly larger values of MQ23. When the latter is switched off, $\tilde{d}_1$ is mainly $\tilde{b}_L$-like, $\tilde{d}_2$ is mainly $\tilde{b}_R$-like. With increasing MQ23, both particles slowly become more $\tilde{s}_L$-like, predominantly decaying into charginos and wino-like neutralinos, together with strange or charm quarks. Although only a small absolute fraction of the down-squarks is $\tilde{s}_L$-like, the increase due to the enlarged allowed area of MQ23 is significant. Especially for the $\tilde{d}_1$, the partner decay into bottom/top is only slightly affected.

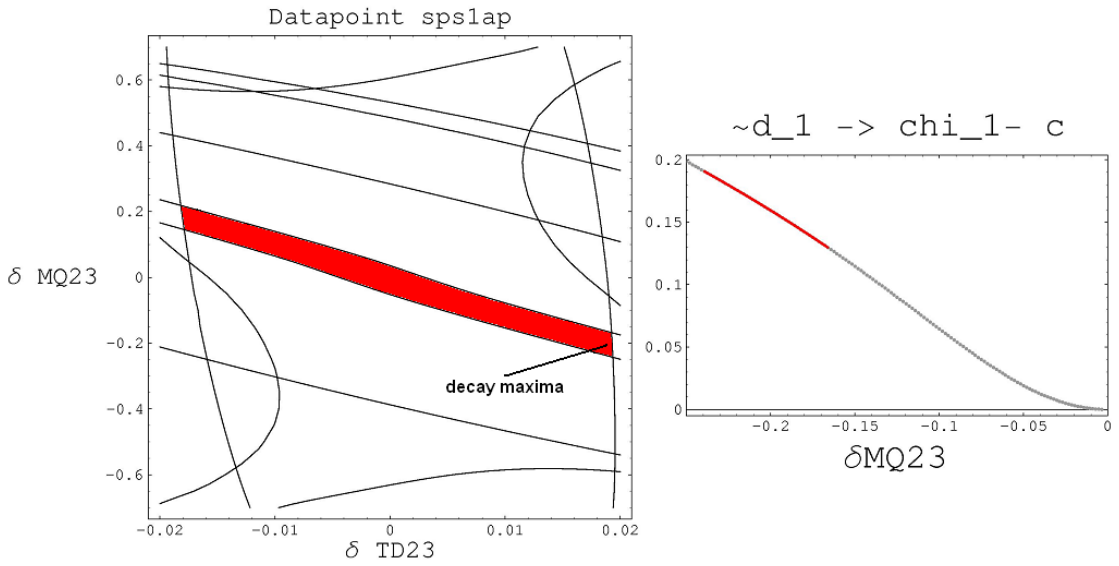

Figure 6.33: left: parameter interplay MQ23/TD23 right: example of the strong MQ23 dependence near the absolute allowed maximum TD23 = 0.019

At γ and I", the above isn't observed due to the additional confinement of TD23 by $B_s \to \mu^+\mu^-$. There is a very similar effect in the MQ23/TU23 plane, where TU23 influences the $b \to s\gamma$ constraints on MQ23 and extends its allowed region in a way that roughly doubles some of the MQ23-dependant branching ratios like $\tilde{u}_1 \to \tilde{\chi}_1^+ b$. Since the effect is much smaller than in the MQ23/TD23-plane and essentially the same, we won't discuss it here.

Apart from that,we found an anomaly in the parameter plane MQ23/MD23 compared to the MQ sweep alone, affecting the decays $\tilde{d}_2 \to \tilde{\chi}_1^- t$ and $\tilde{d}_2 \to \tilde{\chi}_2^0 b$ at all three data points, roughly by a factor of four at I"/γ and a factor of three at SPS1a'.[Fig.6.34]
Looking at the parameter plane and the parameter dependencies, we find a reason. MD23 is strongly affecting the above decays, because at MD23 = 0, the $\tilde{d}_2$ is almost completely $\tilde{b}_R$-like. When switching on MD23, it rapidly induces a large RR-mixing, leading to flavor violation via $\tilde{d}_2 \to \tilde{\chi}_1^0 s/b$. When MD23 continues to grow, the $\tilde{d}_2$ quickly becomes almost exclusively $\tilde{b}_L$-like, which - as we know - predominantly decays into charginos and wino-like neutralinos (exactly the above decays). In consequence, $\tilde{d}_2 \to \tilde{\chi}_1^0 s/b$ vanishes and the branching ratios of the above decays increase. Therefore we find the maxima for these in the high MD23 regions. From the perspective of flavor violation, this effect isn't too interesting, since in the high MD23 regions, the partner decays $\tilde{d}_2 \to \tilde{\chi}_1^- c$ and $\tilde{d}_2 \to \tilde{\chi}_2^0 s$ become very small. At SPS1a', the change in branching ratios is smaller than at the other two data points, since it provides a larger allowed region for MQ23 and, consequently, larger branching ratios in the sweep of MQ23 alone.

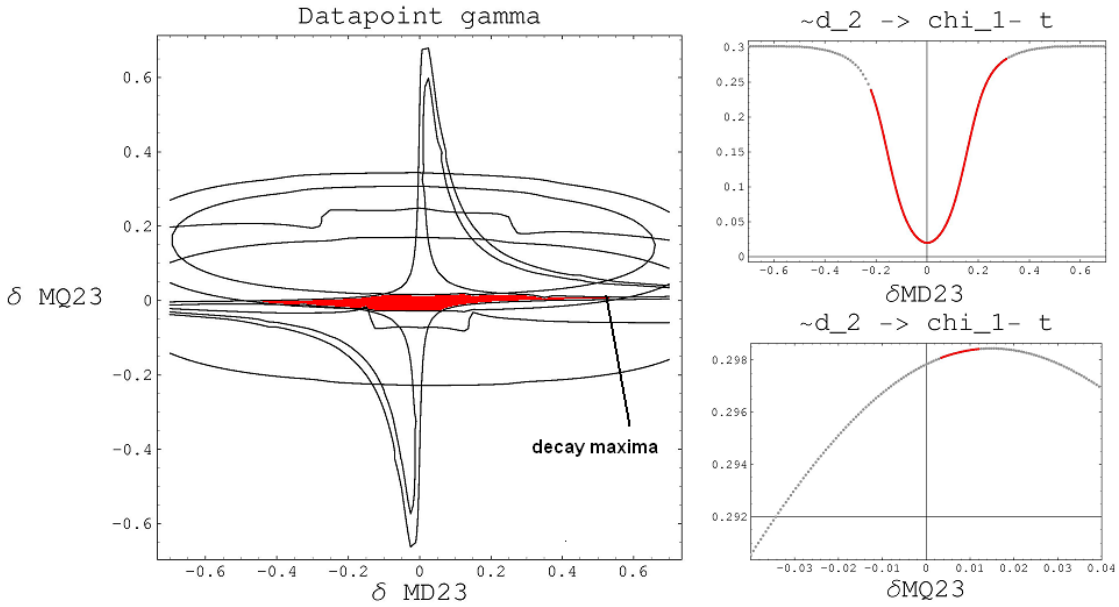

Figure 6.34: left: parameter interplay MQ23/MD23. top right: example of the MD23 at MQ23 = 0. bottom right: MD23 dependence at MQ23 = 0.5, near the absolute maximum

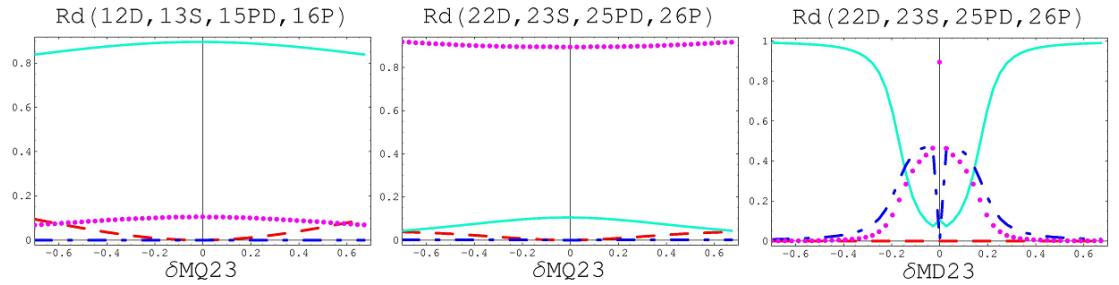

Figure 6.35: mixing matrix elements for the above discussions. S=solid, D=dashed, P=points, PD=point-dashed

7 Summary and Outlook

We showed that in the given nMFV scenarios, we can induce large flavor violation in the area of parameter space allowed by low energy observables by switching on off-diagonal elements of the soft SUSY breaking squark masses and trilinear couplings. At all data points, we observed considerable flavor violation by squark and gluino decays, for example $\tilde{u}_1 \to \tilde{\chi}_1^0 c$ with 30% at γ, $\tilde{u}_2 \to \tilde{\chi}_1^0 c$ and $\tilde{d}_1 \to \tilde{\chi}_1^0 s$, both 10% at γ, and $\tilde{d}_2 \to \tilde{\chi}_1^0 s$ with 30% at SPS1a'. An example for FV gluino decays is $\tilde{g} \to \tilde{u}_1 c$ with about 10% at all datapoints.

We investigated the interplay between pairs of flavor violating parameters and strongly constrained the parameter space by using low energy observables in the B physics sector. With the help of these interplay observations, we then checked if the branching ratios of the discussed decays can be significantly larger when manipulating two parameters at once - especially in the MQ23/TD23 and MQ23/TU23 plane at the SPS1a' data point, this indeed was the case for $\tilde{d}_2 \to \tilde{\chi}_1^- c$ and $\tilde{d}_2 \to \tilde{\chi}_2^0 s$.

These results gave a first insight in how the possible parameter combinations can affect each other, and which regions of nMFV MSSM can be excluded by phenomenology. The next step would be to combine the above considerations to cascade decays like $\tilde{g} \to \tilde{d}_1 b$ with $\tilde{d}_1$ further decaying into $s\tilde{\chi}_1^0$. One would then look at differential distributions of jets at the LHC zu extract information about the underlying parameters.

8 Appendix

8.1 Rotation into physical fields - calculations

8.1.1 $\mathcal{L}_I$ in mass eigenstates

In the first step of the calculation, we use the transformations from section [2.7] to rotate the fields into mass eigenstates. In each line with Yukawa matrices, an identity $U_{qL}^\dagger U_{qL} = U_{qR}^\dagger U_{qR} = \mathbf{1}$ is added to contract some of the rotation and the Yukawa matrices to the diagonal quark mass matrices $\hat{m}_q$ and the V_{CKM} in the second step.

Charginos

First step:

$$\begin{aligned}\mathcal{L}_I|_{\tilde{q}q\tilde{\chi}^\pm} = -g[&\tilde{u}_p^*(R_{uL}^\dagger)_{pg}(U_{uL}^\dagger)_{gf}(U_{dL})_{fk}d_{L_k}V_{1n}^\dagger\tilde{C}_n^+\\ &+\tilde{d}_p^*(R_{dL}^\dagger)_{pg}(U_{dL}^\dagger)_{gf}(U_{uL})_{fk}u_{L_k}U_{1n}^\dagger\tilde{C}_n^-\\ &+\overline{\tilde{C}_n^-}U_{n1}\overline{u}_{L_k}(U_{uL}^\dagger)_{kf}(U_{dL})_{fg}(R_{dL})_{gi}\tilde{d}_i\\ &+\overline{\tilde{C}_n^+}V_{n1}\overline{d}_{L_k}(U_{dL}^\dagger)_{kf}(U_{uL})_{fg}(R_{uL})_{gi}\tilde{u}_i]\end{aligned} \tag{8.1}$$

$$\begin{aligned}&+U_{2n}^\dagger\tilde{C}_n^-\overline{d}_{R_k}(U_{dR}^\dagger)_{kj}(Y_D^T)_{ji}(U_{dL})_{il}(U_{dL}^\dagger)_{lm}(U_{uL})_{mo}(R_{uL})_{op}\tilde{u}_p\\ &+V_{2n}^\dagger\tilde{C}_n^+\overline{u}_{R_k}(U_{uR}^\dagger)_{kj}(Y_U^T)_{ji}(U_{uL})_{il}(U_{uL}^\dagger)_{lm}(U_{dL})_{mo}(R_{dL})_{op}\tilde{d}_p\\ &+U_{2n}^\dagger\tilde{C}_n^-\tilde{d}_p^*(R_{dR}^\dagger)_{po}(U_{dR}^\dagger)_{oj}(Y_D^T)_{ji}(U_{dL})_{il}(U_{dL}^\dagger)_{lm}(U_{uL})_{mk}u_{L_k}\\ &+V_{2n}^\dagger\tilde{C}_n^+\tilde{u}_p^*(R_{uR}^\dagger)_{po}(U_{uR}^\dagger)_{oj}(Y_U^T)_{ji}(U_{uL})_{il}(U_{uL}^\dagger)_{lm}(U_{dL})_{mk}d_{L_k}\end{aligned} \tag{8.2}$$

$$
\begin{aligned}
&+ \overline{\tilde{C}_n^-} U_{n2} \tilde{u}_p^* (R_{uL}^\dagger)_{po} (U_{uL}^\dagger)_{oj} (U_{dL})_{jl} (U_{dL}^\dagger)_{lm} (Y_D^*)_{mi} (U_{dR})_{ik} d_{R_k} \\
&+ \overline{\tilde{C}_n^+} V_{n2} \tilde{d}_p^* (R_{dL}^\dagger)_{po} (U_{dL}^\dagger)_{oj} (U_{uL})_{jl} (U_{uL}^\dagger)_{lm} (Y_U^*)_{mi} (U_{uR})_{ik} u_{R_k} \\
&+ \overline{\tilde{C}_n^-} U_{n2} \overline{u}_{L_k} (U_{uL}^\dagger)_{kj} (U_{dL})_{jm} (U_{dL}^\dagger)_{mo} (Y_D^*)_{oi} (U_{dR})_{il} (R_{dR})_{lp} \tilde{d}_p \\
&+ \overline{\tilde{C}_n^+} V_{n2} \overline{d}_{L_k} (U_{dL}^\dagger)_{kj} (U_{uL})_{jm} (U_{uL}^\dagger)_{mo} (Y_U^*)_{oi} (U_{uR})_{il} (R_{uR})_{lp} \tilde{u}_p
\end{aligned}
\tag{8.3}
$$

Second step:

$$
\begin{aligned}
\mathcal{L}_I|_{\tilde{q}q\tilde{\chi}^\pm} = -g[&\tilde{u}_p^* (R_{uL}^\dagger)_{pg} (V_{CKM})_{gk} d_{L_k} V_{1n}^\dagger \tilde{C}_n^+ \\
&+ \tilde{d}_p^* (R_{dL}^\dagger)_{pg} (V_{CKM}^\dagger)_{gk} u_{L_k} U_{1n}^\dagger \tilde{C}_n^- \\
&+ \overline{\tilde{C}_n^-} U_{n1} \overline{u}_{L_k} (V_{CKM})_{fg} (R_{dL})_{gp} \tilde{d}_p \\
&+ \overline{\tilde{C}_n^+} V_{n1} \overline{d}_{L_k} (V_{CKM}^\dagger)_{fg} (R_{uL})_{gp} \tilde{u}_p]
\end{aligned}
\tag{8.4}
$$

$$
\begin{aligned}
&+ \frac{\sqrt{2}}{\nu_1} U_{2n}^\dagger \tilde{C}_n^- \overline{d}_{R_k} (\hat{m}_d)_{kl} (V_{CKM}^\dagger)_{lo} (R_{uL})_{op} \tilde{u}_p \\
&+ \frac{\sqrt{2}}{\nu_2} V_{2n}^\dagger \tilde{C}_n^+ \overline{u}_{R_k} (\hat{m}_u)_{kl} (V_{CKM})_{lo} (R_{dL})_{op} \tilde{d}_p \\
&+ \frac{\sqrt{2}}{\nu_1} U_{2n}^\dagger \tilde{C}_n^- \tilde{d}_p^* (R_{dR}^\dagger)_{po} (\hat{m}_d)_{oi} (V_{CKM}^\dagger)_{ik} u_{L_k} \\
&+ \frac{\sqrt{2}}{\nu_2} V_{2n}^\dagger \tilde{C}_n^+ \tilde{u}_p^* (R_{uR}^\dagger)_{po} (\hat{m}_u)_{oi} (V_{CKM})_{ik} d_{L_k}
\end{aligned}
\tag{8.5}
$$

$$
\begin{aligned}
&+ \frac{\sqrt{2}}{\nu_1} \overline{\tilde{C}_n^-} U_{n2} \tilde{u}_p^* (R_{uL}^\dagger)_{po} (V_{CKM})_{ol} (\hat{m}_d)_{lk} d_{R_k} \\
&+ \frac{\sqrt{2}}{\nu_2} \overline{\tilde{C}_n^+} V_{n2} \tilde{d}_p^* (R_{dL}^\dagger)_{po} (V_{CKM}^\dagger)_{ol} (\hat{m}_u)_{lk} u_{R_k} \\
&+ \frac{\sqrt{2}}{\nu_1} \overline{\tilde{C}_n^-} U_{n2} \overline{u}_{L_k} (V_{CKM})_{km} (\hat{m}_d)_{ml} (R_{dR})_{lp} \tilde{d}_p \\
&+ \frac{\sqrt{2}}{\nu_2} \overline{\tilde{C}_n^+} V_{n2} \overline{d}_{L_k} (V_{CKM}^\dagger)_{km} (\hat{m}_u)_{ml} (R_{uR})_{lp} \tilde{u}_p
\end{aligned}
\tag{8.6}
$$

Neutralinos

The neutralinos are a bit more work, but also easier due to absence of V_{CKM}.

$$\begin{aligned}\mathcal{L}_I|_{\tilde{q}q\tilde{\chi}^0} = -\sqrt{2}g'[&\frac{1}{6}\tilde{u}_p^*(R_{uL}^\dagger)_{pg}(U_{uL}^\dagger)_{gf}(U_{uL})_{fk}u_{L_k}N_{1n}\tilde{C}_n^0\\ &+\frac{1}{6}\tilde{d}_p^*(R_{dL}^\dagger)_{pg}(U_{dL}^\dagger)_{gf}(U_{dL})_{fk}d_{L_k}N_{1n}\tilde{C}_n^0\\ &+\frac{1}{6}\overline{u}_{L_k}(U_{uL}^\dagger)_{kf}(U_{uL})_{fg}(R_{uL})_{gp}\tilde{u}_pN_{1n}^*\overline{\tilde{C}_n^0}\\ &+\frac{1}{6}\overline{d}_{L_k}(U_{dL}^\dagger)_{kf}(U_{dL})_{fg}(R_{dL})_{gp}\tilde{d}_pN_{1n}^*\overline{\tilde{C}_n^0}\end{aligned} \tag{8.7}$$

$$\begin{aligned}&-\frac{2}{3}\tilde{u}_p^*(R_{uR}^\dagger)_{pg}(U_{uR}^\dagger)_{gf}(U_{uR})_{fk}u_{R_k}N_{1n}^*\overline{\tilde{C}_n^0}\\ &+\frac{1}{3}\tilde{d}_p^*(R_{dR}^\dagger)_{pg}(U_{dR}^\dagger)_{gf}(U_{dR})_{fk}d_{R_k}N_{1n}^*\overline{\tilde{C}_n^0}\\ &-\frac{2}{3}\overline{u}_{R_k}(U_{uR}^\dagger)_{kf}(U_{uR})_{fg}(R_{uR})_{gp}\tilde{u}_pN_{1n}\tilde{C}_n^0\\ &+\frac{1}{3}\overline{d}_{R_k}(U_{dR}^\dagger)_{kf}(U_{dR})_{fg}(R_{dR})_{gp}\tilde{d}_pN_{1n}\tilde{C}_n^0]\end{aligned} \tag{8.8}$$

$$\begin{aligned}-\frac{1}{\sqrt{2}}g[&\tilde{d}_p^*(R_{dL}^\dagger)_{pg}(U_{dL}^\dagger)_{gf}(U_{dL})_{fk}d_{L_k}N_{2n}\tilde{C}_n^0\\ &+\tilde{u}_p^*(R_{uL}^\dagger)_{pg}(U_{uL}^\dagger)_{gf}(U_{uL})_{fk}u_{L_k}N_{2n}\tilde{C}_n^0\\ &+\overline{u}_{L_k}(U_{uL}^\dagger)_{kf}(U_{uL})_{fg}(R_{uL})_{gp}\tilde{u}_pN_{2n}^*\overline{\tilde{C}_n^0}\\ &+\overline{d}_{L_k}(U_{dL}^\dagger)_{kf}(U_{dL})_{fg}(R_{dL})_{gp}\tilde{d}_pN_{2n}^*\overline{\tilde{C}_n^0}]\end{aligned} \tag{8.9}$$

$$\begin{aligned}&-N_{3n}\tilde{C}_n^0\overline{d}_{R_k}(U_{dR}^\dagger)_{kj}(Y_D^T)_{ji}(U_{dL})_{ig}(R_{dL})_{gp}\tilde{d}_p\\ &-N_{4n}\tilde{C}_n^0\overline{u}_{R_k}(U_{uR}^\dagger)_{kj}(Y_U^T)_{ji}(U_{uL})_{ig}(R_{uL})_{gp}\tilde{u}_p\\ &-N_{3n}\tilde{C}_n^0\tilde{d}_p^*(R_{dR}^\dagger)_{pg}(U_{dR}^\dagger)_{gj}(Y_D^T)_{ji}(U_{dL})_{ik}d_{L_k}\\ &-N_{4n}\tilde{C}_n^0\tilde{u}_p^*(R_{uR}^\dagger)_{pg}(U_{uR}^\dagger)_{gj}(Y_U^T)_{ji}(U_{uL})_{ik}u_{L_k}\end{aligned} \tag{8.10}$$

$$
\begin{aligned}
&- N_{3j}^{*}\overline{\tilde{C}_n^0}\tilde{d}_p^{*}(R_{dL}^{\dagger})_{pg}(U_{dL}^{\dagger})_{gj}(Y_D^{*})_{ji}(U_{dR})_{ik}d_{R_k}\\
&- N_{4j}^{*}\overline{\tilde{C}_n^0}\tilde{u}_p^{*}(R_{uL}^{\dagger})_{pg}(U_{uL}^{\dagger})_{gj}(Y_U^{*})_{ji}(U_{uR})_{ik}u_{R_k}\\
&- N_{3j}^{*}\overline{\tilde{C}_n^0}\overline{d}_{L_k}(U_{dL}^{\dagger})_{kj}(Y_D^{*})_{ji}(U_{dR})_{ig}(R_{dR})_{gp}\tilde{d}_p\\
&- N_{4j}^{*}\overline{\tilde{C}_n^0}\overline{u}_{L_k}(U_{uL}^{\dagger})_{kj}(Y_U^{*})_{ji}(U_{uR})_{ig}(R_{uR})_{gp}\tilde{u}_p
\end{aligned}
\tag{8.11}
$$

Second step:

$$
\begin{aligned}
\mathcal{L}_I|_{\tilde{q}q\tilde{\chi}^0} = &-\sqrt{2}g'N_{1n}\tilde{C}_n^0[\frac{1}{6}\tilde{u}_p^{*}(R_{uL}^{\dagger})_{pk}u_{L_k} + \frac{1}{6}\tilde{d}_p^{*}(R_{dL}^{\dagger})_{pk}d_{L_k}\\
&-\frac{2}{3}\overline{u}_{R_k}(R_{uR})_{kp}\tilde{u}_p + \frac{1}{3}\overline{d}_{R_k}(R_{dR})_{kp}\tilde{d}_p]
\end{aligned}
\tag{8.12}
$$

$$
\begin{aligned}
&-\sqrt{2}g'N_{1n}^{*}\overline{\tilde{C}_n^0}[-\frac{2}{3}\tilde{u}_p^{*}(R_{uR}^{\dagger})_{pk}u_{R_k} + \frac{1}{3}\tilde{d}_p^{*}(R_{dR}^{\dagger})_{pk}d_{R_k}\\
&+\frac{1}{6}\overline{u}_{L_k}(R_{uL})_{kp}\tilde{u}_p + \frac{1}{6}\overline{d}_{L_k}(R_{dL})_{kp}\tilde{d}_p]
\end{aligned}
\tag{8.13}
$$

$$
\begin{aligned}
&-\frac{1}{\sqrt{2}}gN_{2n}\tilde{C}_n^0[\tilde{u}_p^{*}(R_{uL}^{\dagger})_{pk}u_{L_k} + \tilde{d}_p^{*}(R_{dL}^{\dagger})_{pk}d_{L_k}]\\
&-\frac{1}{\sqrt{2}}gN_{2n}^{*}\overline{\tilde{C}_n^0}[\overline{u}_{L_k}(R_{uL})_{kp}\tilde{u}_p + \overline{d}_{L_k}(R_{dL})_{kp}\tilde{d}_p]\\
&-\frac{\sqrt{2}}{\nu_1}N_{3n}\tilde{C}_n^0(\overline{d}_{R_k}(\hat{m}_d)_{kg}(R_{dL})_{gp}\tilde{d}_p + \tilde{d}_p^{*}(R_{dR}^{\dagger})_{pg}(\hat{m}_d)_{gk}d_{L_k})\\
&-\frac{\sqrt{2}}{\nu_2}N_{4n}\tilde{C}_n^0(\overline{u}_{R_k}(\hat{m}_u)_{kg}(R_{uL})_{gp}\tilde{u}_p + \tilde{u}_p^{*}(R_{uR}^{\dagger})_{pg}(\hat{m}_u)_{gk}u_{L_k})\\
&-\frac{\sqrt{2}}{\nu_1}N_{3n}^{*}\overline{\tilde{C}_n^0}(\tilde{d}_p^{*}(R_{dL}^{\dagger})_{pg}(\hat{m}_d)_{gk}d_{R_k} + \overline{d}_{L_k}(\hat{m}_d)_{kg}(R_{dR}^{\dagger})_{gp}\tilde{d}_p)\\
&-\frac{\sqrt{2}}{\nu_2}N_{4n}^{*}\overline{\tilde{C}_n^0}(\tilde{u}_p^{*}(R_{uL}^{\dagger})_{pg}(\hat{m}_u)_{gk}u_{R_k} + \overline{u}_{L_k}(\hat{m}_u)_{kg}(R_{uR}^{\dagger})_{gp}\tilde{d}_p)
\end{aligned}
\tag{8.14}
$$

Gluinos

The color indices are supressed:

$$\begin{aligned}\mathcal{L}_I|_{\tilde{q}q\tilde{G}} = -\frac{g_3}{\sqrt{2}}[&\tilde{u}_p^*(R_{uL}^\dagger)_{pg}(U_{uL}^\dagger)_{gf}\lambda_{GM}^a(U_{uL})_{fk}u_{L_k}\tilde{G}^a \\ &+\overline{u}_{L_k}(U_{uL}^\dagger)_{kf}\lambda_{GM}^a(U_{uL})_{fg}(R_{uL})_{gp}\tilde{u}_p\overline{\tilde{G}^a} \\ &+\tilde{d}_p^*(R_{dL}^\dagger)_{pg}(U_{dL}^\dagger)_{gf}\lambda_{GM}^a(U_{dL})_{fk}d_{L_k}\tilde{G}^a \\ &+\overline{d}_{L_k}(U_{dL}^\dagger)_{kf}\lambda_{GM}^a(U_{dL})_{fg}(R_{dL})_{gp}\tilde{d}_p\overline{\tilde{G}^a}\end{aligned} \tag{8.15}$$

$$\begin{aligned}&-\tilde{u}_p^*(R_{uR}^\dagger)_{pg}(U_{uR}^\dagger)_{gf}\lambda_{GM}^a(U_{uR})_{fk}u_{R_k}\overline{\tilde{G}^a} \\ &-\overline{u}_{R_k}(U_{uR}^\dagger)_{kf}\lambda_{GM}^a(U_{uR})_{fg}(R_{uR})_{gp}\tilde{u}_p\tilde{G}^a] \\ &-\tilde{d}_p^*(R_{dR}^\dagger)_{pg}(U_{dR}^\dagger)_{gf}\lambda_{GM}^a(U_{dR})_{fk}d_{R_k}\overline{\tilde{G}^a} \\ &-\overline{d}_{R_k}(U_{dR}^\dagger)_{kf}\lambda_{GM}^a(U_{dR})_{fg}(R_{dR})_{gp}\tilde{d}_p\tilde{G}^a]\end{aligned} \tag{8.16}$$

Second step:

$$\begin{aligned}\mathcal{L}_I|_{\tilde{q}q\tilde{G}} = -\frac{g_3}{\sqrt{2}}[&\tilde{u}_p^*(R_{uL}^\dagger)_{pk}\lambda_{GM}^a u_{L_k}\tilde{G}^a + \overline{u}_{L_k}\lambda_{GM}^a(R_{uL})_{kp}\tilde{u}_p\overline{\tilde{G}^a} \\ &+\tilde{d}_p^*(R_{dL}^\dagger)_{pk}\lambda_{GM}^a d_{L_k}\tilde{G}^a + \overline{d}_{L_k}\lambda_{GM}^a(R_{dL})_{kp}\tilde{d}_p\overline{\tilde{G}^a} \\ &-\tilde{u}_p^*(R_{uR}^\dagger)_{pk}\lambda_{GM}^a u_{R_k}\overline{\tilde{G}^a} - \overline{u}_{R_k}\lambda_{GM}^a(R_{uR})_{kp}\tilde{u}_p\tilde{G}^a] \\ &-\tilde{d}_p^*(R_{dR}^\dagger)_{pk}\lambda_{GM}^a d_{R_k}\overline{\tilde{G}^a} - \overline{d}_{R_k}\lambda_{GM}^a(R_{dR})_{kp}\tilde{d}_p\tilde{G}^a]\end{aligned} \tag{8.17}$$

Vector Bosons

$$\begin{aligned}\mathcal{L}|_{\tilde{q}\tilde{q}V} = -i\frac{g}{\sqrt{2}}[&\tilde{u}_p^*(R_{pg}^\dagger)(U_{uL}^\dagger)_{gf}\partial^\mu_\leftrightarrow(U_{dL})_{fl}(R_{dL})_{lk}\tilde{d}_k W_\mu^+ \\ &+\tilde{d}_p^*(R_{pg}^\dagger)(U_{dL}^\dagger)_{gf}\partial^\mu_\leftrightarrow(U_{uL})_{fl}(R_{uL})_{lk}\tilde{u}_k W_\mu^-] \\ -i\frac{g}{2c_W}[&(\tilde{u}_p^*(R_{uL}^\dagger)_{pg}(U_{uL}^\dagger)_{gf}\partial^\mu_\leftrightarrow(U_{uL})_{fl}(R_{uL})_{lk}\tilde{u}_k Z_\mu \\ &-\tilde{d}_p^*(R_{dL}^\dagger)_{pg}(U_{dL}^\dagger)_{gf}\partial^\mu_\leftrightarrow(U_{dL})_{fl}(R_{dL})_{lk}\tilde{d}_k Z_\mu]\end{aligned} \tag{8.18}$$

$$\begin{aligned}+ig\frac{2s_W^2}{3c_W}[&\tilde{u}_p^*(R_{uL}^\dagger)_{pg}(U_{uL}^\dagger)_{gf}\partial^\mu_\leftrightarrow(U_{uL})_{fl}(R_{uL})_{lk}\tilde{u}_k Z_\mu \\ &+\tilde{u}_p^*(R_{uR}^\dagger)_{pg}(U_{uR}^\dagger)_{gf}\partial^\mu_\leftrightarrow(U_{uR})_{fl}(R_{uR})_{lk}\tilde{u}_k Z_\mu] \\ -ig\frac{s_W^2}{3c_W}[&\tilde{d}_p^*(R_{dL}^\dagger)_{pg}(U_{dL}^\dagger)_{gf}\partial^\mu_\leftrightarrow(U_{dL})_{fl}(R_{dL})_{lk}\tilde{d}_k Z_\mu \\ &+\tilde{d}_p^*(R_{dR}^\dagger)_{pg}(U_{dR}^\dagger)_{gf}\partial^\mu_\leftrightarrow(U_{dR})_{fl}(R_{dR})_{lk}\tilde{d}_k Z_\mu]\end{aligned} \tag{8.19}$$

In the second step, we use $(R_{uL}^\dagger)_{pl}(R_{uL})_{lk} + (R_{uR}^\dagger)_{pl}(R_{uR})_{lk} = \mathbf{1}$. Please note that R_{qL} and R_{qR} alone are NOT unitary matrices.

$$\begin{aligned}\mathcal{L}|_{\tilde{q}\tilde{q}V} = -i\frac{g}{\sqrt{2}}[&\tilde{u}_p^*(R_{pg}^\dagger)\partial^\mu_\leftrightarrow(V_{CKM})_{gl}(R_{dL})_{lk}\tilde{d}_k W_\mu^+ \\ &+\tilde{d}_p^*(R_{pg}^\dagger)(V_{CKM}^\dagger)_{gl}\partial^\mu_\leftrightarrow(R_{uL})_{lk}\tilde{u}_k W_\mu^-]\end{aligned} \tag{8.20}$$

$$\begin{aligned}&-i\frac{g}{2c_W}[(\tilde{u}_p^*(R_{uL}^\dagger)_{pg}\partial^\mu_\leftrightarrow(R_{uL})_{gk}\tilde{u}_k Z_\mu - \tilde{d}_p^*(R_{dL}^\dagger)_{pg}\partial^\mu_\leftrightarrow(R_{dL})_{gk}\tilde{d}_k Z_\mu] \\ &+ig\frac{2s_W^2}{3c_W}[\tilde{u}_p^*\partial^\mu_\leftrightarrow\tilde{u}_p Z_\mu + \tilde{u}_p^*\partial^\mu_\leftrightarrow\tilde{u}_p Z_\mu] - ig\frac{s_W^2}{3c_W}[\tilde{d}_p^*\partial^\mu_\leftrightarrow\tilde{d}_p Z_\mu + \tilde{d}_p^*\partial^\mu_\leftrightarrow\tilde{d}_p Z_\mu]\end{aligned} \tag{8.21}$$

8.1.2 Dirac notation

We introduce the Dirac spinors of the Charginos and Quarks, as well as the Majorana spinors for Gluons and Neutralinos

$$\begin{aligned}
\tilde{\chi}_j^+ &= \begin{pmatrix} \tilde{C}_j^+ \\ \overline{\tilde{C}_j^-} \end{pmatrix} & \tilde{\chi}_j^- &= \begin{pmatrix} \tilde{C}_j^- \\ \overline{\tilde{C}_j^+} \end{pmatrix} \\
\overline{\tilde{\chi}_j^+} &= \begin{pmatrix} \tilde{C}_j^- & \overline{\tilde{C}_j^+} \end{pmatrix} & \overline{\tilde{\chi}_j^-} &= \begin{pmatrix} \tilde{C}_j^+ & \overline{\tilde{C}_j^-} \end{pmatrix} \\
\tilde{\chi}_j^0 &= \begin{pmatrix} \tilde{C}_j^0 \\ \overline{\tilde{C}_j^0} \end{pmatrix} & \overline{\tilde{\chi}_j^0} &= \begin{pmatrix} \tilde{C}_j^0 & \overline{\tilde{C}_j^0} \end{pmatrix}
\end{aligned} \tag{8.22}$$

$$\begin{aligned}
\tilde{g} &= \begin{pmatrix} \tilde{G} \\ \overline{\tilde{G}} \end{pmatrix} & \overline{\tilde{g}} &= \begin{pmatrix} \tilde{G} & \overline{\tilde{G}} \end{pmatrix} \\
\boldsymbol{\Psi}_u &= \begin{pmatrix} u_L \\ u_R \end{pmatrix} & \boldsymbol{\Psi}_d &= \begin{pmatrix} d_L \\ d_R \end{pmatrix} \\
\overline{\boldsymbol{\Psi}}_u &= \begin{pmatrix} \overline{u}_R & \overline{u}_L \end{pmatrix} & \overline{\boldsymbol{\Psi}}_d &= \begin{pmatrix} \overline{d}_R & \overline{d}_L \end{pmatrix}
\end{aligned} \tag{8.23}$$

and use them to write down the Lagrangians in dirac notation. We also replace $\frac{1}{\nu_1} = \frac{g}{2m_W c_\beta}$ and $\frac{1}{\nu_2} = \frac{g}{2m_W s_\beta}$.

Charginos

$$\begin{aligned}
\mathcal{L}_I = -g[&\vec{\tilde{\mathbf{u}}}^* R_{uL}^\dagger (V_{1j}^\dagger \overline{\tilde{\chi}_j^-}) V_{CKM} \hat{P}_L \boldsymbol{\Psi}_\mathbf{d} + \vec{\tilde{\mathbf{d}}}^* R_{dL}^\dagger (U_{1j}^\dagger \overline{\tilde{\chi}_j^+}) V_{CKM}^\dagger \hat{P}_L \boldsymbol{\Psi}_\mathbf{u} \\
&+ \overline{\boldsymbol{\Psi}}_u \hat{P}_R (\tilde{\chi}_j^+ U_{j1}) V_{CKM} R_{dL} \vec{\tilde{\mathbf{d}}} + \overline{\boldsymbol{\Psi}}_d \hat{P}_R (\tilde{\chi}_j^- V_{j1}) V_{CKM}^\dagger R_{uL} \vec{\tilde{\mathbf{u}}}]
\end{aligned} \tag{8.24}$$

$$\begin{aligned}
+ \frac{g}{\sqrt{2} m_W s_\beta} [&\overline{\boldsymbol{\Psi}}_u \hat{P}_L (V_{2j}^\dagger \tilde{\chi}_j^+) \hat{m}_u V_{CKM} R_{dL} \vec{\tilde{\mathbf{d}}} + \vec{\tilde{\mathbf{u}}}^* R_{uR}^\dagger \hat{m}_u V_{CKM} (V_{2j}^\dagger \overline{\tilde{\chi}_j^-}) \hat{P}_L \boldsymbol{\Psi}_d \\
&+ \overline{\boldsymbol{\Psi}}_d \hat{P}_R (\tilde{\chi}_j^- V_{j2}) V_{CKM}^\dagger \hat{m}_u R_{uR} \vec{\tilde{\mathbf{u}}} + \vec{\tilde{\mathbf{d}}}^* R_{dL}^\dagger V_{CKM}^\dagger \hat{m}_u (\overline{\tilde{\chi}_j^+} V_{j2}) \hat{P}_R \boldsymbol{\Psi}_u]
\end{aligned} \tag{8.25}$$

$$+\frac{g}{\sqrt{2}m_W c_\beta}[\overline{\mathbf{\Psi}}_d\hat{P}_L(U^\dagger_{2j}\tilde{\chi}^-_j)\hat{m}_d V^\dagger_{CKM}R_{uL}\vec{\tilde{\mathbf{u}}}+\vec{\tilde{\mathbf{d}}}^*R^\dagger_{dR}\hat{m}_d V^\dagger_{CKM}(U^\dagger_{2j}\overline{\tilde{\chi}^+_j})\hat{P}_L\mathbf{\Psi}_u \\ +\overline{\mathbf{\Psi}}_u\hat{P}_R(\tilde{\chi}^+_jU_{j2})V_{CKM}\hat{m}_dR_{dR}\vec{\tilde{\mathbf{d}}}+\vec{\tilde{\mathbf{u}}}^*R^\dagger_{uL}V_{CKM}\hat{m}_d(\overline{\tilde{\chi}^-_j}U_{j2})\hat{P}_R\mathbf{\Psi}_d] \tag{8.26}$$

$$\begin{aligned}&=\overline{\mathbf{\Psi}}_u[\hat{P}_L(\frac{g}{\sqrt{2}m_Ws_\beta}V^*_{2j}\hat{m}_uV_{CKM}R_{dL}) \\ &\quad+\hat{P}_R(\frac{g}{\sqrt{2}m_Wc_\beta}U_{2j}V_{CKM}\hat{m}_dR_{dR}-gU_{1j}V_{CKM}R_{dL})]\tilde{\chi}^+_j\vec{\tilde{\mathbf{d}}} \\ &+\overline{\mathbf{\Psi}}_d[\hat{P}_L(\frac{g}{\sqrt{2}m_Wc_\beta}U^*_{2j}\hat{m}_dV^\dagger_{CKM}R_{uL}) \\ &\quad+\hat{P}_R(\frac{g}{\sqrt{2}m_Ws_\beta}V_{2j}V^\dagger_{CKM}\hat{m}_uR_{uR}-gV_{1j}V^\dagger_{CKM}R_{uL})]\tilde{\chi}^-_j\vec{\tilde{\mathbf{u}}} \\ &\quad+\mathbf{h.c.}\end{aligned} \tag{8.27}$$

Neutralinos

$$\begin{aligned}\mathcal{L}_I=\overline{\mathbf{\Psi}}_u[\hat{P}_L(&\frac{2\sqrt{2}g'}{3}N^*_{1j}R_{uR}-\frac{\hat{m}_ug}{\sqrt{2}m_Ws_\beta}N^*_{4j}R_{uL}) \\ &+\hat{P}_R(-\frac{\sqrt{2}g'}{6}N_{1j}R_{uL}-\frac{\sqrt{2}g}{2}N_{2j}R_{uL}-\frac{\hat{m}_ug}{\sqrt{2}m_Ws_\beta}N_{4j}R_{uR})]\tilde{\chi}^0_j\vec{\tilde{\mathbf{u}}}\end{aligned} \tag{8.28}$$

$$\begin{aligned}&+\overline{\mathbf{\Psi}}_d[\hat{P}_L(\frac{-\sqrt{2}g'}{3}N^*_{1j}R_{dR}-\frac{\hat{m}_dg}{\sqrt{2}m_Wc_\beta}N^*_{3j}R_{dL}) \\ &\quad+\hat{P}_R(\frac{-\sqrt{2}g'}{6}N_{1j}R_{dL}+\frac{\sqrt{2}g}{2}N_{2j}R_{dL}-\frac{\hat{m}_dg}{\sqrt{2}m_Wc_\beta}N_{3j}R_{dR})]\tilde{\chi}^0_j\vec{\tilde{\mathbf{d}}} \\ &\quad+\mathbf{h.c.}\end{aligned} \tag{8.29}$$

Gluinos

$$\begin{aligned}\mathcal{L}_I=&\overline{\mathbf{\Psi}}_u[\hat{P}_L(\frac{g_3}{\sqrt{2}}\lambda_{GM}R_{uR})+\hat{P}_R(-\frac{g_3}{\sqrt{2}}\lambda_{GM}R_{uL})]\tilde{g}\vec{\tilde{\mathbf{u}}} \\ &+\overline{\mathbf{\Psi}}_d[\hat{P}_L(\frac{g_3}{\sqrt{2}}\lambda_{GM}R_{dR})+\hat{P}_R(-\frac{g_3}{\sqrt{2}}\lambda_{GM}R_{dL})]\tilde{g}\vec{\tilde{\mathbf{d}}} \\ &+\mathbf{h.c.}\end{aligned} \tag{8.30}$$

Erklärung und Danksagung

Hiermit versichere ich, dass ich diese Diplomarbeit selbständig verfasst und keine anderen als die angegebenen Quellen und Hilfsmittel benutzt habe. Die Stellen meiner Arbeit, die dem Wortlaut oder dem Sinn nach anderen Werken entnommen sind, habe ich in jedem Fall unter Angabe der Quelle als Entlehnung kenntlich gemacht. Dasselbe gilt sinngemäß für Tabellen, Karten und Abbildungen. Diese Arbeit hat in dieser oder einer ähnlichen Form noch nicht im Rahmen einer anderen Prüfung vorgelegen.

Mein Dank gilt meinem Betreuer Prof. Werner Porod, ohne dessen geduldige und freundliche Beratungen diese Arbeit nicht zustande gekommen wäre.

Bibliography

[1] J.A. Aguilar-Saavedra et al. [hep-ph/0511344]. *Eur. Phys. J. C46*, 2006.

[2] A. De Roeck et al. [hep-ph/0508198]. *Eur. Phys. J. C49*, 2007.

[3] S.P.Martin. A supersymmetry primer - [hep-ph/9709356]. 2006.

[4] I. Aitchison. Susy and the mssm: an elementary introduction - [hep-ph/0505105]. 2005.

[5] J.Mandula S.Coleman. All possible symmetries of the s-matrix. *Phys. Rev. 159. 1251 to 1256.*, 1967.

[6] Lopuszanski Haag, Sohnius. All possible generators of supersymmetries of the s matrix. *Nucl. Phys. B 88 257.*, 1975.

[7] P.Skands et al. Les houches accord [hep-ph/0311123v3]. 2007.

[8] P.Skands et al. Les houches accord 2 [hep-ph/0801.0045]. 2007.

[9] W. Porod. [hep-ph/0301101]. *Comput. Phys. Commun. 153. 275*, 2003.

[10] T.Gajdosik. Quellen der cp-verletzung im mssm. *PhD Thesis Vienna*, 1997.

[11] Degrassi G et al. Eur. phys. *J C 28 133*, 2003.

[12] M.Artuso et al. B,d and k decays,[hep-ph/0801.1833]. 2008.

[13] T. Skwarnicki K. Lingel and James G. Smith. Penguin decays of b mesons - [hep-ph/9804015]. 1998.

[14] Andrzej J. Buras. Cp violation and rare decays of k and b mesons - [hep-ph/9905437v1]. 1999.

[15] I.I. Bigi et al. [hep-ph/9212227].

[16] G. Isidori G. Buchalla and S. J. Rey. [hep-ph/9705253]. *Nucl. Phys. B 511 594*, 1998.

[17] M.B. Voloshin. [hep-ph/9612483]. *Phys. Lett. B 397 275*, 1997.

[18] A. Khodjamirian et al. [hep-ph/9702318]. *Phys. Lett. B 402 167*, 1997.

[19] L. Randall Z. Ligeti and M.B. Wise. [hep-ph/9702322]. *Phys. Lett. B 402 178*, 1997.

[20] K. Grant et al. [hep-ph/9702380]. *A,Phys. Rev. D 56 3151*, 1997.

[21] M. Neubert S. J. Lee and G. Paz. [hep-ph/0609224].

[22] M. Misiak et al. [hep-ph/609232]. *Phys. Rev. Lett. 98*, 2007.

[23] M. Misiak C. Bobeth and J. Urban. [hep-ph/9910220]. *Nucl. Phys. B 574 291*, 2000.

[24] M. Misiak and M. Steinhauser. [hep-ph/0401041]. *Nucl. Phys. B 683 277*, 2004.

[25] M. Gorbahn and U. Haisch. [hep-ph/0411071]. *Nucl. Phys. B 713 291*, 2005.

[26] U. Haisch M. Gorbahn and M. Misiak. [hep-ph/0504194]. *Phys. Rev. Lett. 95 102004*, 2005.

[27] U. Haisch M. Czakon and M. Misiak. Jhep 0703, 008. *[arXiv:hep-ph/0612329]*, 2007.

[28] K. Melnikov and A. Mitov. [hep-ph/0505097]. *Phys. Lett. B 620 69]*, 2005.

[29] I. Blokland et al. [hep-ph/0506055]. *Phys. Rev. D 72 033014*, 2005.

[30] H. M. Asatrian et al. [hep-ph/0605009]. *Nucl. Phys. B 749 325]*, 2006.

[31] H. M. Asatrian et al. [hep-ph/0607316]. *Nucl. Phys. B 762 212]*, 2007.

[32] H. M. Asatrian et al. [hep-ph/0611123].

[33] C. Greub K. Bieri and M. Steinhauser. [hep-ph/0302051]. *Phys. Rev. D 67, 114019*, 2003.

[34] M. Misiak and M. Steinhauser. [hep-ph/0609241]. *Nucl. Phys. B 764 62*, 2007.

[35] T. Becher and M. Neubert. [hep-ph/0610067]. *Phys. Rev. Lett. 98 022003*, 2007.

[36] J. R. Andersen and E. Gardi. [hep-ph/0609250]. *JHEP 0701 029*, 2007.

[37] I. Bigi and N. Uraltsev. [hep-ph/0202175]. *Int. J. Mod. Phys. A 17 4709*, 2002.

[38] Z. Ligeti A. Kapustin and H.D. Politzer. [hep-ph/9507248]. *Phys. Lett. B 357 653*, 1995.

[39] Z. Ligeti et al. [hep-ph/9903305]. *Phys. Rev. D 60 034019*, 1999.

[40] P. Koppenburg et al. [Belle Collaboration]. [arxiv:hepex/0403004]. *Phys. Rev. Lett. 93 061803*, 2004.

[41] K. Abe et al. [Belle Collaboration]. [arxiv:hep-ex/0103042. *Phys. Lett. B 511 151*, 2001.

[42] B. Aubert et al. [BABAR Collaboration]. [arxiv:hepex/0508004]. *Phys. Rev. D 72 052004*, 2005.

[43] B. Aubert et al. [BaBar Collaboration]. [arxiv:hepex/0607071]. *Phys. Rev. Lett. 97 171803*, 2006.

[44] D0 collaboration. D0-note-conf-5344. 2007.

[45] M. Jamin A. J. Buras and P. H. Weisz. *Nucl. Phys. B 347.491*, 1990.

[46] J. Charles et al. [ckmfitter group, http://ckmfitter.in2p3.fr]. *Eur. Phys. J. C 41 1, [hepph/0406184]*, 2005.

[47] A. Abulencia et al. [cdf collaboration]. *[hep-ex/0609040].*

[48] M. Bona et al. [utfit collaboration]. *arXiv:0707.0636 [hep-ph].*

[49] D.Dujmic. http://today.slac.stanford.edu/a/2006/09-14.htm. 2008.

[50] E.Lunghi T.Hurth and W.Porod. [hep-ph/0312260]. *Nucl. Phys. B704*, 2005.

[51] J.Rosiek A.J.Buras, P.H.Chankowski and L.Slawianowska. [hep-ph/0210145]. *Nucl. Phys. B659*, 2003.

[52] M.Misiak T.Huber, E.Lunghi and D.Wyler. [hep-ph/0512066]. *Nucl. Phys. B740*, 2006.